

Considerations of Polarization in Inclusive Electron Scattering from Nuclei*

T. W. DONNELLY AND A. S. RASKIN

*Laboratory for Nuclear Science and Department of Physics, Center for Theoretical Physics,
Massachusetts Institute of Technology, Cambridge, Massachusetts 02139*

Received April 23, 1985

Inclusive electron scattering of either unpolarized or polarized electrons, (e, e') or (\bar{e}, e'), from polarized nuclei is considered. General formulas are given for arbitrary nuclear transitions and polarizations, in the extreme relativistic limit for the electron, and examples where the nuclear states involved have specific angular momenta and parities are discussed in some detail. © 1986 Academic Press, Inc.

1. INTRODUCTION

One of the fundamental problems of nuclear physics has been to develop a complete understanding of the electromagnetic structure of the nucleus. Specifically, it is of interest to have all of the individual electromagnetic form factors for a given nuclear transition at our disposal, for these quantities provide the most complete characterization of the electromagnetic structure of that transition.

For many years, the use of inclusive electron scattering from nuclei has been a fruitful approach to the experimental determination of nuclear electromagnetic form factors. Underlying such studies is the fundamental theory of quantum electrodynamics describing the electromagnetic interaction of spin- $\frac{1}{2}$ leptons, which has led to theoretical predictions that are in unprecedented agreement with experiment. Thus, in considering lepton scattering from hadrons (i.e., semi-leptonic processes), the leptonic part of the reaction can be presumed to be well known. Specifically, electron scattering allows us to investigate the electromagnetic structure of the relevant nuclear (hadronic) states with confidence, since certain properties of the electromagnetic interaction make electron scattering especially well suited to analysis. In particular, the electromagnetic coupling, characterized by the fine-structure constant $\alpha \equiv e^2/\hbar c \approx 1/137.036$, is relatively small, and thus we only need to consider the lowest order processes involved in order to achieve results which are quite accurate and relatively easy to interpret. Since higher-order processes are suppressed relative to the lowest order ones, the single-photon-exchange process for

* This work is supported through funds provided by the U.S. Department of Energy (D.O.E.) under Contract DE-AC02-76ERO3069.

electron scattering is usually dominant. In fact, in this work we shall consider only the one-photon-exchange contributions together with plane-wave electrons (the plane-wave Born approximation, PWBA). Of course, distorted electron waves can also be handled (leading to the distorted-wave Born approximation, DWBA), but this goes beyond the more limited focus of the present developments. Within the context of the PWBA, the electromagnetic form factors are directly related to the Fourier transforms of the electromagnetic current matrix elements; by fixing the energy transferred to the nucleus (to pick out a transition between specific nuclear states) and varying the momentum transfer, it is possible to learn about the spatial distributions of the nuclear electromagnetic current. This provides the basic interface for comparison with predictions obtained using some specific model for the nuclear states involved.

Alternatively, one might imagine performing similar types of experiments in which the weak or strong interactions are used as a probe of nuclear structure; these experiments could involve, for example, neutrino scattering in the former case or meson or nucleon scattering in the latter. As far as the weak interaction is concerned, the corresponding analysis of the scattering process is completely analogous to that for the electromagnetic interaction, except that the resulting cross sections are much smaller [1, 2, 3]; this limits the applicability of such experiments. On the other hand, hadron scattering, which is characterized by a large coupling strength, involves correspondingly larger cross sections; however, this increased strength (compared to the electroweak coupling) is also a drawback since the effects of the reaction mechanism (namely, the hadron scattering process itself) are difficult to separate from those of the underlying nuclear structure. Thus, electron scattering can be seen to play a special role when studying nuclear structure. Of course, whenever possible, it is desirable to have information from all three (electromagnetic, weak, and strong) types of probes.

Electron scattering studies may be undertaken in principle with or without polarization degrees of freedom being specified for the electrons and/or for the nucleus. Up to the present, the technology required in practice to achieve useful polarized electron beams and nuclear targets has not been readily available. On the other hand, a considerable amount of information has been obtained using unpolarized beams and targets, although there are certain limitations inherent in this class of experiments. Under these conditions, it is only possible to extract from measurements of the inclusive differential scattering cross section two form factors, corresponding to the longitudinal and transverse polarizations of the exchanged virtual photon. This separation, which is made by varying the kinematic factors of the incident and scattered electrons (such as the initial energy and scattering angle) while keeping the energy and momentum transferred constant, is known as the Rosenbluth decomposition [4]. However, for the case of electron scattering from discrete nuclear states which have definite parities and angular momenta, the longitudinal form factor in general consists of an incoherent superposition of the squares of a number of Coulomb (i.e., charge) form factors with various multipolarities. Similarly, the transverse form factor in general is an incoherent super-

position of the squares of a series of electric and magnetic form factors, again with varying multipolarity (in the case of elastic scattering, the electric form factors can be shown to be identically zero, if time-reversal invariance is applied). Thus, in the general case it can be seen that it is not possible to extract all of the individual electromagnetic form factors from experimental cross section measurements, and this puts important restrictions on the amount of nuclear information which may be extracted from experiments involving inclusive electron scattering. Indeed, even when there are only two possible form factors (e.g., in elastic scattering from spin- $\frac{1}{2}$ nuclei, where one has only a single Coulomb and a single magnetic multipole), there are frequently cases where one form factor dominates over the other and it is difficult to extract the small quantity using the Rosenbluth technique.

These limitations have led a number of people to investigate the possibility of extracting additional information through the use of polarized electron beams and/or targets (see especially [5]). The essential point is that new combinations of the form factors (other than incoherent sums of squares) can be obtained by varying the polarization direction, or the polarization itself, of the nucleus; also, the presence of polarization results in additional independent kinematic factors in a sort of super-Rosenbluth formula [6] which can be used to the same purpose. Previously, the only nuclei which had been considered in detail for polarization studies were the nucleon [7-14], the deuteron [14-17], and ^{165}Ho [18, 19]. At present, the prospects for having intense, polarized electron beams are very good [20], as is the possibility of being able to polarize a variety of nuclei, as discussed below (see also Refs. [21, 22, 23]), and so a general treatment of the problem of inclusive electron scattering from polarized nuclei is called for; in particular, in the present article we generalize the formalism (building on the work of Weigert and Rose [5]), casting the basic polarization cross sections in forms which should prove to be useful in the future in discussing experimental results. Anticipating such experimental studies, we apply our general formalism to a selection of specific nuclear transitions which serve to illustrate the high degree of sensitivity inherent in using polarization measurements as a tool to probe nuclear structure.

There are two technical developments which make electron polarization experiments of increasing importance in nuclear physics. First, the construction of high duty factor facilities with high beam intensities makes coincidence experiments involving the analysis of recoil nuclear polarization much easier than in the past. Second, the construction of stretcher rings [22, 23, 24] will allow experiments to be undertaken using internal (e.g., gas jet) targets of polarized nuclei; because of the high intensity of the resulting internal circulating electron beam, the luminosity will approach the point where it will be possible to perform electron scattering experiments over extended ranges of the momentum transfer, even though the targets themselves are relatively thin [22]. In contrast, polarized-target experiments using an external electron beam have not been practical except in a few very special cases, such as hydrogen or holmium; however, even in these cases, the development of targets with both high polarizations and a tolerance to high beam intensities remains a largely unsolved problem [22].

The focus of this paper is on the nuclear structure information which may be extracted from the analysis of inclusive electron scattering from polarized nuclei. The basic formalism is presented in Section 2 and Appendices A and B, and the accompanying tables given in Appendix C. We consider the situation in which the incident electron beam is polarized in an arbitrary direction, and then specialize the resulting formalism to the case in which the beam is longitudinally polarized. The approach which we have taken here is a straightforward extension of familiar analyses of the (e, e') reaction which have been previously developed [1, 25, 26], and also parallels other treatments of electron and nuclear polarization [5]. In addition to treating polarized target situations, our formalism turns out to be very well suited to the situation in which the recoil polarization of the nucleus is measured, regardless of whether or not the initial target was itself polarized; this will be useful since it may be more practical in some cases to measure the recoil polarization of the nucleus than it would be to maintain a polarized target with a high intensity electron beam. In order to complete our analysis of polarization in electron scattering from nuclei, we indicate the equivalence of our results to those obtained previously for the nucleon and the deuteron, and in Section 3 give results for a selection of other nuclei which are of interest, indicating the nuclear structure information which may be accessible from polarization experiments. Some of the basic results of our analysis have been reported in abbreviated forms in various conference proceedings [6, 21, 24, 27, 28, 29], and interested readers may wish to consult them for an overview of our results.

2. FORMALISM

We begin by considering the problem of scattering polarized electrons from nuclei whose polarizations are specified. The incident and/or scattered electrons may be polarized and the initial and/or final nuclear states may have specific polarizations in this general case. The Feynman diagram corresponding to the lowest order (one-photon-exchange) process, together with the appropriate factors which are associated with the lines and vertices, is given in Fig. 1. The four-

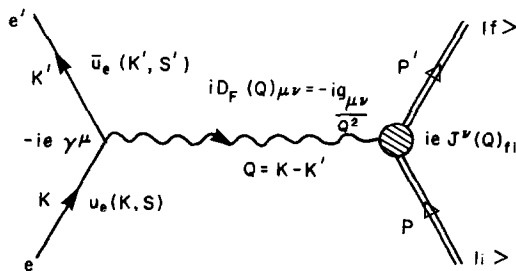


FIG. 1. Feynman diagram and rules for the electron-nucleus scattering process in the one-photon-exchange or first-order Born approximation.

momenta of the incident and scattered electrons are labeled K and K' , respectively (see Appendix A for details concerning our conventions); in particular, $K = (\varepsilon, \mathbf{k})$ and $K' = (\varepsilon', \mathbf{k}')$, where \mathbf{k} and \mathbf{k}' are the three-momenta of the electrons and ε and ε' are their corresponding energies. Note that we are using the space-time metric $g_{\mu\nu}$ of Bjorken and Drell [30], and are taking $\hbar = c = 1$ (see Appendix A). Then, the four-momentum transfer is given by $Q = K - K' = P_f - P_i$, and satisfies the requirement that $Q^2 = (\varepsilon - \varepsilon')^2 - (\mathbf{k} - \mathbf{k}')^2 \leq 0$. Here P_i and P_f are the initial and final four-momenta, respectively, of the nucleus. Also, $Q = (\omega, \mathbf{q})$, where the three-momentum transfer $\mathbf{q} = \mathbf{k} - \mathbf{k}' = \mathbf{p}_f - \mathbf{p}_i$ and the energy transfer $\omega = \varepsilon - \varepsilon' = E_f - E_i$. The incoming and outgoing electron Dirac spinors u_e and \bar{u}_e are labeled with the corresponding four-momenta K and K' and spins S and S' . The electric charge e is taken to be positive, and the virtual photon is represented by the propagator $D_F(Q)_{\mu\nu} = -g_{\mu\nu}/Q^2$.

Following Bjorken and Drell [30], we obtain the differential scattering cross section in the laboratory frame (i.e., with $\mathbf{p}_i = 0$ and $P_i^0 = E_i = M_{\text{target}}$):

$$d\sigma = \frac{1}{\beta} \frac{m_e}{\varepsilon} \overline{\sum}_{\text{if}} |\mathcal{M}_{\bar{n}}|^2 \frac{m_e}{\varepsilon'} \frac{d^3\mathbf{k}'}{(2\pi)^3} \frac{M_{\text{target}}}{E_f} \frac{d^3\mathbf{p}_f}{(2\pi)^3} (2\pi)^4 \delta^{(4)}(K + P_i - K' - P_f), \quad (2.1)$$

where $\beta = |\mathbf{k}|/\varepsilon = |\mathbf{v}_e|$ and where $\overline{\sum}_{\text{if}}$ corresponds to the appropriate average over initial states and sum over final states as discussed below. Throughout this paper, we will be dealing with the laboratory system only, and so we will not explicitly label any of the cross sections as such. The invariant matrix element $\mathcal{M}_{\bar{n}}$ corresponding to the given process is

$$\mathcal{M}_{\bar{n}} = \frac{ie}{Q^2} \left(\frac{\varepsilon\varepsilon'}{m_e^2} \right)^{1/2} j_e(K', S'; K, S)_\mu J^\mu(P_f, P_i)_{\bar{n}}, \quad (2.2)$$

where the electromagnetic current for the electron is equal to

$$j_e(K', S'; K, S)_\mu = -e \left(\frac{m_e^2}{\varepsilon\varepsilon'} \right)^{1/2} \bar{u}_e(K', S') \gamma_\mu u_e(K, S), \quad (2.3)$$

and where $J^\mu(P_f, P_i)_{\bar{n}} = J^\mu(Q)_{\bar{n}}$ is the nuclear electromagnetic transition current in momentum space. If we assume that the momentum of the scattered nucleus is not measured, while that of the electron is (i.e., we consider inclusive electron scattering), then the integration over \mathbf{p}_f must be performed, and so we have that

$$\left(\frac{d\sigma}{d\Omega_e} \right)_{\bar{n}} = \frac{m_e^2 k'}{(2\pi)^2 k} f_{\text{rec}}^{-1} \overline{\sum}_{\text{if}} |\mathcal{M}_{\bar{n}}|^2, \quad (2.4)$$

where the nuclear recoil correction factor f_{rec} is given by

$$f_{\text{rec}} = 1 + \frac{\varepsilon k' - \varepsilon' k \cos \theta_e}{k' M_{\text{target}}}. \quad (2.5)$$

Consider now the invariant matrix element $\mathcal{M}_{\bar{n}} = -i(e^2/Q^2) \bar{u}_e(K', S') \gamma_\mu u_e(K, S) J^\mu(Q)_{\bar{n}}$; then,

$$\overline{\sum_{\text{if}}} |\mathcal{M}_{\bar{n}}|^2 = \frac{(4\pi\alpha)^2}{(Q^2)^2} \eta_e(K', S'; K, S)_{\mu\nu} W^{\mu\nu}(Q)_{\bar{n}}, \quad (2.6)$$

where the electron tensor $\eta_e(K', S'; K, S)_{\mu\nu}$ is defined by

$$\eta_e(K', S'; K, S)_{\mu\nu} \equiv \overline{\sum_{\text{if}}} [\bar{u}_e(K', S') \gamma_\mu u_e(K, S)]^* [\bar{u}_e(K', S') \gamma_\nu u_e(K, S)], \quad (2.7)$$

and the nuclear tensor

$$W^{\mu\nu}(Q)_{\bar{n}} \equiv \overline{\sum_{\text{if}}} J^{\mu*}(Q)_{\bar{n}} J^\nu(Q)_{\bar{n}}. \quad (2.8)$$

It then follows that the cross section can be expressed as

$$\left(\frac{d\sigma}{d\Omega_e} \right)_{\bar{n}} = \frac{\alpha^2}{(Q^2)^2} \frac{4m_e^2 k'}{k} f_{\text{rec}}^{-1} \eta_e(K', S'; K, S)_{\mu\nu} W^{\mu\nu}(Q)_{\bar{n}}. \quad (2.9)$$

We now consider the electron tensor in more detail, beginning with the case in which both the initial and final electron spins are known. Under these circumstances, it follows that there is no sum/average to be performed. To evaluate the electron tensor easily, we use the standard technique of inserting positive energy (electron) and spin projection operators into the proper places in the expression for η_e so as to allow the summation over all four components of the Dirac spinors [30]. Then, using the completeness relation for the Dirac spinors, we have that

$$\eta_e(K', S'; K, S)_{\mu\nu} = \frac{1}{16m_e^2} \text{Trace} \{ \gamma_\mu (1 + \gamma_5 \mathcal{S}') (\mathbf{K}' + m_e) \gamma_\nu (1 + \gamma_5 \mathcal{S}) (\mathbf{K} + m_e) \}, \quad (2.10)$$

where $A \equiv \gamma_\mu A^\mu$ and $\gamma_5 \equiv i\gamma^0\gamma^1\gamma^2\gamma^3$. It then follows from the well-known trace identities involving the γ -matrices that

$$\begin{aligned} \eta_e(K', S'; K, S)_{\mu\nu}^{\text{eff}} = & \frac{1}{8m_e^2} (P_\mu P_\nu (1 - S \cdot S') + Q^2 g_{\mu\nu} (1 + S \cdot S' - 2\Sigma \cdot \Sigma')) \\ & + Q^2 (\Sigma_\mu \Sigma'_\nu + \Sigma'_\mu \Sigma_\nu) + (P_\mu U_\nu + U_\mu P_\nu) \\ & + 2im_e \epsilon_{\mu\nu\alpha\beta} (S + S')^\alpha Q^\beta, \end{aligned} \quad (2.11)$$

where we have defined the quantities $P_\mu \equiv K_\mu + K'_\mu$ and $U_\mu \equiv (Q \cdot S') \Sigma'_\mu - (Q \cdot S) \Sigma_\mu$, where by construction $\Sigma_\mu \equiv S_\mu - ((Q \cdot S)/Q^2) Q_\mu$ and $\Sigma'_\mu \equiv S'_\mu - ((Q \cdot S')/Q^2) Q_\mu$ satisfy $Q \cdot \Sigma = Q \cdot \Sigma' = 0$. Note that we have eliminated terms proportional to Q_μ or Q_ν , since they would vanish when the electron tensor is con-

tracted with the nuclear tensor, due to the current conservation condition $Q_\mu J^\mu(Q)_{\text{eff}} = 0$ (this is indicated by the superscript "eff" in Eq. (2.11)).

Now, consider the electron spin four-vector S , which must satisfy the requirements that $S \cdot S = -1$ and $K \cdot S = 0$ [30]. For the case of general electron polarization, the spin three-vector \mathbf{s} can be written as $\mathbf{s} = h s (\cos \zeta \mathbf{u}_\parallel + \sin \zeta \mathbf{u}_\perp)$, where \mathbf{u}_\parallel and \mathbf{u}_\perp are unit vectors parallel and perpendicular to the electron momentum \mathbf{k} , respectively, $h = \pm 1$, ζ is the angle between the spin \mathbf{s} and the momentum \mathbf{k} , and where s is taken to be a positive quantity. Then, it follows from the properties of S that

$$s = (1 - \beta^2 \cos^2 \zeta)^{-1/2} = \frac{\gamma}{\sqrt{\cos^2 \zeta + \gamma^2 \sin^2 \zeta}} \quad (2.12)$$

and $S^0 = h\beta s \cos \zeta$, where $\gamma = (1 - \beta^2)^{-1/2} = \varepsilon/m_e$ is the usual relativistic factor. For the case of longitudinal polarization, $\zeta = 0$ and so $S = h\gamma(\beta, \mathbf{u}_L)$, where $\mathbf{u}_L = \mathbf{u}_\parallel$, while for transverse polarization, $\zeta = \pi/2$ and $S = h(0, \mathbf{u}_\perp)$. Also, to completely specify the orientation of the spin vector relative to \mathbf{k} , we require an additional angle η ; $\mathbf{u}_\perp = \cos \eta \mathbf{u}_S + \sin \eta \mathbf{u}_N$, where \mathbf{u}_N is a unit vector along $\mathbf{k} \times \mathbf{k}'$ (normal to the scattering plane) and $\mathbf{u}_S = \mathbf{u}_N \times \mathbf{u}_L$ ("sideways"; see Fig. 2).

The general cross section for the scattering of arbitrarily polarized electrons from nuclei can then be seen to contain terms of the following types:

(A) terms with neither h nor h' , which occur even if no electron polarizations are involved;

(B) terms with h but not h' , which occur when only the incident electron beam is polarized;

(C) terms with h' but not h , which occur if only the polarization of the scattered electrons is measured; and,

(D) terms with the product hh' , which can occur only if the incident beam is polarized and the polarization of the scattered electrons is measured.

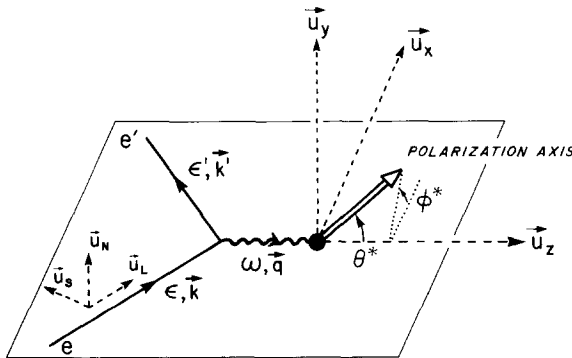


FIG. 2. Kinematics and coordinate systems for the scattering of polarized electrons from polarized nuclear targets.

As it is more difficult to measure the polarization of the scattered electron than it is to prepare a polarized electron beam, we will usually consider only the situation in which the final electron polarization is unmeasured (although see Eq. (2.35)). Then, terms of types (C) and (D) listed above are absent from the cross section, and so the remaining terms yield an electron scattering cross section of the form

$$\left(\frac{d\sigma}{d\Omega_e}\right)_{\bar{fi}}^h = \Sigma_{\bar{fi}} + h\Delta_{\bar{fi}}, \quad (2.13)$$

where \bar{fi} refers to a transition from an initial nuclear state labelled i to a final nuclear state labelled f . The term $\Sigma_{\bar{fi}}$ contains the electron dependence of type (A), while the term $\Delta_{\bar{fi}}$ contains the dependence of type (B). In fact, $\Sigma_{\bar{fi}}$ is just the electron-spin-averaged cross section

$$\left(\frac{d\sigma}{d\Omega_e}\right)_{\bar{fi}}^{\text{unpol}} = \frac{1}{2} \left\{ \left(\frac{d\sigma}{d\Omega_e}\right)_{\bar{fi}}^{+1} + \left(\frac{d\sigma}{d\Omega_e}\right)_{\bar{fi}}^{-1} \right\} = \Sigma_{\bar{fi}}, \quad (2.14)$$

and $\Delta_{\bar{fi}}$ is the electron polarization cross section

$$\left(\frac{d\sigma}{d\Omega_e}\right)_{\bar{fi}}^{\text{pol}} = \frac{1}{2} \left\{ \left(\frac{d\sigma}{d\Omega_e}\right)_{\bar{fi}}^{+1} - \left(\frac{d\sigma}{d\Omega_e}\right)_{\bar{fi}}^{-1} \right\} = \Delta_{\bar{fi}}. \quad (2.15)$$

If the final electron polarization is not measured, then the previous expression for the electron tensor reduces to

$$4m_e^2 \eta_e(K'; K, S)_{\mu\nu}^{\text{eff}} = K_\mu K'_\nu + K'_\mu K_\nu - g_{\mu\nu}(K \cdot K' - m_e^2) - im_e \varepsilon_{\mu\nu\alpha\beta} Q^\alpha S^\beta \quad (2.16a)$$

$$\equiv \chi_e(K'; K, S)_{\mu\nu}, \quad (2.16b)$$

where $K \cdot K' - m_e^2 = -\frac{1}{2}Q^2$, and so

$$\left(\frac{d\sigma}{d\Omega_e}\right)_{\bar{fi}}^h = \frac{\alpha^2}{(Q^2)^2} \frac{k'}{k} f_{\text{rec}}^{-1} \mathcal{R}_{\bar{fi}}, \quad (2.17)$$

where $\mathcal{R}_{\bar{fi}} \equiv \chi_e(K'; K, S)_{\mu\nu} W^{\mu\nu}(Q)_{\bar{fi}}$.

In general, we have that the contraction of the electron tensor with that of the nucleus can be expressed in the form

$$4m_e^2 \eta_e(K', S'; K, S)_{\mu\nu}^{\text{eff}} W^{\mu\nu}(Q)_{\bar{fi}} = v_0 \sum_K V_K \mathcal{R}_{\bar{fi}}^K, \quad (2.18)$$

where the label K takes on the values L , T , TT , TL , T' , TL' , \underline{TT} , \underline{TL} , and \underline{TL}' . The labels L and T refer to the longitudinal and transverse components of the virtual photon polarization, respectively, and hence correspond to the nuclear electromagnetic current components *with respect to the direction* \mathbf{q} . The unprimed terms result from the product of the symmetric parts of the electron and nuclear tensors,

and so enter in $\Sigma_{\bar{n}}$, while the primed terms involve the antisymmetric parts of the tensors, and so enter in $\Delta_{\bar{n}}$; the symmetric-antisymmetric cross terms vanish. The significance of the underlining will become apparent in due course. The various $\mathcal{R}_{\bar{n}}^K$ are nuclear response functions which contain all of the nuclear structure information; v_0 and the V_K are electron kinematic and polarization factors, and in the absence of any final electron polarization are given by

$$v_0 = (\varepsilon + \varepsilon')^2 - q^2, \quad (2.19a)$$

$$V_L = \left(\frac{Q^2}{q^2}\right)^2, \quad (2.19b)$$

$$V_T = \frac{1}{v_0} \left\{ 2 \left(\frac{kk' \sin \theta_e}{q} \right)^2 - Q^2 \right\}, \quad (2.19c)$$

$$V_{TT} = -\frac{2}{v_0} \left(\frac{kk' \sin \theta_e}{q} \right)^2, \quad (2.19d)$$

$$V_{TL} = \frac{\sqrt{2}(\varepsilon + \varepsilon')}{v_0} \left(\frac{kk' \sin \theta_e}{q} \right) \left(\frac{Q^2}{q^2} \right), \quad (2.19e)$$

$$V_T = \frac{2hm_e s}{qv_0} [(q^2\beta - \omega(k - k' \cos \theta_e)) \cos \zeta + \omega k' \sin \theta_e \sin \zeta \cos \eta], \quad (2.19f)$$

$$V_{TL'} = \frac{\sqrt{2}hm_e s}{v_0} \left(\frac{Q^2}{q^2} \right) [k' \sin \theta_e \cos \zeta + (k - k' \cos \theta_e) \sin \zeta \cos \eta], \quad (2.19g)$$

$$V_{TL''} = \frac{\sqrt{2}hm_e s q}{v_0} \left(\frac{Q^2}{q^2} \right) \sin \zeta \sin \eta. \quad (2.19h)$$

Note that $V_{TT} = V_{TL} = 0$; these two terms enter only when both the initial and the final electron polarizations are specified.

By examining the detailed form of the kinematic factors V_K for this special case where the sum over the final electron spin has been performed, it can be seen that $\Delta_{\bar{n}}$ has the form

$$\Delta_{\bar{n}} = S_L \Delta_{\bar{n}}^{(0)} + \Delta_{\bar{n}}^{(1)}, \quad (2.20)$$

where $S_L = 1$ for longitudinal electron polarization and $S_L = 0$ for transverse polarizations (these ideas will be discussed in greater detail in [31]). The term $\Delta_{\bar{n}}^{(1)}$ is of order γ^{-1} relative to $\Delta_{\bar{n}}^{(0)}$ (see Eqs. (2.11) and (2.19)), and so we may safely assume that $\Delta_{\bar{n}}^{(1)}$ may be dropped at electron energies of interest in most nuclear physics experiments. Thus, one has arrived at the conclusion that only longitudinally polarized electrons are of practical interest, in which case h becomes the electron helicity.

We will now consider the case of the scattering of purely longitudinally polarized electrons from polarized nuclei in much greater detail. We will be assuming

throughout this paper that $\gamma \gg 1$ (the extreme relativistic limit (ERL) for the electrons); again, this fact will generally not be explicitly indicated in the formalism. As explained previously, these special cases of the general problem will be the most useful ones for nuclear physics experiments; the results for general lepton polarizations and kinematics, which may for example be useful for muon scattering experiments, will be given in [31]. Since $\zeta = 0$ for longitudinally polarized electrons and $\beta \mapsto 1$ in the ERL, it follows that $S = hK/m_e$ in this limit. Then,

$$\chi_e(K'; K, S)_{\mu\nu}^{\text{ERL}} = K_\mu K'_\nu + K'_\mu K_\nu + \frac{1}{2}Q^2 g_{\mu\nu} - ih\varepsilon_{\mu\nu\alpha\beta} K^\alpha K'^\beta \quad (2.21)$$

and

$$\left(\frac{d\sigma}{d\Omega_e}\right)_{\text{fi}}^h = \frac{\alpha^2}{(Q^2)^2} \frac{\varepsilon'}{\varepsilon} f_{\text{rec}}^{-1} \mathcal{R}_{\text{fi}}, \quad (2.22)$$

where

$$f_{\text{rec}} = 1 + \frac{2\varepsilon \sin^2 \theta_e/2}{M_{\text{target}}} \quad (2.23)$$

is the nuclear recoil correction in the ERL. Also, $Q^2 = -4\varepsilon\varepsilon' \sin^2 \theta_e/2$ and $v_0 = 4\varepsilon\varepsilon' \cos^2 \theta_e/2$ in the ERL, and so

$$\frac{\alpha^2}{(Q^2)^2} \frac{\varepsilon'}{\varepsilon} v_0 = \sigma_{\text{Mott}} = \left(\frac{\alpha \cos \theta_e/2}{2\varepsilon \sin^2 \theta_e/2}\right)^2, \quad (2.24)$$

the Mott cross section in the ERL. The electron kinematic factors $V_{\mathbf{K}}$ take on simple forms for longitudinal polarization in the ERL; $V_{\mathbf{K}} \mapsto v_{\mathbf{K}}$ for the unprimed terms, while $V_{\mathbf{K}'} \mapsto hv_{\mathbf{K}'}$ for the primed terms and $V_{\mathbf{TL}'} \mapsto 0$, where

$$v_{\mathbf{L}} = \left(\frac{Q^2}{q^2}\right)^2, \quad (2.25a)$$

$$v_{\mathbf{T}} = -\frac{1}{2} \left(\frac{Q^2}{q^2}\right) + \tan^2 \frac{\theta_e}{2}, \quad (2.25b)$$

$$v_{\mathbf{TT}} = \frac{1}{2} \left(\frac{Q^2}{q^2}\right), \quad (2.25c)$$

$$v_{\mathbf{TL}} = (1/\sqrt{2}) \left(\frac{Q^2}{q^2}\right) \sqrt{-(Q^2/q^2) + \tan^2(\theta_e/2)}, \quad (2.25d)$$

$$v_{\mathbf{T}'} = \sqrt{-(Q^2/q^2) + \tan^2(\theta_e/2)} \tan \frac{\theta_e}{2}, \quad (2.25e)$$

and

$$v_{\mathbf{TL}'} = (1/\sqrt{2}) \left(\frac{Q^2}{q^2}\right) \tan \frac{\theta_e}{2}. \quad (2.25f)$$

Note that v_L and v_T are the usual kinematic factors which occur in the Rosenbluth formula for the scattering of unpolarized electrons from unpolarized nuclei, while v_{TT} and v_{TL} occur in the analysis of $(e, e'x)$ coincidence reactions [32]. Also, the kinematic factors $v_{T'}$ and $v_{TL'}$, which are peculiar to polarized electron scattering, are proportional to $\tan \theta_e/2$ and so $\Delta_{\bar{n}}$ will be suppressed relative to $\Sigma_{\bar{n}}$ at small scattering angles. An alternative parametrization of the kinematic factors which is in common use is in terms of $\tau \equiv -Q^2/4M_{\text{target}}^2 \geq 0$ and the scattering angle θ_e ; then for elastic scattering the energy transfer $\omega = 2M_{\text{target}}\tau$, the three-momentum transfer is given by $q^2 = 4M_{\text{target}}^2\tau(1+\tau)$, and so $Q^2/q^2 = -1/(1+\tau)$.

Now, we must consider contracting the nuclear tensor $W^{\mu\nu}(Q)_{\bar{n}}$ with the electron tensor $\chi_e(K'; K, S)_{\mu\nu}$. Again, we let $P = K + K'$, and so

$$\mathcal{R}_{\bar{n}} = |P_\mu J^\mu(\mathbf{q})_{\bar{n}}|^2 + Q^2 J_\mu^*(\mathbf{q})_{\bar{n}} J^\mu(\mathbf{q})_{\bar{n}} - 2hi\epsilon_{\mu\nu\alpha\beta} K^\alpha K'^\beta J^\mu(\mathbf{q})_{\bar{n}} J^\nu(\mathbf{q})_{\bar{n}}, \quad (2.26)$$

where we have used current conservation. However, we have that $J^0(\mathbf{q})_{\bar{n}} = \rho(\mathbf{q})_{\bar{n}}$ is the Fourier transform of the transition charge density, while

$$\mathbf{J}(\mathbf{q})_{\bar{n}} = \sum_{m=0, \pm 1} J(\mathbf{q}; m)_{\bar{n}} \mathbf{e}^*(\mathbf{q}; 1, m) \quad (2.27)$$

is the expansion of the Fourier transform of the transition three-current distributions (convection and magnetization) [25, 32, 33] in terms of the standard unit spherical vectors $\mathbf{e}(\mathbf{q}; 1, m)$ defined by [34]:

$$\mathbf{e}(\mathbf{q}; 1, 0) = \mathbf{u}_z, \quad (2.28a)$$

$$\mathbf{e}(\mathbf{q}; 1, \pm 1) = \mp (1/\sqrt{2})(\mathbf{u}_x \pm i\mathbf{u}_y). \quad (2.28b)$$

Throughout this paper, we employ the coordinate system in which the z axis is along the direction of the three-momentum transfer \mathbf{q} , and the y axis, which lies along $\mathbf{k} \times \mathbf{k}'$, is perpendicular to the scattering plane; the xz plane is then defined by \mathbf{k} and \mathbf{k}' (see Fig. 2). From current conservation,

$$Q^0 J^0(\mathbf{q})_{\bar{n}} - \mathbf{q} \cdot \mathbf{J}(\mathbf{q})_{\bar{n}} = \omega \rho(\mathbf{q})_{\bar{n}} - q J(\mathbf{q}; 0)_{\bar{n}} = 0, \quad (2.29)$$

so that $J(\mathbf{q}; 0)_{\bar{n}} = (\omega/q) \rho(\mathbf{q})_{\bar{n}}$.

Then, eliminating $J(\mathbf{q}; 0)_{\bar{n}}$ from the expression for $\mathcal{R}_{\bar{n}}$ results in

$$(\mathcal{R}_{\bar{n}})^{\text{unpol}} = |P^0 J^0(\mathbf{q})_{\bar{n}} - \mathbf{P} \cdot \mathbf{J}(\mathbf{q})_{\bar{n}}|^2 + (Q^2)^2 (|J^0(\mathbf{q})_{\bar{n}}|^2 - \mathbf{J}^*(\mathbf{q})_{\bar{n}} \cdot \mathbf{J}(\mathbf{q})_{\bar{n}}) \quad (2.30a)$$

$$\equiv v_0(v_L \mathcal{R}_{\bar{n}}^L + v_T \mathcal{R}_{\bar{n}}^T + v_{TT} \mathcal{R}_{\bar{n}}^{TT} + v_{TL} \mathcal{R}_{\bar{n}}^{TL}), \quad (2.30b)$$

where the nuclear response functions $\mathcal{R}_{\bar{n}}^K$ are then defined by

$$\mathcal{R}_{\bar{n}}^L \equiv |\rho(\mathbf{q})_{\bar{n}}|^2, \quad (2.31a)$$

$$\mathcal{R}_{\bar{n}}^T \equiv |J(\mathbf{q}; +1)_{\bar{n}}|^2 + |J(\mathbf{q}; -1)_{\bar{n}}|^2, \quad (2.31b)$$

$$\mathcal{R}_{\bar{n}}^{TT} \equiv 2\Re\{J^*(\mathbf{q}; +1)_{\bar{n}} J(\mathbf{q}; -1)_{\bar{n}}\}, \quad (2.31c)$$

and

$$\mathcal{R}_{\bar{n}}^{\text{TL}} \equiv -2\Re\{\rho^*(\mathbf{q})_{\bar{n}}(J(\mathbf{q}; +1)_{\bar{n}} - J(\mathbf{q}; -1)_{\bar{n}})\}. \quad (2.31d)$$

Consider now the polarized part of $\mathcal{R}_{\bar{n}}$:

$$(\mathcal{R}_{\bar{n}})^{\text{pol}} = -2hi\varepsilon_{\mu\nu\alpha\beta}K^\alpha K'^\beta J^{\mu*}(\mathbf{q})_{\bar{n}}J^\nu(\mathbf{q})_{\bar{n}} \quad (2.32a)$$

$$= hv_0(v_{\text{T}}\mathcal{R}_{\bar{n}}^{\text{T}'} + v_{\text{TL}}\mathcal{R}_{\bar{n}}^{\text{TL}'}), \quad (2.32b)$$

as can be shown by a straightforward calculation, where the quantities $\mathcal{R}_{\bar{n}}^{\text{T}'}$ and $\mathcal{R}_{\bar{n}}^{\text{TL}'}$ are defined by

$$\mathcal{R}_{\bar{n}}^{\text{T}'} \equiv |J(\mathbf{q}; +1)_{\bar{n}}|^2 - |J(\mathbf{q}; -1)_{\bar{n}}|^2, \quad (2.33a)$$

and

$$\mathcal{R}_{\bar{n}}^{\text{TL}'} \equiv -2\Re\{\rho^*(\mathbf{q})_{\bar{n}}(J(\mathbf{q}; +1)_{\bar{n}} + J(\mathbf{q}; -1)_{\bar{n}})\}. \quad (2.33b)$$

Then, the differential cross section is equal to

$$\left(\frac{d\sigma}{d\Omega_e}\right)_{\bar{n}}^h = \sigma_{\text{Mott}}f_{\text{rec}}^{-1}\{(v_{\text{L}}\mathcal{R}_{\bar{n}}^{\text{L}} + v_{\text{T}}\mathcal{R}_{\bar{n}}^{\text{T}} + v_{\text{TT}}\mathcal{R}_{\bar{n}}^{\text{TT}} + v_{\text{TL}}\mathcal{R}_{\bar{n}}^{\text{TL}}) + h(v_{\text{T}}\mathcal{R}_{\bar{n}}^{\text{T}'} + v_{\text{TL}}\mathcal{R}_{\bar{n}}^{\text{TL}'})\} \quad (2.34a)$$

$$\equiv \Sigma_{\bar{n}} + h\Delta_{\bar{n}}, \quad (2.34b)$$

and all of the nuclear structure physics is contained in the six nuclear response functions $\mathcal{R}_{\bar{n}}^{\text{K}}$. In the somewhat more general case in which the helicity of the incident beam is known *and* the final electron helicity h' is measured, we have that

$$\left(\frac{d\sigma}{d\Omega_e}\right)_{\bar{n}}^{hh'} = \frac{1}{2}(1 + hh')\Sigma_{\bar{n}} + \frac{1}{2}(h + h')\Delta_{\bar{n}}, \quad (2.35)$$

and so the cross section for an experiment in which only the final electron helicity is measured is the same as that for an experiment in which only the initial helicity is known, except that $h \mapsto h'$ and we have an additional factor of $\frac{1}{2}$ due to the required average over the initial helicities. Note that if $h' = -h$, then $1 + hh' = h + h' = 0$ and the cross section vanishes; thus, the electron helicity is conserved in the scattering process in the extreme relativistic limit for the electron.

We have seen that there are three independent components of the nuclear four-current, since one of the components can be eliminated using current conservation. Then, because $\mathcal{R}_{\bar{n}}$ is bilinear in these components, we expect there to be nine independent nuclear response functions. For longitudinal electron polarization, we have seen only six functions; the other three functions will be evident for the case of general electron spin [31], since their corresponding kinematic factors either require both initial and final electron polarization or are of order γ^{-1} relative to the

six kinematic factors defined previously. However, since we are considering only the case of a longitudinally polarized electron beam and the extreme relativistic limit in detail in this paper, we shall have no further use for these extra quantities. In fact, it turns out that these three response functions do not contain any new nuclear structure information beyond that obtainable with the six previously defined response functions. For the sake of completeness, the remaining three nuclear structure functions are given here in terms of the current components:

$$\mathcal{R}_{\bar{n}}^{\text{TT}} \equiv 2\mathfrak{F}\{J^*(\mathbf{q}; +1)_{\bar{n}} J(\mathbf{q}; -1)_{\bar{n}}\}, \quad (2.36a)$$

$$\mathcal{R}_{\bar{n}}^{\text{TL}} \equiv -2\mathfrak{F}\{\rho^*(\mathbf{q})_{\bar{n}}(J(\mathbf{q}; +1)_{\bar{n}} + J(\mathbf{q}; -1)_{\bar{n}})\}, \quad (2.36b)$$

and

$$\mathcal{R}_{\bar{n}}^{\text{TL}'} \equiv -2\mathfrak{F}\{\rho^*(\mathbf{q})_{\bar{n}}(J(\mathbf{q}; +1)_{\bar{n}} - J(\mathbf{q}; -1)_{\bar{n}})\}. \quad (2.36c)$$

What now remains to be done is to determine the functional dependence of the nuclear structure functions $\mathcal{R}_{\bar{n}}^{\text{K}}$ in terms of the usual nuclear electromagnetic multipole form factors. We define auxiliary (real) nuclear response functions as follows:

$$\mathcal{R}_{\bar{n}}^{m'm} \equiv J^*(\mathbf{q}; m')_{\bar{n}} J(\mathbf{q}; m)_{\bar{n}} + J(\mathbf{q}; m')_{\bar{n}} J^*(\mathbf{q}; m)_{\bar{n}} \quad (2.37a)$$

$$= \mathcal{R}_{\bar{n}}^{mm'}. \quad (2.37b)$$

Then, we can write

$$\mathcal{R}_{\bar{n}}^{\text{L}} = \frac{1}{2} \frac{q^2}{\omega^2} \mathcal{R}_{\bar{n}}^{00}, \quad (2.38a)$$

$$\mathcal{R}_{\bar{n}}^{\text{T}} = \frac{1}{2} (\mathcal{R}_{\bar{n}}^{11} + \mathcal{R}_{\bar{n}}^{-1, -1}), \quad (2.38b)$$

$$\mathcal{R}_{\bar{n}}^{\text{TT}} = \mathcal{R}_{\bar{n}}^{1, -1}, \quad (2.38c)$$

$$\mathcal{R}_{\bar{n}}^{\text{TL}} = -\frac{q}{\omega} (\mathcal{R}_{\bar{n}}^{01} - \mathcal{R}_{\bar{n}}^{0, -1}), \quad (2.38d)$$

$$\mathcal{R}_{\bar{n}}^{\text{T}'} = \frac{1}{2} (\mathcal{R}_{\bar{n}}^{11} - \mathcal{R}_{\bar{n}}^{-1, -1}), \quad (2.38e)$$

and

$$\mathcal{R}_{\bar{n}}^{\text{TL}'} = -\frac{q}{\omega} (\mathcal{R}_{\bar{n}}^{01} + \mathcal{R}_{\bar{n}}^{0, -1}). \quad (2.38f)$$

The current components $J(\mathbf{q}; m)_{\bar{n}}$ are given by $J(\mathbf{q}; m)_{\bar{n}} = \mathbf{e}(\mathbf{q}; 1, m) \cdot \mathbf{J}(\mathbf{q})_{\bar{n}}$, where we have that $\mathbf{J}(\mathbf{q})_{\bar{n}} = \int d^3\mathbf{x} e^{i\mathbf{q} \cdot \mathbf{x}} \langle f | \hat{\mathbf{J}}(\mathbf{x}) | i \rangle$; note that the caret in the term $\hat{\mathbf{J}}(\mathbf{x})$ denotes that we are dealing with a second-quantization operator acting in the nuclear Hilbert space. Hence, we must consider the expansions [34]

$$\mathbf{e}(\mathbf{q}; 1, m) e^{i\mathbf{q} \cdot \mathbf{x}} = \begin{cases} -i\sqrt{4\pi} \sum_{J \geq 0} [J] i^J \frac{1}{q} \nabla (M_J^0(q\mathbf{x})) & \text{if } m = 0 \\ -\sqrt{2\pi} \sum_{J \geq 1} [J] i^J \left\{ m M_{JJ}^m(q\mathbf{x}) + \frac{1}{q} \nabla \times \mathbf{M}_{JJ}^m(q\mathbf{x}) \right\} & \text{if } m = \pm 1, \end{cases} \quad (2.39)$$

where $[J] \equiv \sqrt{2J+1}$ and

$$M_J^m(q\mathbf{x}) \equiv j_J(qx) Y_J^m(\Omega_x), \quad (2.40a)$$

$$M_{JL}^m(q\mathbf{x}) \equiv j_L(qx) Y_{JL}^m(\Omega_x), \quad (2.40b)$$

and the vector spherical harmonics are given by

$$\mathbf{Y}_{JL}^m(\Omega_x) \equiv [Y_L(\Omega_x) \otimes \mathbf{e}(\mathbf{q}; 1)]_J^m. \quad (2.41)$$

We now define the transverse electric and magnetic multipole operators by [1, 25, 32],

$$\hat{T}_{Jm}^{\text{el}}(q) \equiv \int d^3\mathbf{x} \frac{1}{q} \{ \nabla \times \mathbf{M}_{JJ}^m(q\mathbf{x}) \} \cdot \hat{\mathbf{J}}(\mathbf{x}), \quad (2.42a)$$

$$\hat{T}_{Jm}^{\text{mag}}(q) \equiv \int d^3\mathbf{x} \mathbf{M}_{JJ}^m(q\mathbf{x}) \cdot \hat{\mathbf{J}}(\mathbf{x}), \quad (2.42b)$$

and the longitudinal multipole operator by

$$\hat{L}_{Jm}(q) \equiv \int d^3\mathbf{x} \frac{i}{q} (\nabla M_J^m(q\mathbf{x})) \cdot \hat{\mathbf{J}}(\mathbf{x}). \quad (2.43)$$

From current conservation, we have that $\nabla \cdot \hat{\mathbf{J}}(\mathbf{x}) = -\partial \hat{\rho}(\mathbf{x}) / \partial t = -i[\hat{H}, \hat{\rho}(\mathbf{x})]$. It then follows that

$$\nabla \cdot \mathbf{J}(\mathbf{x})_{\bar{n}} = -i \langle f | [\hat{H}, \hat{\rho}(\mathbf{x})] | i \rangle = -i\omega \rho(\mathbf{x})_{\bar{n}} \quad (2.44)$$

and so $\langle f | \hat{L}_{Jm}(q) | i \rangle = -(\omega/q) \langle f | \hat{M}_{Jm}(q) | i \rangle$, where the Coulomb multipole operator is defined by

$$\hat{M}_{Jm}(q) \equiv \int d^3\mathbf{x} M_J^m(q\mathbf{x}) \hat{\rho}(\mathbf{x}). \quad (2.45)$$

Thus,

$$J(\mathbf{q}; 0)_{\bar{n}} = \frac{\omega}{q} \sqrt{4\pi} \sum_{J \geq 0} [J] i^J \langle f | \hat{M}_{J0}(q) | i \rangle \quad (2.46)$$

and

$$J(\mathbf{q}; \pm 1)_{\bar{n}} = -\sqrt{2\pi} \sum_{J \geq 1} [J] i^J \{ \langle f | \hat{T}_{J, \pm 1}^{\text{el}}(q) | i \rangle \pm \langle f | \hat{T}_{J, \pm 1}^{\text{mag}}(q) | i \rangle \}, \quad (2.47)$$

and hence,

$$\mathcal{R}_{\bar{n}}^{m'm} = 8\pi \sum_{JJ'} [J'] [J] \Re \{ (-i)^{J'} i^J \langle f | \hat{T}_{J'm}(q) | i \rangle^* \langle f | \hat{T}_{Jm}(q) | i \rangle \}, \quad (2.48)$$

where

$$\hat{T}_{Jm} = \begin{cases} -(\omega/q)\hat{M}_{J0}(q) & \text{if } m = 0, \\ (1/\sqrt{2})(\hat{T}_{Jm}^{el}(q) + m\hat{T}_{Jm}^{mag}(q)) & \text{if } m = \pm 1. \end{cases} \quad (2.49)$$

Let us now focus on a transition $i \rightarrow f$ between discrete nuclear states with good angular momenta J_i and J_f , respectively, as well as parities π_i and π_f , respectively. Furthermore, let us also assume that the target nucleus is polarized, i.e., the target is prepared with its magnetic substates (labeled by M_{J_i}) populated in a nonuniform manner with probabilities $p_{(i)}(M_{J_i})$. The multipole operators $\hat{T}_{Jm}(q)$ apply to a system whose axis of quantization is the z axis defined by the three-momentum transfer \mathbf{q} ; however, the nuclear states themselves are quantized with respect to some as yet arbitrary quantization axis, which is taken to be specified by the spherical coordinates θ^* and ϕ^* with respect to \mathbf{q} (see Fig. 2). Thus, we must express the nucleus' quantum state vectors in terms of state vectors defined with respect to the z axis; explicitly, we have that

$$|J_i M_{J_i}^*\rangle = \sum_{M'_{J_i}} \mathcal{D}_{M'_{J_i} M_{J_i}}^{(J_i)}(\theta^*, \phi^*) |J_i M'_{J_i}\rangle, \quad (2.50)$$

where the eigenkets $|J_i M_{J_i}^*\rangle$ and $|J_i M'_{J_i}\rangle$ refer to the systems with axes of quantization along (θ^*, ϕ^*) and \mathbf{q} , respectively, and where $\mathcal{D}_{M'_{J_i} M_{J_i}}^{(J_i)}(\theta^*, \phi^*)$ is the rotation matrix corresponding to the transformation to the starred system. Then,

$$\begin{aligned} &\langle J_f M_{J_f}^* | \hat{T}_{Jm}(q) | J_i M_{J_i}^* \rangle \\ &= \sum_{M'_{J_i} M'_{J_f}} \langle J_f M'_{J_f} | \hat{T}_{Jm}(q) | J_i M'_{J_i} \rangle \mathcal{D}_{M'_{J_f} M_{J_f}}^{(J_f)*}(\theta^*, \phi^*) \mathcal{D}_{M'_{J_i} M_{J_i}}^{(J_i)}(\theta^*, \phi^*), \end{aligned} \quad (2.51)$$

where we have assumed for simplicity that the final nuclear polarization is measured with respect to the same axis of quantization as the target. While this assumption is not necessarily very useful as far as experiments are concerned, it will allow us to do the calculations for the two cases of interest (i.e., when either the initial or the final nuclear polarization, but not both, is known) simultaneously (for the general case, see Ref. [31]).

Then, we wish to evaluate the quantities

$$\overline{\mathcal{R}_{\text{fi}}^{m'm}} = (2J_f + 1) \sum_{M_{J_i} M_{J_f}} p_{(i)}(M_{J_i}) p_{(f)}(M_{J_f}) \mathcal{R}_{\text{fi}}^{m'm}, \quad (2.52)$$

where the factor $(2J_f + 1)$ takes into account the proper average over initial states—sum over final states required for the cross section. It turns out that it is convenient to express the nuclear polarizations in terms of the spherical Fano statistical tensors defined by (see, e.g., Ref. [26])

$$f_{J_i}^{(i)} \equiv \sum_{M_{J_i}} (-1)^{J_i - M_{J_i}} \langle J_i M_{J_i} J_i - M_{J_i} | I_i 0 \rangle p_{(i)}(M_{J_i}). \quad (2.53)$$

For the inverse we then have

$$p_{(i)}(M_{J_i}) = \sum_{I_i} (-1)^{J_i - M_{J_i}} [I_i] \begin{pmatrix} J_i & J_i & I_i \\ M_{J_i} & -M_{J_i} & 0 \end{pmatrix} f_{I_i}^{(i)}; \quad (2.54)$$

similar relationships are valid for the final state polarization. In particular, we have that $f_0^{(i)} = 1/\sqrt{2J_i + 1}$, regardless of the detailed population of the magnetic substates. In the case of an unpolarized target, $p_{(i)}(M_{J_i}) = 1/(2J_i + 1)$ and $f_{I_i}^{(i)} = f_0^{(i)} \delta_{I_i,0}$. Frequently, we will be interested in the situation for which $p_{(i)}(M_{J_i}) = \delta_{J_i, M_{J_i}}$, which we will refer to as 100% polarization, in which case the general formula reduces to

$$f_{I_i}^{(i)} = \frac{(2J_i)! \sqrt{2I_i + 1}}{\sqrt{(2J_i + I_i + 1)!(2J_i - I_i)!}}. \quad (2.55)$$

Furthermore, we note that if the nucleus is aligned (i.e., if $p_{(i)}(M_{J_i}) = p_{(i)}(-M_{J_i})$ for all M_{J_i}), then it can be shown that $f_{I_i}^{(i)} = 0$ for I_i odd.

We now wish to evaluate the real part of $(-i)^{J'} i^J \langle f | \hat{T}_{J'm'}(q) | i \rangle^* \langle f | \hat{T}_{Jm}(q) | i \rangle$. It can easily be shown that $(-i)^{J'} i^J = (-1)^{(J'-J)/2} P_{J'+J}^+ + i(-1)^{(J'-J+1)/2} P_{J'+J}^-$, with projections $P_n^\pm \equiv \frac{1}{2}(1 \pm (-1)^n)$, where n is an integer. Define the real quantities $A_{J'J}^{m'm}$ and $B_{J'J}^{m'm}$ by

$$A_{J'J}^{m'm} + iB_{J'J}^{m'm} \equiv \langle J_f \| \hat{T}_{J'(m')}(q) \| J_i \rangle^* \langle J_f \| \hat{T}_{J(m)}(q) \| J_i \rangle, \quad (2.56)$$

and let

$$\begin{pmatrix} J' & J & \mathcal{J} \\ m' & -m & M \end{pmatrix} Y_{\mathcal{J}}^M(\theta^*, \phi^*) \equiv ([\mathcal{J}]/\sqrt{4\pi}) \{ \mathcal{F}_{J'm':Jm}^{\mathcal{J}}(\theta^*, \phi^*) + i\mathcal{G}_{J'm':Jm}^{\mathcal{J}}(\theta^*, \phi^*) \}, \quad (2.57)$$

where $M = m - m'$, and the $\mathcal{F}_{J'm':Jm}^{\mathcal{J}}(\theta^*, \phi^*)$ and $\mathcal{G}_{J'm':Jm}^{\mathcal{J}}(\theta^*, \phi^*)$ are real functions. Then, $\overline{\mathcal{A}_{J'J}^{m'm}}$ will in general involve both of the functions $\mathcal{F}_{J'm':Jm}^{\mathcal{J}}(\theta^*, \phi^*)$ and $\mathcal{G}_{J'm':Jm}^{\mathcal{J}}(\theta^*, \phi^*)$.

However, the terms involving $\mathcal{G}_{J'm':Jm}^{\mathcal{J}}(\theta^*, \phi^*)$ can be eliminated by considering the parity properties of the multipole operators, since we are considering parity to be a good quantum number for the nuclear states under consideration. Define the electromagnetic matrix elements t_{CJ} (Coulomb), t_{EJ} (electric), and t_{MJ} (magnetic) as follows:

$$t_{CJ}(q) \equiv \langle J_f \| \hat{M}_J(q) \| J_i \rangle, \quad (2.58a)$$

$$t_{EJ}(q) \equiv \langle J_f \| \hat{T}_J^{\text{el}}(q) \| J_i \rangle, \quad (2.58b)$$

and

$$t_{MJ}(q) \equiv \langle J_f \| i\hat{T}_J^{\text{mag}}(q) \| J_i \rangle; \quad (2.58c)$$

it can be shown, as a result of parity conservation and time-reversal invariance, that

these may all be chosen to be real quantities [35]. Let $\pi \equiv \pi_i \pi_f$; then, the matrix elements t_{CJ} and t_{EJ} vanish unless $\pi = (-1)^J$, while the t_{MJ} vanish unless $\pi = (-1)^{J+1}$, if parity is conserved in the electron-nucleus interaction. Since we are ignoring the effects of the weak interaction in our treatment, the assumption of parity conservation applies, and it can then be shown that all of the terms of the form $t_{\sigma'J} t_{\sigma J}$ contained in the various $A_{JJ}^{m'm}$ have $\pi^2 = (-1)^{J+J} = +1$, i.e., there is an implied factor of P_{J+J}^+ . Similarly, the terms in $B_{JJ}^{m'm}$ have $\pi^2 = (-1)^{J'+J+1} = +1$, and so there is an implied factor of P_{J+J}^- . Then,

$$P_{J+J}^- A_{JJ}^{m'm} = P_{J+J}^- (P_{J+J}^+ A_{JJ}^{m'm}) = 0;$$

similar results hold true for $P_{J+J}^+ B_{JJ}^{m'm}$. Then, if we consider the explicit form for the $\mathcal{R}_{\bar{n}}^{m'm}$ in terms of the $A_{JJ}^{m'm}$ and $B_{JJ}^{m'm}$, it can be shown that the terms involving $\mathcal{G}_{Jm';Jm}^{\mathcal{J}}(\theta^*, \phi^*)$ vanish.

Thus, we have that

$$\begin{aligned} \overline{\mathcal{R}_{\bar{n}}^{m'm}} &= \frac{8\pi(-1)^m}{[J_i]^2} \sum_{\mathcal{J}} [\mathcal{J}] \sum_{J'J} [J'] \Phi_{\bar{n}}^{\mathcal{J}JJ} \mathcal{F}_{Jm';Jm}^{\mathcal{J}}(\theta^*, \phi^*) \\ &\times \{ (-1)^{(J'+J)/2} P_{J+J}^+ A_{JJ}^{m'm} + (-1)^{(J'+J+1)/2} P_{J+J}^- B_{JJ}^{m'm} \}, \end{aligned} \quad (2.59)$$

where

$$\begin{aligned} \mathcal{F}_{Jm';Jm}^{\mathcal{J}}(\theta^*, \phi^*) &= (-1)^M \sqrt{(\mathcal{J}-M)!/(\mathcal{J}+M)!} \begin{pmatrix} J' & J & \mathcal{J} \\ m' & -m & M \end{pmatrix} P_{\mathcal{J}}^M(\cos \theta^*) \cos M\phi^*, \end{aligned} \quad (2.60)$$

with $M = m - m'$. The term $\Phi_{\bar{n}}^{\mathcal{J}JJ}$ summarizes all of the nuclear polarization information; for the three special cases of interest, $\Phi_{\bar{n}}^{\mathcal{J}JJ}$ is given by

$$\Phi_{\bar{n}}^{\mathcal{J}JJ} = (-1)^{J_i+J_f} (-1)^{J'} [J_i]^2 [J] \begin{Bmatrix} J' & J & \mathcal{J} \\ J_i & J_i & J_f \end{Bmatrix} f_{\mathcal{J}}^{(i)}, \quad (2.61a)$$

$$\Phi_{\bar{n}}^{\mathcal{J}JJ} = (-1)^{J_i+J_f} (-1)^{J'+\mathcal{J}} [J_f]^2 [J] \begin{Bmatrix} J' & J & \mathcal{J} \\ J_f & J_f & J_i \end{Bmatrix} f_{\mathcal{J}}^{(f)}, \quad (2.61b)$$

and

$$\Phi_{\bar{n}}^{\mathcal{J}JJ} = \delta_{\mathcal{J}0} \delta_{J'J} \Delta(J_i J_f J), \quad (2.61c)$$

where the slash indicates that the corresponding nuclear polarization (initial and/or final) is undetermined. Explicitly, \bar{n} means that the initial polarization is known and the final nuclear polarization is not measured, while \bar{f} indicates that the nuclear target is unpolarized and the polarization of the recoiling nucleus is measured.

Then, \bar{f} refers to an experiment in which neither the initial nor the final nuclear polarizations are known.

It then follows from the properties of the $\mathcal{F}_{J,m';Jm}^{\mathcal{J}}(\theta^*, \phi^*)$ and the $A_{J'J}^{m'm}$ and $B_{J'J}^{m'm}$ that

$$\begin{aligned} \frac{1}{2} (\overline{\mathcal{R}_{\bar{f}}^{m'm}} \pm \overline{\mathcal{R}_{\bar{f}}^{-m',-m}}) &= \frac{8\pi(-1)^m}{[J_i]^2} \sum_{\mathcal{J}} [\mathcal{J}] \sum_{J'J} [J'] \Phi_{\bar{f}}^{\mathcal{J}J'} \mathcal{F}_{J,m';Jm}^{\mathcal{J}}(\theta^*, \phi^*) P_{\mathcal{J}+m'-m}^{\pm} \\ &\times \{ (-1)^{(J'+J)/2} P_{J'+J}^+ A_{J'J}^{m'm} + (-1)^{(J'+J+1)/2} P_{J'+J}^- B_{J'J}^{m'm} \}, \end{aligned} \quad (2.62)$$

for use in Eq. (2.38).

Making use of these results, we have that the nuclear response functions in the case of an experiment involving a polarized target for which the final polarization is undetected can be written as

$$\mathcal{R}_{\bar{f}}^L = 4\pi \sum_{\substack{\mathcal{J} \geq 0 \\ \text{even}}} P_{\mathcal{J}}(\cos \theta^*) f_{\mathcal{J}}^{(i)} \mathcal{W}_{\mathcal{J}}^L(q)_{\bar{f}}, \quad (2.63a)$$

$$\mathcal{R}_{\bar{f}}^T = 4\pi \sum_{\substack{\mathcal{J} \geq 0 \\ \text{even}}} P_{\mathcal{J}}(\cos \theta^*) f_{\mathcal{J}}^{(i)} \mathcal{W}_{\mathcal{J}}^T(q)_{\bar{f}}, \quad (2.63b)$$

$$\mathcal{R}_{\bar{f}}^{TT} = 4\pi \sum_{\substack{\mathcal{J} \geq 2 \\ \text{even}}} P_{\mathcal{J}}^2(\cos \theta^*) \cos 2\phi^* f_{\mathcal{J}}^{(i)} \mathcal{W}_{\mathcal{J}}^{TT}(q)_{\bar{f}}, \quad (2.63c)$$

$$\mathcal{R}_{\bar{f}}^{TL} = 4\pi \sum_{\substack{\mathcal{J} \geq 2 \\ \text{even}}} P_{\mathcal{J}}^1(\cos \theta^*) \cos \phi^* f_{\mathcal{J}}^{(i)} \mathcal{W}_{\mathcal{J}}^{TL}(q)_{\bar{f}}, \quad (2.63d)$$

$$\mathcal{R}_{\bar{f}}^{T'} = 4\pi \sum_{\substack{\mathcal{J} \geq 1 \\ \text{odd}}} P_{\mathcal{J}}(\cos \theta^*) f_{\mathcal{J}}^{(i)} \mathcal{W}_{\mathcal{J}}^{T'}(q)_{\bar{f}}, \quad (2.63e)$$

and

$$\mathcal{R}_{\bar{f}}^{TL'} = 4\pi \sum_{\substack{\mathcal{J} \geq 1 \\ \text{odd}}} P_{\mathcal{J}}^1(\cos \theta^*) \cos \phi^* f_{\mathcal{J}}^{(i)} \mathcal{W}_{\mathcal{J}}^{TL'}(q)_{\bar{f}}, \quad (2.63f)$$

where the nuclear information is contained in the various reduced response functions $\mathcal{W}_{\mathcal{J}}^K(q)_{\bar{f}}$ as follows:

$$\mathcal{W}_{\mathcal{J}}^L(q)_{\bar{f}} = (-1)^{J_i+J} [\mathcal{J}] \sum_{J'J \geq 0} (-1)^{(J'-J)/2} [J'] [J] \begin{pmatrix} J' & J & \mathcal{J} \\ 0 & 0 & 0 \end{pmatrix} \begin{Bmatrix} J' & J & \mathcal{J} \\ J_i & J_i & J_i \end{Bmatrix} t_{CJ} t_{CJ}, \quad (2.64a)$$

$$\begin{aligned} \mathcal{W}_{\mathcal{J}}^{\text{T}}(q)_{\bar{n}} = & -(-1)^{J_i+J_t}[\mathcal{J}] \sum_{J \geq 1} [J'] [J] \begin{pmatrix} J' & J & \mathcal{J} \\ 1 & -1 & 0 \end{pmatrix} \begin{Bmatrix} J' & J & \mathcal{J} \\ J_i & J_i & J_t \end{Bmatrix} \\ & \times [(-1)^{(J'-J)/2} P_{J'+J}^+(t_{EJ'} t_{EJ} + t_{MJ'} t_{MJ}) \\ & + (-1)^{(J'-J+1)/2} P_{J'+J}^-(t_{EJ'} t_{MJ} - t_{MJ'} t_{EJ})], \end{aligned} \quad (2.64b)$$

$$\begin{aligned} \mathcal{W}_{\mathcal{J}}^{\text{TT}}(q)_{\bar{n}} = & -(-1)^{J_i+J_t}([\mathcal{J}]/\sqrt{(\mathcal{J}-1)\mathcal{J}(\mathcal{J}+1)(\mathcal{J}+2)}) \\ & \times \sum_{J \geq 1} [J'] [J] \begin{pmatrix} J' & J & \mathcal{J} \\ 1 & 1 & -2 \end{pmatrix} \begin{Bmatrix} J' & J & \mathcal{J} \\ J_i & J_i & J_t \end{Bmatrix} \\ & \times [(-1)^{(J'-J)/2} P_{J'+J}^+(t_{EJ'} t_{EJ} - t_{MJ'} t_{MJ}) \\ & - (-1)^{(J'-J+1)/2} P_{J'+J}^-(t_{EJ'} t_{MJ} + t_{MJ'} t_{EJ})], \end{aligned} \quad (2.64c)$$

$$\begin{aligned} \mathcal{W}_{\mathcal{J}}^{\text{TL}}(q)_{\bar{n}} = & 2\sqrt{2}(-1)^{J_i+J_t}([\mathcal{J}]/\sqrt{\mathcal{J}(\mathcal{J}+1)}) \\ & \times \sum_{\substack{J' \geq 0 \\ J \geq 1}} [J'] [J] \begin{pmatrix} J' & J & \mathcal{J} \\ 0 & 1 & -1 \end{pmatrix} \begin{Bmatrix} J' & J & \mathcal{J} \\ J_i & J_i & J_t \end{Bmatrix} t_{CJ'} \\ & \times [(-1)^{(J'-J)/2} P_{J'+J}^+ t_{EJ} - (-1)^{(J'-J+1)/2} P_{J'+J}^- t_{MJ}], \end{aligned} \quad (2.64d)$$

$$\mathcal{W}_{\mathcal{J}}^{\text{T}'}(q)_{\bar{n}} = \mathcal{W}_{\mathcal{J}}^{\text{T}}(q)_{\bar{n}}, \quad (2.64e)$$

and

$$\mathcal{W}_{\mathcal{J}}^{\text{TL}'}(q)_{\bar{n}} = -\mathcal{W}_{\mathcal{J}}^{\text{TL}}(q)_{\bar{n}}, \quad (2.64f)$$

where the T and TL terms have \mathcal{J} even, while the T' and TL' terms have the same forms as for the T and TL terms, respectively, except that now \mathcal{J} is odd (see Appendix C for a tabulation of the numerical coefficients required for these reduced response functions for a variety of nuclear transitions). It should be noted that only the Fano tensors of even rank occur in the terms which contribute to $\Sigma_{\bar{n}}$, while only the odd-rank tensors contribute to $\Delta_{\bar{n}}$. Thus, it follows that, if the target is aligned (as defined previously), then $\Delta_{\bar{n}}$ vanishes, since it only involves the odd Fano tensors. This is a general statement which is valid for arbitrary values of J_i and J_t ; thus, an unaligned target will provide more information than will an aligned one, but only if the incident electron beam is polarized. For completeness, we have that the three nuclear response functions which involve a $1/\gamma$ suppression due to their corresponding kinematic factors are given by

$$\mathcal{R}_{\bar{n}}^{\text{TT}} = 4\pi \sum_{\substack{\mathcal{J} \geq 2 \\ \text{even}}} P_{\mathcal{J}}^2(\cos \theta^*) \sin 2\phi^* f_{\mathcal{J}}^{(i)} \mathcal{W}_{\mathcal{J}}^{\text{TT}}(q)_{\bar{n}}, \quad (2.65a)$$

$$\mathcal{R}_f^{\text{TL}} = -4\pi \sum_{\substack{\mathcal{J} \geq 2 \\ \text{even}}} P_{\mathcal{J}}^1(\cos \theta^*) \sin \phi^* f_{\mathcal{J}}^{(i)} \mathcal{W}_{\mathcal{J}}^{\text{TL}}(q)_f, \quad (2.65b)$$

$$\mathcal{R}_f^{\text{TL}'} = -4\pi \sum_{\substack{\mathcal{J} \geq 1 \\ \text{odd}}} P_{\mathcal{J}}^1(\cos \theta^*) \sin \phi^* f_{\mathcal{J}}^{(i)} \mathcal{W}_{\mathcal{J}}^{\text{TL}'}(q)_f; \quad (2.65c)$$

again, we note that no new nuclear structure information is accessible from a measurement of these quantities (i.e., the same reduced response functions are already present in Eq. (2.63)).

Then, Eqs. (2.23), (2.24), (2.25), (2.34), (2.53), (2.63), and (2.64) contain all of the formalism required for electron scattering from polarized nuclei. These results are equivalent to those obtained by Weigert and Rose [5] in the extreme relativistic limit for the electron, except that they do not include the effects of nuclear recoil as contained in f_{rec} and their Eq. (4.16c) has a typographical error; the vector-coupling coefficient in their definition of the function $F_v^{(01)}(LL'J_fJ_i)$ should be $C(LL'v; 0, 1)$, as is evident from their notation.

Similar results hold true for the case in which the target is unpolarized but the final nuclear polarization is measured. It can be seen from the expressions for $\Phi_f^{\mathcal{J}J'J}$ and from the formulas for the $\mathcal{W}_{\mathcal{J}}^{\text{K}}(q)_f$ that there exist simple relationships between the reduced response functions $\mathcal{W}_{\mathcal{J}}^{\text{K}}(q)_f$ and $\mathcal{W}_{\mathcal{J}}^{\text{K}}(q)_{\bar{f}}$:

$$\mathcal{W}_{\mathcal{J}}^{\text{K}}(q)_{\bar{f}} = \pm \left(\frac{2J_f + 1}{2J_i + 1} \right) \mathcal{W}_{\mathcal{J}}^{\text{K}}(q)_f, \quad (2.66)$$

where the plus sign occurs for $\text{K} = \text{L}, \text{T}, \text{TT},$ and TL' and the minus sign occurs for $\text{K} = \text{TL}$ and T' . Note that the interchange of the initial and final states implied by this "turn-around" relation has also been performed in the multipole matrix elements $t_{CJ}, t_{EJ},$ and t_{MJ} ; it follows from the properties of these matrix elements that

$$\langle i \| \hat{T}_{\sigma J}(q) \| f \rangle = (-1)^{J_f - J_i} (-1)^{J + \eta} \langle f \| \hat{T}_{\sigma J}(q) \| i \rangle, \quad (2.67)$$

where $\eta = 0$ for the Coulomb operator and $\eta = 1$ for the transverse multipole operators [25, 33]. Also, we must of course replace the $f_{\mathcal{J}}^{(i)}$ with the $f_{\mathcal{J}}^{(f)}$ in the expressions for the $\mathcal{R}_{\bar{f}}^{\text{K}}$.

The reduced response functions can now be seen to contain all of the nuclear structure information in the form of bilinear products of the various Coulomb, electric, and magnetic multipole matrix elements for the nuclear transition $i \rightarrow f$. In particular, $\mathcal{W}_{\mathcal{J}}^{\text{L}}$ contains only Coulomb matrix elements, in general with interferences between different multipolarities CJ/CJ' . Similarly, $\mathcal{W}_{\mathcal{J}}^{\text{T}}, \mathcal{W}_{\mathcal{J}}^{\text{TT}},$ and $\mathcal{W}_{\mathcal{J}}^{\text{T}'}$ contain only transverse multipoles which interfere as $EJ/EJ', MJ/MJ',$ and EJ/MJ' in general. Finally, $\mathcal{W}_{\mathcal{J}}^{\text{TL}}$ and $\mathcal{W}_{\mathcal{J}}^{\text{TL}'}$ have only Coulomb-transverse interferences of the general form CJ/EJ' and CJ/MJ' . Furthermore, only those values of \mathcal{J} satisfying the constraint $0 \leq \mathcal{J} \leq 2J_{\text{pol}}$ are allowed, where J_{pol} is equal to either J_i or J_f ,

depending on whether the initial or the final nuclear polarization is known, respectively. In all cases, the interfering multipoles must satisfy $|J' - J| \leq \mathcal{J} \leq J' + J$.

The rank-zero ($\mathcal{J} = 0$) reduced response functions are especially simple (see Eq. (2.64)):

$$\mathcal{W}_0^L(q)_n = \sqrt{2J_i + 1} F_L^2(q)^n = (1/\sqrt{2J_i + 1}) \sum_{J \geq 0} t_{C,J}^2(q), \quad (2.68a)$$

and

$$\mathcal{W}_0^T(q)_n = \sqrt{2J_i + 1} F_T^2(q)^n = (1/\sqrt{2J_i + 1}) \sum_{J \geq 1} (t_{E,J}^2(q) + t_{M,J}^2(q)), \quad (2.68b)$$

where $F_L^2(q)^n$ and $F_T^2(q)^n$ are the usual longitudinal and transverse form factors, respectively. These are the quantities which enter in the familiar unpolarized cross section,

$$\Sigma_0^n \equiv 4\pi\sigma_{\text{Mott}} f_{\text{rec}}^{-1} F^2(q, \theta_e)^n, \quad (2.69)$$

where the (unpolarized) form factor is given by

$$F^2(q, \theta_e)^n = f_0^{(i)}(v_L \mathcal{W}_0^L(q)_n + v_T \mathcal{W}_0^T(q)_n) \quad (2.70a)$$

$$= v_L F_L^2(q)^n + v_T F_T^2(q)^n. \quad (2.70b)$$

It is useful to rewrite the expressions for Σ_n and Δ_n separating out the above $\mathcal{J} = 0$ (unpolarized) contribution so as to display the complete (θ^*, ϕ^*) dependence of the cross sections and to separate this dependence from their (q, θ_e) behavior. Explicitly, we then have that

$$\Sigma_n \equiv \Sigma_0^n \left[1 + \sum_{\substack{\mathcal{J} \geq 2 \\ \text{even}}} (P_{\mathcal{J}}(\cos \theta^*) R_{\mathcal{J}}^0(q, \theta_e)_n + P_{\mathcal{J}}^1(\cos \theta^*) \cos \phi^* R_{\mathcal{J}}^1(q, \theta_e)_n + P_{\mathcal{J}}^2(\cos \theta^*) \cos 2\phi^* R_{\mathcal{J}}^2(q, \theta_e)_n) \right], \quad (2.71)$$

and

$$\Delta_n \equiv \Sigma_0^n \left[\sum_{\substack{\mathcal{J} \geq 1 \\ \text{odd}}} (P_{\mathcal{J}}(\cos \theta^*) R_{\mathcal{J}}^0(q, \theta_e)_n + P_{\mathcal{J}}^1(\cos \theta^*) \cos \phi^* R_{\mathcal{J}}^1(q, \theta_e)_n) \right]. \quad (2.72)$$

The quantities $R_{\mathcal{J}}^{\mu}(q, \theta_e)_n$, which are related to the usual vector and tensor polarizations, are then given by

$$\mathcal{J} = \text{even: } R_{\mathcal{J}}^0(q, \theta_e)_n = f_{\mathcal{J}}^{(i)}(v_L \mathcal{W}_{\mathcal{J}}^L(q)_n + v_T \mathcal{W}_{\mathcal{J}}^T(q)_n) / F^2(q, \theta_e)^n, \quad (2.73a)$$

$$R_{\mathcal{J}}^1(q, \theta_e)_n = f_{\mathcal{J}}^{(i)} v_{TL} \mathcal{W}_{\mathcal{J}}^{TL}(q)_n / F^2(q, \theta_e)^n, \quad (2.73b)$$

$$R_{\mathcal{J}}^2(q, \theta_e)_n = f_{\mathcal{J}}^{(i)} v_{TT} \mathcal{W}_{\mathcal{J}}^{TT}(q)_n / F^2(q, \theta_e)^n, \quad (2.73c)$$

$$\mathcal{J} = \text{odd: } R_{\mathcal{J}}^0(q, \theta_e)_{fi} = f_{\mathcal{J}}^{(i)} v_{T'} \mathcal{W}_{\mathcal{J}}^{T'}(q)_{fi} / F^2(q, \theta_e)_{fi}, \quad (2.73d)$$

$$R_{\mathcal{J}}^1(q, \theta_e)_{fi} = f_{\mathcal{J}}^{(i)} v_{TL'} \mathcal{W}_{\mathcal{J}}^{TL'}(q)_{fi} / F^2(q, \theta_e)_{fi}, \quad (2.73e)$$

where the above $\mathcal{J} = 0$ results imply that $R_{\mathcal{J}}^0(q, \theta_e)_{fi} = 1$. Furthermore, we can remove all of the dependence on the Fano tensors by defining the polarization tensors

$$S_{\mathcal{J}}^{\mathcal{M}}(q, \theta_e)_{fi} = f_0^{(i)} R_{\mathcal{J}}^{\mathcal{M}}(q, \theta_e)_{fi} / f_{\mathcal{J}}^{(i)}, \quad (2.74)$$

where $S_0^0(q, \theta_e)_{fi} = 1$; finally, we have that the relationship between the $S_{\mathcal{J}}^{\mathcal{M}}(q, \theta_e)_{fi}$ and the familiar tensor polarizations $t_{\mathcal{J}\mathcal{M}}$ is

$$(t_{\mathcal{J}\mathcal{M}})_{fi} = (-1)^{\mathcal{M}} \left(\frac{1 + \delta_{\mathcal{M}0}}{2} \right) \sqrt{(\mathcal{J} + \mathcal{M})! / (\mathcal{J} - \mathcal{M})!} S_{\mathcal{J}}^{\mathcal{M}}(q, \theta_e)_{fi}, \quad (2.75)$$

where

$$\left(\frac{d\sigma}{d\Omega_e} \right)_{fi} = \Sigma_0 \sum_{\mathcal{J}\mathcal{M}} (t_{\mathcal{J}\mathcal{M}})_{fi} T_{\mathcal{J}\mathcal{M}}^*,$$

and the analyzing powers $T_{\mathcal{J}\mathcal{M}}$ for the scattering process satisfy $T_{\mathcal{J}\mathcal{M}}^* = (-1)^{\mathcal{J} - \mathcal{M}} T_{\mathcal{J}, -\mathcal{M}}$ [36]. To determine the analogous polarization tensors for the case that the final nuclear polarization is known (instead of the initial polarization), we must make use of the "turn-around" relation (2.66); then, it follows that the $R_{\mathcal{J}}^{\mathcal{M}}$, $S_{\mathcal{J}}^{\mathcal{M}}$, and $t_{\mathcal{J}\mathcal{M}}$ all transform like $(Z_{\mathcal{J}}^{\mathcal{M}})_{if} = (-1)^{\mathcal{J} - \mathcal{M}} (Z_{\mathcal{J}}^{\mathcal{M}})_{fi}$.

The basic quantities of interest are the $\mathcal{W}_{\mathcal{J}}^{\mathcal{K}}(q)_{fi}$, since they contain all of the nuclear structure information involved in the electromagnetic transition $i \rightarrow f$. The complete set of reduced response functions may in principle be determined experimentally, for example, by performing the following steps:

(1) By controlling the helicity of the incident electron beam, Σ_{fi} may be separated from Δ_{fi} (see Eq. (2.13)).

(2) For each of these contributions, controlling the polarization angles (θ^*, ϕ^*) then allows the various polarization tensors ($R_{\mathcal{J}}^{\mathcal{M}}$ in Eqs. (2.71), (2.72), and (2.73), $S_{\mathcal{J}}^{\mathcal{M}}$ in Eq. (2.74) or $t_{\mathcal{J}\mathcal{M}}$ in Eq. (2.75), depending on one's preference) to be separately determined.

(3) Knowing the quantities $R_{\mathcal{J}}^{\mathcal{M}}$, and using the standard Rosenbluth separation techniques to decompose $R_{\mathcal{J}=\text{even}}^0$ into L and T contributions, all of the reduced response functions $\mathcal{W}_{\mathcal{J}}^{\mathcal{K}}$ may be extracted.

It can be seen that the number of possible reduced response functions which are present is given by $6J_{\text{pol}} + \lambda$, where $\lambda = 1$ or 2 for half-integral or integral values of J_{pol} , respectively, where J_{pol} is as specified previously. However, if the incident electron beam is not polarized, i.e., if Δ_{fi} is not measured, then this number is reduced

to $4J_{\text{pol}} + 2(\lambda - 1)$; in both cases, one must remember that the various $\mathcal{W}_{\mathcal{J}}^{\text{K}}(q)_{\text{fi}}$ need not be independent.

Several special cases deserve a bit more attention. First, for $J_i = 0$ or $\frac{1}{2}$, we have that $\Sigma_{\text{fi}} = \Sigma_0^{\text{fi}}$; this is just the usual unpolarized (e, e') cross section. Thus, new information in Σ_{fi} is obtained only for those nuclei with $J_i \geq 1$. Second, for $J_i = 0$ we have that $\Delta_{\text{fi}} = 0$, whereas for $J_i = \frac{1}{2}$ we obtain

$$\Delta_{\text{fi}} = \Sigma_0^{\text{fi}}(\cos \theta^* R_1^0(q, \theta_c)_{\text{fi}} + \sin \theta^* \cos \phi^* R_1^1(q, \theta_c)_{\text{fi}}), \quad (2.76)$$

which contains new nuclear information (i.e., beyond the usual unpolarized result).

Let us now conclude this section by considering the special case of elastic scattering (see also Ref. [37]). Then, the preceding equations for the reduced response functions $\mathcal{W}_{\mathcal{J}}^{\text{K}}(q)_{\text{fi}}$ simplify to closed-form expressions. If time-reversal-invariance is assumed, along with parity, it then follows that the electric multipoles are all identically zero, and only the even Coulomb and odd magnetic multipoles occur [25, 33, 37]. If we define the elastic form factors by

$$F_J(q) = \begin{cases} 1/[J_0] \langle J_0 \| \hat{M}_J(q) \| J_0 \rangle, & \text{if } J = \text{even}, \\ 1/[J_0] \langle J_0 \| i\hat{T}_J^{\text{mag}}(q) \| J_0 \rangle, & \text{if } J = \text{odd}, \end{cases} \quad (2.77)$$

then we can write

$$\mathcal{W}_{\mathcal{J}}^{\text{K}}(q)_{\text{fi}} = \sum_{J,J'} A_{J,J',\mathcal{J}}^{\text{K}}(J_0) F_J(q) F_{J'}(q). \quad (2.78)$$

The coefficients $A_{J,J',\mathcal{J}}^{\text{K}}(J_0)$ are given by

$$A_{J,J',\mathcal{J}}^{\text{K}}(J_0) = \begin{cases} \alpha_{J,J',\mathcal{J}}(J_0) & \text{if } \text{K} = \text{L}, \quad J', J = \text{even} \\ \beta_{J,J',\mathcal{J}}^0 X_{J,J',\mathcal{J}}(J_0) & \text{if } \text{K} = \text{T or T}', \quad J', J = \text{odd} \\ (2\sqrt{2}/\sqrt{\mathcal{J}(\mathcal{J}+1)}) \beta_{J,J',\mathcal{J}}^1 X_{J,J',\mathcal{J}}(J_0) & \text{if } \text{K} = \text{TL or TL}', \quad J' = \text{even}, J = \text{odd} \\ (1/\sqrt{(\mathcal{J}-1)\mathcal{J}(\mathcal{J}+1)(\mathcal{J}+2)}) \beta_{J,J',\mathcal{J}}^2 X_{J,J',\mathcal{J}}(J_0) & \text{if } \text{K} = \text{TT}, \quad J', J = \text{odd}, \end{cases} \quad (2.79)$$

where

$$X_{J,J',\mathcal{J}}(J_0) \equiv (-1)^{2J_0} [J_0]^2 [J'] [J] [\mathcal{J}] \begin{Bmatrix} J' & J & \mathcal{J} \\ J_0 & J_0 & J_0 \end{Bmatrix}, \quad (2.80a)$$

$$\alpha_{J,J',\mathcal{J}} \equiv (-1)^{(J'+J)/2} \begin{pmatrix} J & J' & \mathcal{J} \\ 0 & 0 & 0 \end{pmatrix}, \quad (2.80b)$$

and

$$\beta_{J,J',\mathcal{J}}^M \equiv (-1)^{(J'+J-M)/2} \begin{pmatrix} J & J' & \mathcal{J} \\ 1 & M-1 & -M \end{pmatrix}. \quad (2.80c)$$

Note that $X_{J'J\mathcal{J}}(J_0)$ is totally symmetric with respect to the interchange of any two of the indices J' , J , and \mathcal{J} . The coefficients $A_{J'J\mathcal{J}}^K(J_0)$ for $J_0 \leq 2$ are tabulated in Appendix C along with the more general results required for inelastic scattering. In particular, it can be shown that

$$\mathcal{W}_1^T(q)_f = -\frac{1}{2}\sqrt{3/J_0(J_0+1)} \mathcal{W}_0^T(q)_f \quad (2.81)$$

for *elastic* scattering.

We now turn in the following section to detailed discussions of specific $J_i^{n_i} \mapsto J_f^{n_f}$ transitions, where particular nuclei are chosen to illustrate the general formalism summarized in the present section.

3. DISCUSSION AND SPECIFIC EXAMPLES

Let us now turn from the preceding general discussion and consider electron scattering from some illustrative nuclei. These nuclei will involve values of J_i in the range from 1/2 to 9/2, and will be discussed in ascending order with respect to their spins. In each case, we will first consider elastic scattering after which we will discuss inelastic scattering to low-lying discrete excited states with selected values of J_f and $\Delta\pi$. For the most part, we emphasize low- Z nuclei where the plane-wave Born approximation (PWBA) is reasonable; as will be discussed when we encounter $Z = 27$ (^{59}Co), for high- Z nuclei the distorted-wave Born approximation (DWBA) should be used (especially for elastic scattering), and this goes beyond the context of the present work.

As part of our discussion of these representative nuclei, we will examine the behaviour of several quantities of interest. The first of these quantities consists of the various asymmetries of the form

$$A_{ij} = (\Sigma_i - \Sigma_j) / \Sigma_0, \quad (3.1)$$

where i and j here refer to a given choice of the target polarization direction as specified by the angles (θ^*, ϕ^*) , corresponding to the directions L (along the direction of the electron beam), N (normal to the scattering plane), and S (sideways), and where Σ_0 is the unpolarized cross section; also, we will restrict ourselves to targets which are 100% polarized in the given direction. The three particular directions which we will be considering are shown in Fig. 2; as can be seen, they are defined relative to the incident electron beam (i.e., they are fixed in the lab system), and so θ^* and ϕ^* vary as the momentum transfer \mathbf{q} changes. Explicitly, the angles corresponding to the three directions are given by

$$\text{L: } \cos \theta^* = (\varepsilon - \varepsilon' \cos \theta_c) / q, \quad (3.2a)$$

$$\phi^* = 0; \quad (3.2b)$$

$$\text{N: } \cos \theta^* = 0, \quad (3.2c)$$

$$\phi^* = \pi/2; \quad (3.2d)$$

$$\text{S: } \cos \theta^* = -\frac{\varepsilon'}{q} \cos \theta_e, \quad (3.2e)$$

$$\phi^* = 0. \quad (3.2f)$$

Note that, for $J_{\text{pol}} \leq \frac{3}{2}$, it can be shown that $\Sigma_0 = (\Sigma_L + \Sigma_S + \Sigma_N)/3$. Because the asymmetries are defined with a factor of Σ_0 in the denominator, rather than $\Sigma_i + \Sigma_j$, the resulting asymmetries need not have magnitudes of less than 100%; the advantage of this definition is that all of the polarization dependence is contained in the numerator, and not in the denominator as well, thereby making it easier to interpret the effects of polarization on the A_{ij} . Other quantities which are of interest are the (electron) polarization ratios $(\Delta/\Sigma)_i$ for the L and S directions mentioned previously; because of the behaviour of the associated Legendre polynomials $P_{\mathcal{J}}^{\mathcal{M}}(\cos \theta^*)$ for \mathcal{J} odd and $\theta^* = \pi/2$, we have that $(\Delta/\Sigma)_N$ is identically zero.

Since we will be displaying the momentum dependence of the asymmetries and polarization ratios for a large variety of nuclei and nuclear transitions, it will be useful to have a standard method for differentiating between the various curves which will be shown on the same graph. The asymmetries A_{ij} will be indicated by solid, dashed, and dotted lines as follows:

$$A_{\text{NS}}: \text{ —}, \quad (3.3a)$$

$$A_{\text{LN}}: \text{ ---}, \quad (3.3b)$$

$$A_{\text{LS}}: \text{ \cdots}, \quad (3.3c)$$

where $A_{\text{LN}} + A_{\text{NS}} = A_{\text{LS}}$; the polarization ratios will be denoted by solid and dashed lines:

$$(\Delta/\Sigma)_L: \text{ —}, \quad (3.4a)$$

$$(\Delta/\Sigma)_S: \text{ ---}; \quad (3.4b)$$

as stated previously, $(\Delta/\Sigma)_N \equiv 0$.

Throughout most of this section, we consider a variety of complex nuclei (i.e., with $A > 4$), and so we have to make some choices concerning the assumed nuclear model to illustrate the qualitative behaviour of the polarization asymmetries and ratios. Our descriptions of the various selected nuclei involve the extreme-single-particle model, the shell model in some restricted model-space, or deformed Nilsson models, and we will occasionally compare the results obtained with these different models for the same nuclear transition; note, however, that the formulas for the $R_{\mathcal{J}}^{\mathcal{M}}$ are completely general, and do not depend on the choice of the model. In addition, we will include the effects of core polarization and meson-exchange currents in our

calculations for some nuclei in order to illustrate the sensitivity of the various polarization quantities to differences in the details of the underlying nuclear structure. For our present purposes, we are really only interested in the qualitative aspects of nuclear and electron polarizations, since we lack any experimental data, and so we will use harmonic oscillator wavefunctions to describe the single-particle states of complex nuclei [37, 38]; however, this simplification is not necessary as far as the formalism is concerned, and other single-particle wavefunctions (such as a Hartree-Fock basis or perhaps from a Woods-Saxon well, for example) can be used if desired [39].

(i) *Elastic Scattering*: $J_i = J_f = \frac{1}{2}$

In this case, only the C0 and M1 multipole form factors are possible:

$$F_L(q) \equiv (1/\sqrt{2}) \langle \frac{1}{2} \| \hat{M}_0(q) \| \frac{1}{2} \rangle, \quad \text{C0} \quad (3.5a)$$

and

$$F_T(q) \equiv (1/\sqrt{2}) \langle \frac{1}{2} \| i\hat{T}_1^{\text{mag}}(q) \| \frac{1}{2} \rangle, \quad \text{M1} \quad (3.5b)$$

where we are using the standard notation for the longitudinal and transverse form factors, respectively. Then, we have that $\Sigma_f = \Sigma_0^f$, as stated in Section 2, where the unpolarized cross section is

$$\Sigma_0^f = 4\pi\sigma_{\text{Mott}} f_{\text{rec}}^{-1} F^2(q, \theta_e)^f, \quad (3.6a)$$

with

$$F^2(q, \theta_e)^f = v_L F_L^2(q)^f + v_T F_T^2(q)^f, \quad (3.6b)$$

and, using Table C6 in Appendix C,

$$\Delta_f = -\Sigma_0^f f_1^{(i)} \{ \sqrt{2} F_T^2(q) \cos \theta^* v_T + 2 \sqrt{2} F_L(q) F_T(q) \sin \theta^* \cos \phi^* v_{TL} \} / F^2(q, \theta_e)^f. \quad (3.7)$$

Note that, for a completely polarized nucleus with $p_{(i)}(1/2) = 1$ and $p_{(i)}(-1/2) = 0$, the rank-1 Fano tensor $f_1^{(i)} = 1/\sqrt{2}$.

With a polarized target but without any electron polarization, one does not learn anything beyond the usual unpolarized (e, e') cross section. In cases where the magnitudes of the two form factors are very disparate, it is difficult to separate the smaller form factor from the larger one using the usual Rosenbluth separation method of keeping q and ω fixed while varying θ_e (i.e., fixing v_L and varying v_T), because the form factors occur as their squares. However, if one has both a polarized target *and* a polarized electron beam, then one may determine Δ_f which involves the interference term $F_L(q) F_T(q)$ and hence is a much more sensitive probe of the smaller form factor. Furthermore, in such a complete polarization

experiment, it is possible to determine the relative sign between the two form factors, something which is not possible for the simple Rosenbluth analysis.

The fundamental example of a nucleus exhibiting this behaviour is provided by the nucleon itself, for which the transverse form factor dominates over the longitudinal one at high momentum transfer [14, 40]. The electric (actually, charge) and magnetic form factors, $G_E(q)$ and $G_M(q)$, respectively, used by these authors are related to the $F_L(q)$ and $F_T(q)$ defined above by

$$\sqrt{4\pi}F_L = (1 + \tau) G_E, \quad (3.8a)$$

and

$$\sqrt{4\pi}F_T = -\sqrt{2\tau(1 + \tau)} G_M, \quad (3.8b)$$

where the quantity $\tau = -Q^2/4M^2$ was defined in Section 2. It should be noted that our analysis of the electron-nucleus scattering process involved only the contribution of the leading-order term in the relativistic expansion for the nuclear current, and we assume that the frames of reference for the initial and final nuclear states are the same; neither of these assumptions is rigorously applicable for the nucleon or other low- A nuclei, although corrections to our simpler analysis occur only at order τ^2 .

For the case of a polarized nucleon target, the usual vector polarizations p_x and p_z are related to the t_{jM} and R_j^M defined in Section 2 as follows:

$$p_x = -\sqrt{2}t_{11} = (1/\sqrt{2})R_1^1/f_1 \quad (3.9a)$$

and

$$p_z = t_{10} = (1/\sqrt{2})R_1^0/f_1, \quad (3.9b)$$

where we have that $R_1^0(q)_f = -v_T F_T^2/F^2$ and $R_1^1(q)_f = -2v_{TL} F_L F_T/F^2$, assuming 100% polarization. The fact that p_y is identically zero is due to the use of the one-photon-exchange approximation in evaluating the cross section. If we now consider the case of a recoil polarization experiment, we have the substitutions $R_1^0(q)_f \mapsto -R_1^0(q)_i$ and $R_1^1(q)_f \mapsto R_1^1(q)_i$ which follow from the "turn-around" relation discussed previously (see Eq. (2.66)); for elastic scattering, the initial and final nuclear states are the same ($i = f$). Thus, F_T can be determined up to a sign by measuring p_z , while p_x is directly proportional to $F_L F_T$ and so can be used to determine F_L and its sign relative to F_T ; as noted above, in the absence of electron polarization, the usual Rosenbluth separation will not allow the determination of this relative sign.

For the proton, G_{Ep} dominates over G_{Mp} at low momentum transfer; on the other hand, for $-Q^2$ exceeding 1 (GeV/c)², G_{Mp} dominates the cross section, and we lack any information concerning the longitudinal (charge) form factor G_{Ep} beyond 4 (GeV/c)² [41-45], whereas G_{Mp} has been measured out to

$-Q^2 = 22 (\text{GeV}/c)^2$ [41–46]. Likewise, for the case of the neutron, the magnetic form factor is best known, and has been determined using a Rosenbluth decomposition of the quasi-free scattering of electrons from the deuteron for $-Q^2$ below $10 (\text{GeV}/c)^2$ [45, 47, 48]. However, G_{En} is very small and so is in general very poorly known; it is usually determined from elastic and quasi-elastic electron-deuteron scattering, and what knowledge we have extends out to $-Q^2 \approx 10 (\text{GeV}/c)^2$ [45, 47, 48]. The electric form factor is directly related to the charge distribution of the neutral neutron, and clearly is one of the fundamental pieces of information involved in our understanding of the structure of the nucleon (and hence of complex nuclei to some degree as well). Again, the disparity in magnitude between the electric and magnetic form factors for the proton and neutron make polarized-nucleon experiments useful if one wishes to measure more precisely G_{En} (and to a lesser extent G_{Ep}) [49, 50].

Similar considerations are valid for ${}^3\text{H}$ [51, 52, 53] and ${}^3\text{He}$ [54, 55], which are also spin- $\frac{1}{2}$ nuclei for which the above formulas apply. Again, our understanding of the nuclear structure inherent in the three-nucleon systems will be greatly enhanced by a determination of F_L and F_T over an extended range of the momentum transfer. If we restrict ourselves to descriptions of these nuclei which involve only nucleonic degrees of freedom, then the three-body system is special in that it can be calculated exactly given a specific choice of the nucleon–nucleon interaction, thereby allowing quantitative tests of the validity of the various models of the strong force. ${}^3\text{H}$ and ${}^3\text{He}$ are almost-stable mirror nuclei, and so a comparison of the (e, e') results for these nuclei will allow the separation of the scattering process into its isoscalar and isovector pieces; then, for example, it may be possible to separate the effect of the isovector meson-exchange currents from the less well understood isoscalar meson-exchange effects. At present, a number of experiments (without polarization) have been performed for ${}^3\text{He}$, over an extended range of the momentum transfer [54, 55]; furthermore, data for tritium at the higher momentum transfers will also soon become available [53]. While these unpolarized measurements will go a long way in defining the electromagnetic structure of the $A = 3$ ground states, there may in future experiments be advantages in also determining the interference $F_L F_T$ using polarized electrons and targets as discussed above for the nucleon.

To conclude our discussion of elastic scattering from polarized spin- $\frac{1}{2}$ nuclei, let us turn to one illustrative example of a complex nucleus; namely, let us consider the case of elastic scattering from ${}^{13}\text{C}$, where we use Cohen and Kurath wavefunctions [56], with an harmonic oscillator basis having $b = 1.59$ fm. As a result of discussions of the luminosities and techniques available with targets internal to a stretcher ring, it is estimated that a reasonable lower bound for the cross section for which experiments are feasible is about $10^{-33} \text{ cm}^2/\text{sr}$ (i.e., for a luminosity of $10^{33} \text{ cm}^{-2} \text{ sec}^{-1}$) [22]. For the ${}^{13}\text{C}$ case, this limiting value is reached for a momentum transfer of about 500 MeV/c at an electron energy of 500 MeV; as the energy is increased, the limit is attained at a steadily increasing value of the momentum transfer. It should be noted that, for a given target mass and excitation energy, there exists a relationship between the momentum transfer q and the scattering

angle θ_e , at a fixed electron energy. Typical curves showing θ_e as a function of q for a variety of electron energies are displayed in Fig. 3; while these curves actually correspond to elastic scattering from a nucleus with a mass of $6535 \text{ MeV}/c^2$ (${}^7\text{Li}$, in fact), they are approximately valid for all of the other complex nuclei being considered, including ${}^{13}\text{C}$, since the target masses are all much greater than the electron energies under consideration.

The coherent Coulomb monopole form factor dominates out to about $300 \text{ MeV}/c$, beyond which the magnetic dipole form factor becomes comparable in magnitude. As can be seen from Fig. 4, the zero in the Coulomb form factor at $q \approx 365 \text{ MeV}/c$ results in the variation observed in the values of the polarization ratios at this momentum transfer; $(\Delta/\Sigma)_S$ reaches its maximum of 75% at this value of q , while $(\Delta/\Sigma)_L$ passes through a zero as it goes from its maximum of 25% to its minimum of -60% . Thus, the use of a polarized ${}^{13}\text{C}$ target can be seen to lead to reasonably large effects (i.e., of more than a few percent).

(ii) *Inelastic Scattering*: $J_i = \frac{1}{2}, J_f = \frac{3}{2}, \Delta\pi = no$

In this case, the possible multipoles are

$$F_{M1}(q) = (1/\sqrt{2}) \langle \frac{3}{2} \| i\hat{T}_1^{\text{mag}}(q) \| \frac{1}{2} \rangle, \quad \text{M1} \quad (3.10a)$$

$$F_{C2}(q) = (1/\sqrt{2}) \langle \frac{3}{2} \| \hat{M}_2(q) \| \frac{1}{2} \rangle, \quad \text{C2} \quad (3.10b)$$

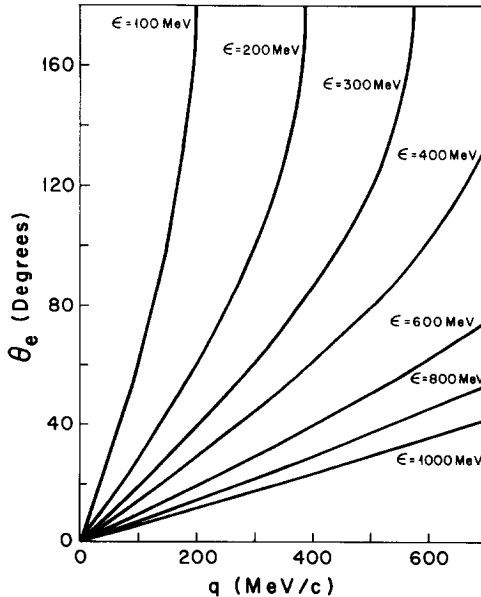


FIG. 3. Scattering angle as a function of the momentum transfer for elastic electron scattering from ${}^7\text{Li}$.

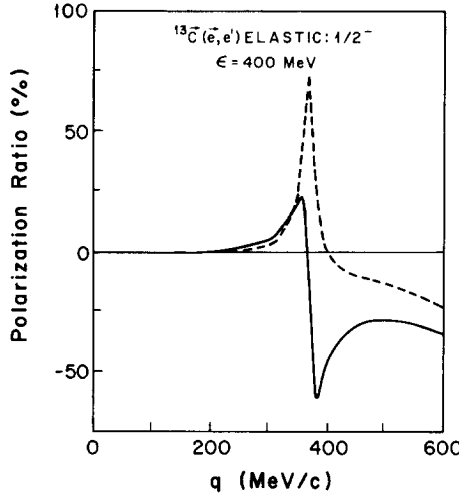


FIG. 4. Elastic electron scattering from polarized $^{13}\text{C} (\frac{1}{2}^-)$. The two polarization ratios defined at the beginning of the section are shown using the convention of (3.4): $(A/\Sigma)_L$ (—), and $(A/\Sigma)_S$ (---); $(A/\Sigma)_N$ is identically zero.

and

$$F_{E2}(q) = (1/\sqrt{2}) \langle \frac{3}{2} \parallel \hat{T}_2^{e1}(q) \parallel \frac{1}{2} \rangle, \quad \text{E2} \quad (3.10c)$$

with $F_L^2(q)^n = F_{C2}^2(q)$ and $F_T^2(q)^n = F_{M1}^2(q) + F_{E2}^2(q)$. The usual Rosenbluth separation would only allow the determination of F_L^2 and F_T^2 ; however, the latter form factor contains two pieces F_{M1}^2 and F_{E2}^2 which cannot be separated in the absence of any polarization. Again, $\Sigma_n = \Sigma_0^n$, and A_n has the same form as for the case of elastic scattering from a spin- $\frac{1}{2}$ nucleus (see Eqs. (3.6) and (3.7)), except that, using Table C8 in Appendix C, we obtain

$$R_1^0(q, \theta_e)_n = \frac{1}{2} v_T [F_{M1}^2 - F_{E2}^2 - 2\sqrt{3} F_{M1} F_{E2}] / F^2(q, \theta_e)^n, \quad (3.11a)$$

and

$$R_1^1(q, \theta_e)_n = -v_{TL} F_{C2} (F_{M1} + \sqrt{3} F_{E2}) / F^2(q, \theta_e)^n. \quad (3.11b)$$

An example of such a transition is the $N(939) \mapsto \Delta(1232)$ transition, where the Δ is the lowest ($J = \frac{3}{2}, T = \frac{3}{2}$) spin-isospin excitation of the nucleon. In this case, the magnetic dipole form factor dominates over the two quadrupole form factors, and so a Rosenbluth separation into the transverse and longitudinal pieces is very difficult to achieve. However, in a situation with a polarized nucleon target and with a polarized electron beam [22], the R_1^1 term will permit a measurement of the C2/M1 interference piece (and, to a lesser extent, the C2/E2 piece), thereby providing greater sensitivity to the small, but interesting, quadrupole matrix elements. Within

the context of the spherically symmetric quark model, the Δ resonance is treated as a spin-excitation of the nucleon: the $N \mapsto \Delta$ transition is just a pure M1 spin-flip of a $1s$ quark, and the quadrupole form factors would then be identically zero. However, $L=2$ contributions could be significant if the Δ has nonspherical admixtures, resulting from a tensor quark-quark interaction (due to the color hyperfine interaction), which would cause S- and D-wave mixing.

The quantities which are usually considered for this transition are the amplitudes labelled by the orbital angular momentum l of the pion in the πN resonance and by the signs $+$ or $-$, where the total angular momentum $j = l \pm \frac{1}{2}$. Then, the amplitudes involved here (S_{1+} , E_{1+} , and M_{1+}) are related to our form factors [57, 58]. Experimentally, it is known from pion photoproduction that $E_{1+}/M_{1+} = -0.014 \pm 0.016$ at $Q^2=0$, while the momentum dependence of the E_{1+} and M_{1+} amplitudes is found from inclusive $p(e, e')\Delta$ and coincidence $p(e, e')\pi^0$ reactions [57-61]: E_{1+} is close to zero except for $-Q^2 < 0.3$ (GeV/c)², while S_{1+} is definitely nonzero, being on the order of 5-10% of the M_{1+} amplitude [58]. The merits of using inclusive electron scattering with polarizations (when feasible) to complement the exclusive (coincidence) reactions with their accompanying final-state interactions should be clear.

For the purposes of illustrating these ideas for complex nuclei, we now consider a second example of a $\frac{1}{2} \mapsto \frac{3}{2}$ transition as provided by the electro-excitation of ^{13}C to its $\frac{3}{2}^-$ excited state at 3.68 MeV; again, we employ Cohen and Kurath wavefunctions [56] to describe the three form factors, just as we did for elastic scattering as discussed above. In this case, the C2 form factor dominates over the M1 and E2 ones beyond 100 MeV/c, while the M1 form factor is greater than the E2 one up to 300 MeV/c. Again, Σ_L exceeds 10^{-33} cm²/sr up to 450 MeV/c for an energy of 400 MeV; as the incident energy is increased, so does the corresponding limiting value of q . As can be seen from Fig. 5, the absence of the coherent Coulomb monopole form factor eliminates the rapid variations in the polarization ratios seen for elastic scattering from ^{13}C ; instead, we observe generally small effects

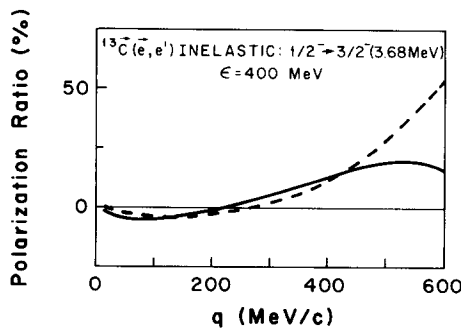


FIG. 5. Inelastic electron scattering from polarized $^{13}\text{C}(\frac{1}{2}^- \mapsto \frac{3}{2}^-)$. The two polarization ratios defined at the beginning of the section are shown using the convention of (3.4): $(D/\Sigma)_L$ (—), and $(D/\Sigma)_S$ (---); $(D/\Sigma)_N$ is identically zero.

for momentum transfers below 400 MeV/c, although one cannot generalize this statement to all inelastic cases (see below for examples where larger effects are seen).

An alternative method for studying nuclear structure using unpolarized or polarized electrons involves the inelastic ($e, e'\gamma$) reaction. In such experiments, the target nucleus is *not* polarized, but the photon resulting from the de-excitation of the excited state is detected in coincidence with the scattered electron (if polarized electrons are used, then the polarization of the photon must also be measured for new information to be obtained). The analysis for this process is very similar to the formalism developed in Section 2 for electron scattering from polarized nuclei [62], and ($e, e'\gamma$) studies may complement (e, e') experiments for inelastic transitions for which only small effects are observed. This particular transition for ^{13}C happens to be such a case.

(iii) *Elastic Scattering*: $J_i = J_f = 1$

The possible multipoles are now given by

$$F_0(q) = (1/\sqrt{3}) \langle 1 \| \hat{M}_0(q) \| 1 \rangle, \quad \text{C0} \quad (3.12a)$$

$$F_1(q) = (1/\sqrt{3}) \langle 1 \| i\hat{T}_1^{\text{mag}}(q) \| 1 \rangle, \quad \text{M1} \quad (3.12b)$$

and

$$F_2(q) = (1/\sqrt{3}) \langle 1 \| \hat{M}_2(q) \| 1 \rangle, \quad \text{C2} \quad (3.12c)$$

and we have that Σ_0^{fi} is given by Eq. (3.3) with $F_L^2(q)^{\text{fi}} = F_0^2(q) + F_2^2(q)$ and $F_T^2(q)^{\text{fi}} = F_1^2(q)$. Thus, with unpolarized scattering, only the sum of the squares of the C0 and C2 contributions can be determined, rather than the individual Coulomb form factors themselves. With polarized targets, however, we have that

$$\begin{aligned} \Sigma_{\text{fi}} = \Sigma_0^{\text{fi}} \{ & 1 + P_2(\cos \theta^*) R_2^0(q, \theta_e)_{\text{fi}} + P_2^1(\cos \theta^*) \cos \phi^* R_2^1(q, \theta_e)_{\text{fi}} \\ & + P_2^2(\cos \theta^*) \cos 2\phi^* R_2^2(q, \theta_e)_{\text{fi}} \}, \end{aligned} \quad (3.13a)$$

and

$$\Delta_{\text{fi}} = \Sigma_0^{\text{fi}} (P_1(\cos \theta^*) R_1^0(q, \theta_e)_{\text{fi}} + P_1^1(\cos \theta^*) \cos \phi^* R_1^1(q, \theta_e)_{\text{fi}}), \quad (3.13b)$$

where

$$R_2^0(q, \theta_e)_{\text{fi}} = -f_2^{(i)} \{ v_L (2\sqrt{3} F_2(F_0 + (\sqrt{2}/4) F_2)) + v_T (\frac{1}{2}\sqrt{\frac{3}{2}} F_1^2) \} / F^2(q, \theta_e)^{\text{fi}}, \quad (3.14a)$$

$$R_2^1(q, \theta_e)_{\text{fi}} = v_{\text{TL}} f_2^{(i)} \{ (3/\sqrt{2}) F_1 F_2 \} / F^2(q, \theta_e)^{\text{fi}}, \quad (3.14b)$$

$$R_2^2(q, \theta_e)_{\text{fi}} = v_{\text{TT}} f_2^{(i)} \{ \frac{1}{4}\sqrt{3/2} F_1^2 \} / F^2(q, \theta_e)^{\text{fi}}, \quad (3.14c)$$

$$R_1^0(q, \theta_e)_{\text{fi}} = -v_T f_1^{(i)} \{ (3\sqrt{2}/4) F_1^2 \} / F^2(q, \theta_e)^{\text{fi}}, \quad (3.14d)$$

and

$$R_1^1(q, \theta_e)_{\bar{n}} = -v_{\text{TL}} f_1^{(i)} \{2\sqrt{3} F_1(F_0 + (\sqrt{2}/4) F_2)\} / F^2(q, \theta_e)^{\bar{n}}, \quad (3.14e)$$

using Table C12 in Appendix C. Again, if we assume 100% polarization, then the rank-1 and -2 Fano tensors are $f_1^{(i)} = 1/\sqrt{2}$ and $f_2^{(i)} = 1/\sqrt{6}$, respectively.

First, let us consider the information which may be determined in the absence of polarized electrons. As can be seen, a measurement of R_2^0 , either as here with a polarized target or by measuring the recoil polarization, together with the longitudinal and transverse form factors as determined without having any nuclear polarization, will allow the extraction of the C0 and C2 form factors separately. The usual Rosenbluth separation will give us $F_1(q)$ (up to an arbitrary sign), and the relative sign between the M1 and the C0 and C2 multipoles can be determined by measuring R_2^1 . Thus, it follows that it is in general not necessary to have knowledge of $A_{\bar{n}}$ to determine all of the multipoles (see the general discussion in Sect. 2 and in Appendix B). Note that R_2^1 (and also R_1^0) only involves $(F_1)^2$, and so just provides a test of the consistency of the measurement; alternatively, some fitting procedure involving all of the reduced response functions $\mathcal{W}_{\bar{J}}^K(q)$ could be used to determine the entire set of form factors.

The fundamental example of a spin-1 nucleus is of course the deuteron (${}^2\text{H}$). The usual definitions of the charge, magnetic, and quadrupole form factors $G_C(q)$, $G_M(q)$, and $G_Q(q)$ prevalent in previous papers are related to our definitions by

$$\sqrt{4\pi} F_0 = (1 + \tau) G_C, \quad (3.15a)$$

$$\sqrt{4\pi} F_1 = -(2/\sqrt{3}) \sqrt{\tau(1 + \tau)} G_M, \quad (3.15b)$$

and

$$\sqrt{4\pi} F_2 = (2\sqrt{2/3}) \tau(1 + \tau) G_Q, \quad (3.15c)$$

where again we note that our form factors only involve the contribution from the leading-order term in the nonrelativistic expansion for the nuclear current (see the discussion above in subsection (i) for the nucleon). Then, the nonvanishing vector and tensor polarizations which are accessible from elastic electron scattering from a polarized target are given in the Madison convention by [36]

$$p_z = \sqrt{2/3} t_{10} = (\sqrt{2/3}) \frac{R_1^0}{f_1}, \quad (3.16a)$$

$$p_x = -(2/\sqrt{3}) t_{11} = (\sqrt{2/3}) \frac{R_1^1}{f_1}, \quad (3.16b)$$

$$p_{zz} = \sqrt{2} t_{20} = \sqrt{2/3} \frac{R_2^0}{f_2}, \quad (3.16c)$$

$$p_{xz} = -\sqrt{3} t_{21} = \sqrt{3/2} \frac{R_2^1}{f_2}, \quad (3.16d)$$

and

$$p_{xx} - p_{yy} = 2\sqrt{3}t_{22} = 2\sqrt{6}\frac{R_2^2}{f_2}. \quad (3.16e)$$

Note that the expression for p_{zz} in terms of t_{20} (T_{20} in their notation) as given in [14] is off by a sign; also, [63] should have a factor of $\sqrt{3}N$ rather than $\sqrt{2}N$ in their Eq. (4b).

The three form factors depend directly on the detailed behaviour of the deuteron wavefunction, and thus a measurement of their values over an extended range of momentum transfer may place some restrictions on possible models for the nucleon–nucleon interaction. Also, the effects of relativistic corrections and meson-exchange currents can be probed at high momentum transfer, where they are expected to be important; in addition, the transition from the meson–baryon description of the nucleus to the quark–gluon description may be observable at such momentum transfers. An experiment measuring the recoil t_{20} tensor polarization of the deuteron has recently been performed at the Bates Laboratory with an unpolarized low duty-factor electron beam using a water target and a conventional ${}^3\text{He}(\bar{d}, p)$ polarimeter; the first results from this experiment are shown in Fig. 6 [64]. It is hoped that the development of improved techniques, especially higher energy polarimeters [22] and higher duty-factor beams, will make it possible to extend such measurements out to the interesting higher momentum transfer region where the different state-of-the-art NN potentials lead to values of t_{20} which differ significantly from one another.

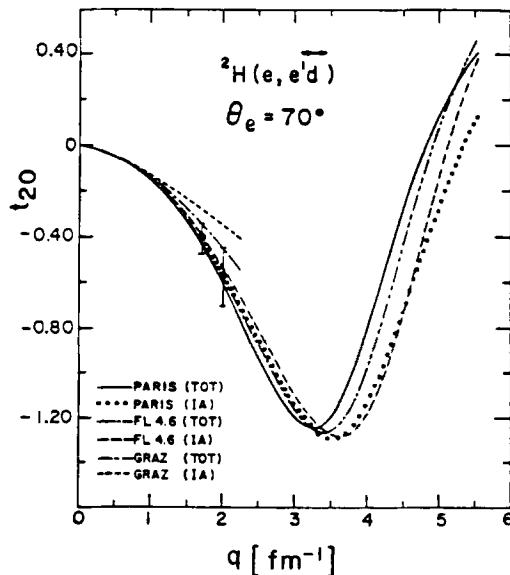


FIG. 6. Recoil t_{20} tensor polarization for elastic electron scattering from the deuteron (from [64]).

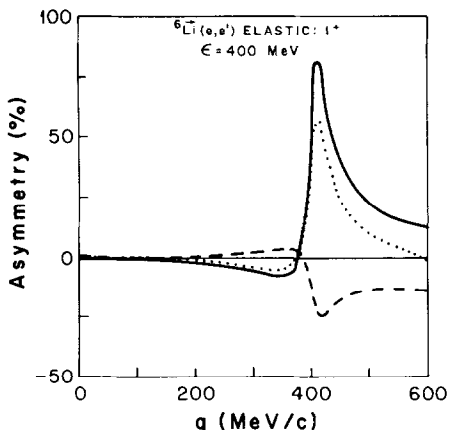


FIG. 7. Elastic electron scattering from polarized ${}^6\text{Li}$ (1^+). The three asymmetries defined in Eq. (3.1) are shown using the convention of (3.3): A_{NS} (—), A_{LN} (---), and A_{LS} (···).

Turning now to approaches involving polarized targets, an experiment which would be suitable for an electron stretcher ring [23] involves an internal target consisting of tensor-polarized deuterium nuclei. A target thickness of approximately 10^{14} atoms/cm² would be required for this type of experiment, making use of the long beam lifetime (about 8 h) in such a facility; in fact, even greater thicknesses of about 4×10^{15} atoms/cm² look feasible. Such a high density of polarized deuterium nuclei can be achieved using optically pumped polarized alkali atoms which transfer polarization to deuterium atoms via an atomic spin-exchange interaction [65]. Looking somewhat further into the future, with the 40 mA circulating current of 1 GeV electrons expected at the proposed Bates stretcher ring [22] luminosities of order 10^{33} cm⁻² sec⁻¹ will be possible, and so it will be possible to measure the target polarization t_{20} out to a momentum transfer of about 1 GeV/c.

In addition to the deuteron, other examples of nuclei with ground states having $J^\pi = 1^+$ are provided by ${}^6\text{Li}$ and ${}^{14}\text{N}$. For the case of ${}^6\text{Li}$, some of the results obtained using phenomenological wavefunctions [3, 35] are displayed in Figs. 7 and 8. As stated previously, we will restrict ourselves to the situation in which the target nucleus is completely polarized along some direction relative to the momentum transfer q . For ${}^6\text{Li}$, a plot of Σ_L versus q indicates that one can only hope to perform experiments out to the maximum momentum transfer of approximately 375 MeV/c for electron energies of less than 1 GeV; however, the interesting high- q region (beyond 400 MeV/c) will be inaccessible in such experiments, unless practical luminosities exceeding 10^{33} cm⁻² sec⁻¹ can be reached.

To illustrate the sensitivity of the cross section Σ to the choice of the nuclear polarization direction, we consider the asymmetries A_{ij} as shown in Fig. 7 for an electron energy of 400 MeV. As can be seen, large asymmetries are present only in those regions where the cross sections are less than the limit of 10^{-33} cm²/sr; for

smaller momentum transfers, $|A_{ij}| < 10\%$. This result is due in part to the dominance of the coherent Coulomb monopole form factor at low momentum transfer for the case of elastic scattering, since the monopole involves a factor of Z ; however, this effect is also related to the qualitative similarity of the C2 and M1 form factors over the entire range of momentum transfer and to the fact that the ground state of ${}^6\text{Li}$ has $T=0$, resulting in a relatively suppressed isoscalar M1 form factor. Thus, in this case the magnitudes of the asymmetries exceed 10% only for momentum transfers near 415 MeV/c, which corresponds to a zero of the C0 form factor; note that in general the dominance of the coherent C0 form factor applies only for q below about 100 MeV/c. It should also be noted that the rapid variation in the asymmetries observed in this case is in fact a general feature of elastic scattering, and results from the interferences between the other form factors weighted with the various kinematic and polarization factors. At higher electron energies, we obtain similar results; there are not any significant differences over the range of useful momentum transfer.

For completeness, we show in Fig. 8 the polarization ratios $(\Delta/\Sigma)_i$ for $\varepsilon = 400$ MeV, which would be obtained only if both a polarized electron beam and a polarized target are available. Again, we observe rapid variations in this ratio in the vicinity of the zero of the Coulomb monopole; however, in this case there are also regions of q below 375 MeV/c for which the ratio differs significantly from zero. For $q < 300$ MeV/c, that is, for small θ_e , the leading factor of $\tan \theta_e/2$ in the kinematic factors v_{TL} and v_{T} (see Eq. (2.25)) tends to suppress the magnitude of Δ . At higher energies, the behaviour of the ratio remains essentially unchanged, except for the fact that the size of the peaks at $q \approx 415$ MeV/c decreases as the energy

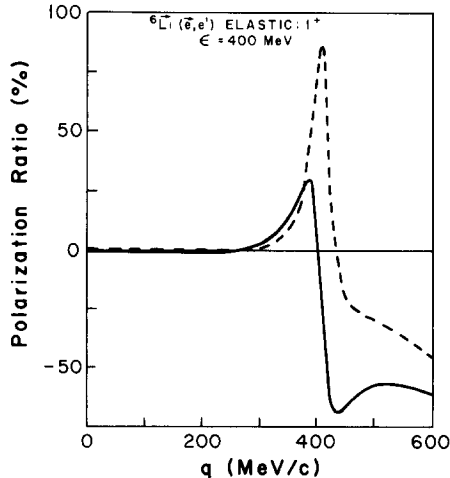


FIG. 8. Elastic electron scattering from polarized ${}^6\text{Li}$ (1^+). The two polarization ratios defined at the beginning of the section are shown using the convention of (3.4): $(\Delta/\Sigma)_L$ (—), and $(\Delta/\Sigma)_S$ (---); $(\Delta/\Sigma)_N$ is identically zero.

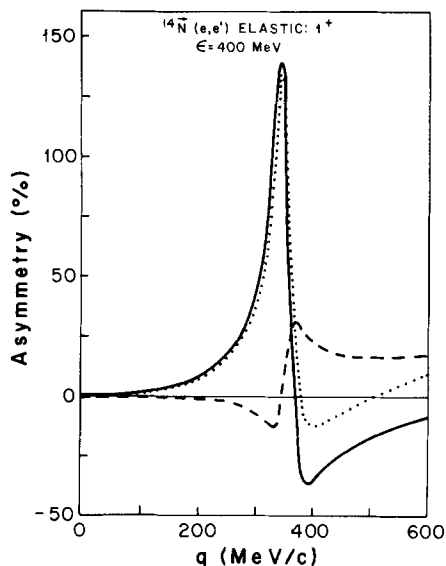


FIG. 9. Elastic electron scattering from polarized $^{14}\text{N}(1^+)$. The three asymmetries defined in Eq. (3.1) are shown using the convention of (3.3): A_{NS} (—), A_{LN} (---), and A_{LS} (···).

increases. Finally, the large magnitude for the ratio at high momentum transfers is due to the behaviour of $\tan \theta_e/2$ as θ_e goes to 180° .

One aspect of the functional form of Δ for elastic scattering from 1^+ nuclei which should be emphasized is the fact that the magnetic dipole form factor $F_{\text{M1}}(q)$ can be factored out; thus, Δ will vanish at momentum transfers which correspond to the zeros of this form factor. For the case of ^6Li , and using our model wavefunctions, $F_{\text{M1}}(q)$ has a zero at about 250 MeV/c, but since $|\Delta/\Sigma|$ is very small at low momentum transfers, this effect is completely suppressed. Furthermore, it can be seen that

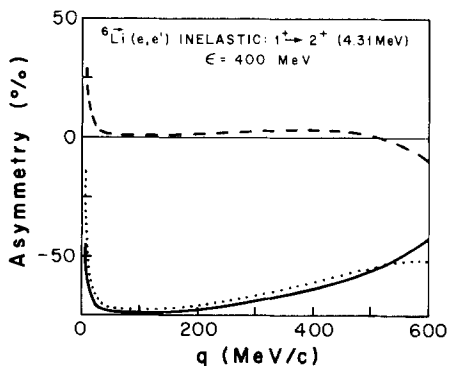


FIG. 10. Inelastic electron scattering from polarized $^6\text{Li}(1^+ \rightarrow 2^+)$. The three asymmetries defined in Eq. (3.1) are shown using the convention of (3.3): A_{NS} (—), A_{LN} (---), and A_{LS} (···).

Δ can also have zeros other than those which correspond to the magnetic dipole zeros; these zeros, which result from the interferences between the various form factors, the nuclear polarizations, and the electron kinematic factors, can be shifted out to different momentum transfers by varying ϵ and θ_e .

We now consider the case of elastic scattering from ^{14}N where we are again using Cohen and Kurath wavefunctions [56], now with $b = 1.60$ fm for the harmonic oscillator $1p$ -shell basis. In this case, Σ_L is greater than 10^{-33} cm²/sr for $q < 550$ MeV/c for an energy of 300 MeV; thus, this case will be somewhat more interesting, since the (coherent) Coulomb monopole has a zero at $q \approx 355$ MeV/c. In fact, for the wavefunctions that we are using, the magnetic dipole form factor has no zero, and so the zeros observed for Δ/Σ are entirely due to interference effects. Now, consider the three asymmetries A_{ij} at $\epsilon = 400$ MeV as shown in Fig. 9; again, we can see a rapid (and large) variation in the vicinity of the zero at 355 MeV/c. Note that A_{LS} and A_{NS} differ significantly from zero for momentum transfers exceeding 200 MeV/c; thus, it should be possible to extract the form factors for a wide range of momentum transfer from 200 MeV/c to about 500 MeV/c, where Σ_L drops below 10^{-33} cm²/sr. Also, as the energy increases, the behaviour of the asymmetries exhibits a significant change in value only for $q > 355$ MeV/c, although the basic shape of the curves remains the same.

Finally, we consider the polarization ratios $(\Delta/\Sigma)_i$ at an energy of 400 MeV. Again, the ratios tend to be relatively small at low momentum transfers until the zero of the charge form factor is approached. Beyond $q \approx 400$ MeV/c, the ratios tend to remain nearly constant, due to the effect of $\tan \theta_e/2$ at large angles. The main effect of increasing the electron energy is to decrease the magnitude of the minimum of Δ/Σ at $q \approx 355$ MeV/c.

(iv) *Inelastic Scattering: $J_i = 1$, $J_f = 2$ and 3, $\Delta\pi = no$*

As examples of these nuclear transitions, we now consider the case of inelastic scattering from ^6Li ; the two transitions discussed are from the 1^+ ground state to the 2^+ (4.31 MeV) and the 3^+ (2.185 MeV) excited states. For both cases, we are using phenomenological one-body density matrix elements [3]. Due to the absence

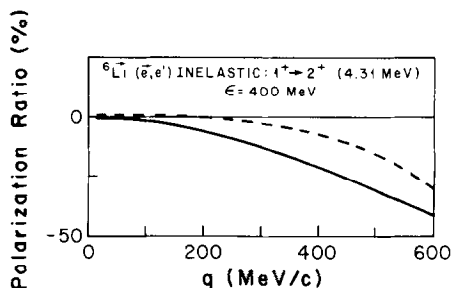


FIG. 11. Inelastic electron scattering from polarized ^6Li ($1^+ \rightarrow 2^+$). The two polarization ratios defined at the beginning of the section are shown using the convention of (3.4): $(\Delta/\Sigma)_L$ (—), and $(\Delta/\Sigma)_S$ (---); $(\Delta/\Sigma)_N$ is identically zero.

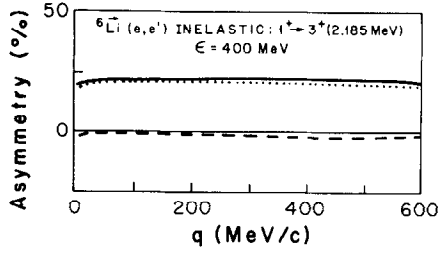


FIG. 12. Inelastic electron scattering from polarized ${}^6\text{Li}(1^+ \rightarrow 3^+)$. The three asymmetries defined in Eq. (3.1) are shown using the convention of (3.3): A_{NS} (—), A_{LN} (---), and A_{LS} (···).

of the coherent Coulomb monopole form factor for inelastic scattering, we expect to observe relatively large asymmetries and polarization ratios over an extended range of the momentum transfer. Also, because the polarization tensors $S_{ij}^{\mathcal{M}}$ are rather complicated functions of the possible form factors, we are not writing them out explicitly; interested readers should consult Table C14 in Appendix C for $J_f = 2$ and Eqs. (2.63) and (2.64) for $J_f = 3$.

The first transition is characterized by the C2, E2, M1, and M3 form factors; for our phenomenological model, the Coulomb form factor is much larger than the other three, and the form factors employed here lack any zeros (other than the one at zero momentum transfer), since we are again dealing with an isoscalar transition. The cross section Σ_L exceeds the practical limit of 10^{-33} cm²/sr for the momentum transfer range $q < 425$ MeV/c for an energy of 350 MeV; at higher energies, this limit on q is relaxed. Because all of the form factors have the same basic shape, i.e., they are zero at zero momentum transfer, reach their maximum magnitude at about 250 MeV/c, and return to zero at large q , the A_{ij} and the $(\Delta/\Sigma)_i$ tend to lack very much structure (see Figs. 10 and 11). Also, note that the asymmetries A_{LS} and A_{NS} are very large in magnitude (-75%) over the entire range of useful momentum transfers, while $(\Delta/\Sigma)_i$ tends to be significant only for q between 300 and 600 MeV/c.

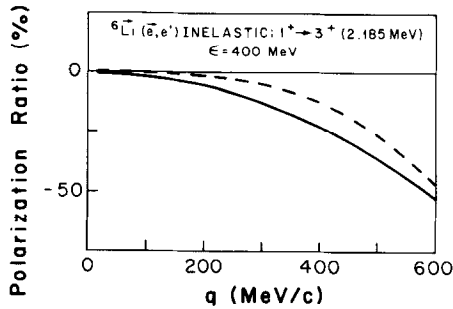


FIG. 13. Inelastic electron scattering from polarized ${}^6\text{Li}(1^+ \rightarrow 3^+)$. The two polarization ratios defined at the beginning of the section are shown using the convention of (3.4): $(\Delta/\Sigma)_L$ (—), and $(\Delta/\Sigma)_S$ (---); $(\Delta/\Sigma)_N$ is identically zero.

Similar results are true for the transition $1^+ \mapsto 3^+$. The C2, E2, and M1 form factors which are possible (we do not have C4 and E4 contributions if we consider only one-body operators in a $1p$ model space) all have the same basic shape as for the previous transition, since again $T_i = T_f = 0$, and the Coulomb quadrupole dominates over the entire momentum range. Also, $\Sigma_L > 10^{-33} \text{ cm}^2/\text{sr}$ for $q < 425 \text{ MeV}/c$ just as for the previous transition, and the asymmetries A_{LS} and A_{NS} are approximately equal to 20% for $q < 600 \text{ MeV}/c$ (see Figs. 12 and 13).

(v) *Elastic Scattering*: $J_i = J_f = \frac{3}{2}$

We now turn to a more complicated example of elastic scattering, where we have the following multipoles:

$$F_0(q) = \frac{1}{2} \langle \frac{3}{2} \| \hat{M}_0(q) \| \frac{3}{2} \rangle, \quad \text{C0} \quad (3.17a)$$

$$F_1(q) = \frac{1}{2} \langle \frac{3}{2} \| i\hat{T}_1^{\text{mag}}(q) \| \frac{3}{2} \rangle, \quad \text{M1} \quad (3.17b)$$

$$F_2(q) = \frac{1}{2} \langle \frac{3}{2} \| \hat{M}_2(q) \| \frac{3}{2} \rangle, \quad \text{C2} \quad (3.17c)$$

and

$$F_3(q) = \frac{1}{2} \langle \frac{3}{2} \| i\hat{T}_3^{\text{mag}}(q) \| \frac{3}{2} \rangle, \quad \text{M3} \quad (3.17d)$$

and $F_L^2(q)^{\text{fi}} = F_0^2(q) + F_2^2(q)$ and $F_T^2(q)^{\text{fi}} = F_1^2(q) + F_3^2(q)$. The cross section Σ_{fi} takes the same form as for the spin-1 case (see Eq. (3.13a)), except that we have, using Table C18 in Appendix C,

$$R_2^0(q, \theta_e)_{\text{fi}} = -f_2^{(i)} \{ 4v_L(F_0F_2) + v_T(\frac{4}{3}(F_1 + \sqrt{3/2}F_3)^2) \} / F^2(q, \theta_e)^{\text{fi}}, \quad (3.18a)$$

$$R_2^1(q, \theta_e)_{\text{fi}} = v_{\text{TL}} f_2^{(i)} \{ (4/\sqrt{5}) F_2(F_1 - \sqrt{2/3}F_3) \} / F^2(q, \theta_e)^{\text{fi}}, \quad (3.18b)$$

and

$$R_2^2(q, \theta_e)_{\text{fi}} = v_{\text{TT}} f_2^{(i)} \{ \frac{2}{3}(F_1^2 - F_3^2 + (1/\sqrt{6})F_1F_3) \} / F^2(q, \theta_e)^{\text{fi}}. \quad (3.18c)$$

The polarization cross section now includes rank-3 tensors:

$$\begin{aligned} \Delta_{\text{fi}} = \Sigma_0^{\text{fi}} \{ & P_1(\cos \theta^*) R_1^0(q, \theta_e)_{\text{fi}} + P_1^1(\cos \theta^*) \cos \phi^* R_1^1(q, \theta_e)_{\text{fi}} + P_3(\cos \theta^*) R_3^0(q, \theta_e)_{\text{fi}} \\ & + P_3^1(\cos \theta^*) \cos \phi^* R_3^1(q, \theta_e)_{\text{fi}} \}, \end{aligned} \quad (3.19)$$

where, again using Table C18,

$$R_1^0(q, \theta_e)_{\text{fi}} = -v_T f_1^{(i)} \{ (2/\sqrt{5})(F_1^2 + F_3^2) \} / F^2(q, \theta_e)^{\text{fi}}, \quad (3.20a)$$

$$R_1^1(q, \theta_e)_{\text{fi}} = -v_{\text{TL}} f_1^{(i)} \{ 4(F_1(F_0 + \frac{2}{3}F_2) + (\sqrt{6}/5)F_2F_3) \} / F^2(q, \theta_e)^{\text{fi}}, \quad (3.20b)$$

$$R_3^0(q, \theta_e)_{\text{fi}} = v_T f_3^{(i)} \{ (2/\sqrt{5})F_3(F_3 + 2\sqrt{6}F_1) \} / F^2(q, \theta_e)^{\text{fi}}, \quad (3.20c)$$

and

$$R_3^1(q, \theta_e)_R = v_{TL} f_3^{(i)} \{ 2 \sqrt{2/3} (F_3 (F_0 + \frac{3}{5} F_2) + (\sqrt{6/5}) F_2 F_1) \} / F^2(q, \theta_e)^6. \quad (3.20d)$$

For 100% polarization, the Fano tensors are given by $f_1^{(i)} = 3 \sqrt{5/10}$, $f_2^{(i)} = \frac{1}{2}$, and $f_3^{(i)} = \sqrt{5/10}$.

Because we are only considering elastic scattering, the electric multipole form factors are all identically zero, and this reduction in the number of form factors implies that, for $J_0 = \frac{3}{2}$, it is not necessary to have a polarized electron beam to determine all four of the form factors (up to the arbitrary overall sign). Explicitly, we have from Eq. (3.18) that the various reduced response functions accessible in such an experiment are given by

$$\mathcal{W}_0^L = 2(F_0^2 + F_2^2), \quad (3.21a)$$

$$\mathcal{W}_2^L = -4F_0 F_2, \quad (3.21b)$$

$$\mathcal{W}_0^T = 2(F_1^2 + F_3^2), \quad (3.21c)$$

$$\mathcal{W}_2^T = -\frac{4}{3}(F_1 + \sqrt{3/2} F_3)^2, \quad (3.21d)$$

$$\mathcal{W}_2^{TT} = \frac{2}{3}(F_1 + \sqrt{3/2} F_3)(F_1 - \sqrt{2/3} F_3), \quad (3.21e)$$

and

$$\mathcal{W}_2^{TL} = (4/\sqrt{5}) F_2 (F_1 - \sqrt{2/3} F_3). \quad (3.21f)$$

Then, the magnitudes of the form factors F_i are given by

$$F_0^2 = \frac{1}{2} \mathcal{W}_0^L + \frac{\mathcal{W}_2^T}{16} \left(\frac{\mathcal{W}_2^{TL}}{\mathcal{W}_2^{TT}} \right)^2, \quad (3.22a)$$

$$F_2^2 = \frac{1}{2} \mathcal{W}_0^L - F_0^2, \quad (3.22b)$$

$$F_1^2 = \frac{3\mathcal{W}_0^T}{10} (1 + X), \quad (3.22c)$$

and

$$F_3^2 = \frac{3\mathcal{W}_0^T}{10} \left(\frac{2}{3} - X \right), \quad (3.22d)$$

where

$$X \equiv \frac{\mathcal{W}_2^T + 12\mathcal{W}_2^{TT}}{3\mathcal{W}_0^T} = \frac{(2/3) - (F_3/F_1)^2}{1 + (F_3/F_1)^2}, \quad (3.23)$$

while the corresponding signs λ_i are given by

$$\lambda_2 = -\frac{\lambda_0 \mathcal{W}_2^L}{4 |F_0| |F_2|}, \tag{3.24a}$$

$$\lambda_1 = \sqrt{5} \lambda_2 \mathcal{W}_2^{TL} / \{4 |F_2| (|F_1| - \sqrt{2/3} \lambda_{13} |F_3|)\}, \tag{3.24b}$$

and

$$\lambda_3 = \lambda_{13} \lambda_1, \tag{3.24c}$$

where

$$\lambda_{13} \equiv \sqrt{2/3} (\mathcal{W}_2^{TT} - \mathcal{W}_0^T - 2\mathcal{W}_2^T) / \{ \mathcal{W}_0^T \sqrt{(1+X)(\frac{2}{3}-X)} \}. \tag{3.25}$$

Thus, we see that it is possible to determine all four of the form factors (up to the arbitrary overall sign) even without having any electron polarization. Note that the quantity X involves only the ratio $|F_3/F_1|$ and so may be sensitive to the different effects of meson-exchange currents or core polarization on the two transverse form factors.

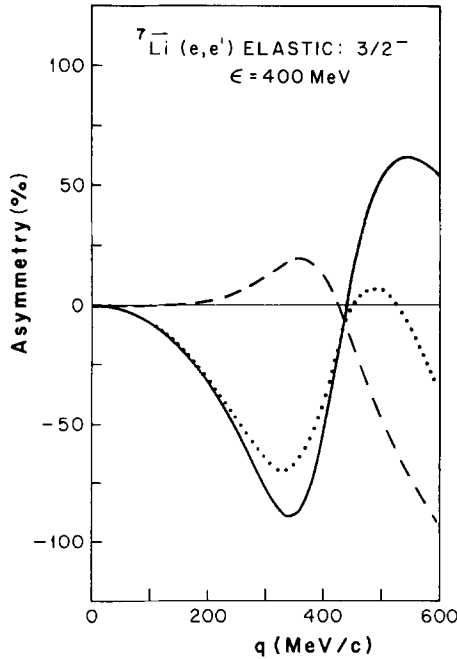


FIG. 14. Elastic electron scattering from polarized ${}^7\text{Li}(\frac{3}{2}^-)$. The three asymmetries defined in Eq. (3.1) are shown using the convention of (3.3): A_{NS} (—), A_{LN} (---), and A_{LS} (···).

As specific examples of ground states of nuclei with spin- $\frac{3}{2}$, we consider ${}^7\text{Li}$ and ${}^{39}\text{K}$; being alkalis, these have the added advantage of being practical for the production of polarized targets [23]. For this reason, we shall consider the ${}^7\text{Li}$ case in some detail. Again, Cohen and Kurath wave functions are used, with an harmonic oscillator basis having $b = 1.65$ fm [56]. In this case, Σ_L decreases monotonically as q increases, and the limit of 10^{-33} cm²/sr is reached at $q \approx 500$ MeV/c. The asymmetries A_{ij} for an electron energy of 400 MeV are displayed in Fig. 14. Note that A_{LS} and A_{NS} differ significantly from zero over essentially the entire range of momentum transfer, while A_{LN} has this property only beyond 300 MeV/c. This is a very interesting feature for elastic scattering and is due to the fact that the nucleus has a relatively low value of Z , since otherwise one would expect the coherent Coulomb monopole to be the dominant form factor up to its zero (at about $q \approx 510$ MeV/c, in this case). However, for ${}^7\text{Li}$, the C0 form factor drops to the level of the C2, M1, and M3 form factors at about 300 MeV/c, and so this effect is suppressed. In addition, one should note that there is a significant difference between the behaviour of the asymmetries for different electron energies at the same momentum transfer; these variations are due to variations in the kinematic factors v_K , since all of the other quantities are held constant. Again, this relates to the fact that the coherent Coulomb monopole does not overwhelm the other form factors except at small momentum transfers, so that there can be a great deal of interference between the various polarization tensors; thus, this effect is not as pronounced for elastic scattering from nuclei with large Z .

Now, consider the polarization ratios $(\Delta/\Sigma)_i$ for $\epsilon = 400$ MeV as shown in Fig. 15. Note that the ratios are small except for $q > 400$ MeV/c due to the fact that the kinematic factors for Δ have a leading term of $\tan \theta_e/2$ which tends to suppress Δ for a given incident electron energy; this effect is enhanced by the dominance of the

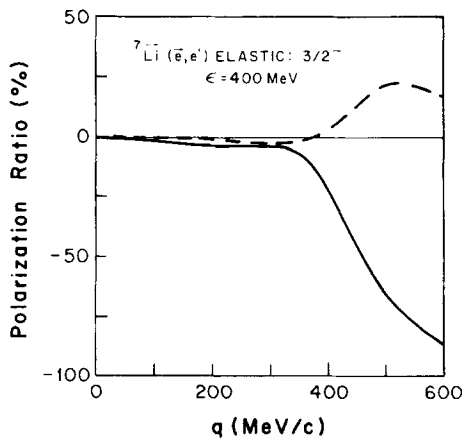


FIG. 15. Elastic electron scattering from polarized ${}^7\text{Li}(\frac{3}{2}^-)$. The two polarization ratios defined at the beginning of the section are shown using the convention of (3.4): $(\Delta/\Sigma)_L$ (—), and $(\Delta/\Sigma)_S$ (---); $(\Delta/\Sigma)_N$ is identically zero.

C_0 form factor at low momentum transfers, since Σ goes as $F_{C_0}^2$ while Δ is only linear in F_{C_0} . Thus, Δ/Σ goes as $1/Z$, which clearly results in a suppression in the values of the polarization ratios for heavy nuclei. On the other hand, it should be noted that the figure of merit for an experiment in which Σ and Δ are separated by switching the electron helicity is given by $\mathcal{P}\Sigma/(1-\mathcal{P})$, where $\mathcal{P} = (\Delta/\Sigma)^2$; then, since Σ goes as Z^2 while Δ goes as Z , the figure of merit varies approximately as $(Z/Z^2)^2 Z^2 \approx 1$. Thus, it is possible that an accurate measurement of Δ/Σ may be much easier than it would appear on first sight to be, even though Δ/Σ goes as $1/Z$. In contrast, the determination of the transverse form factor F_T^2 through a Rosenbluth separation or magnetic electron scattering (at 180°) would have a figure of merit which goes as $1/Z^2$ at low momentum transfer, making such experiments difficult to perform when Z is large.

Another way to display the ratios Δ/Σ is to consider the scattering angle θ_e to be fixed and vary the electron energy. As shown in Fig. 16, once the leading behavior of Δ as contained in the kinematic factors is removed, one sees that there can be a great deal of variation in the ratios and, in fact, the ratios can be appreciable for small momentum transfers; for example, if $\theta_e = 135^\circ$, then $(\Delta/\Sigma)_L$ reaches -25% at $q \approx 300$ MeV/c, while $(\Delta/\Sigma)_S$ reaches -30% at $q \approx 200$ MeV/c and increases through zero near 320 MeV/c until it attains the value of $+25\%$ at 400 MeV/c. The difference in the low- q dependence of the polarization ratios for the constant energy and constant scattering angle cases arises because the $\tan \theta_e/2$ dependence in the

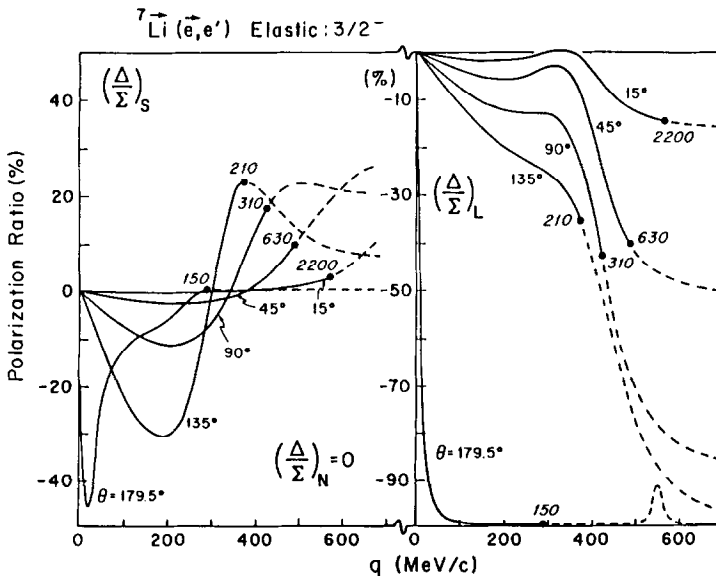


FIG. 16. Elastic electron scattering from polarized ${}^7\text{Li}$ ($\frac{3}{2}^-$). The two polarization ratios defined at the beginning of this section are shown; $(\Delta/\Sigma)_N$ is identically zero. Note that the scattering angle θ_e is being held fixed. The dashed lines indicate that the cross sections are below 10^{-33} cm 2 /sr; the numbers give the corresponding energies ϵ in MeV.

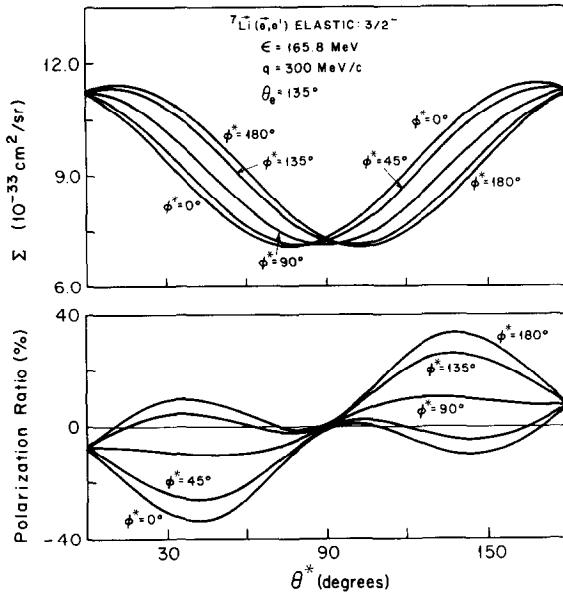


FIG. 17. Elastic electron scattering from polarized ${}^7\text{Li}(\frac{3}{2}^-)$. The cross section Σ and the polarization ratio Δ/Σ are displayed as functions of the polarization direction of the nucleus (θ^* , ϕ^*) for given electron scattering kinematics.

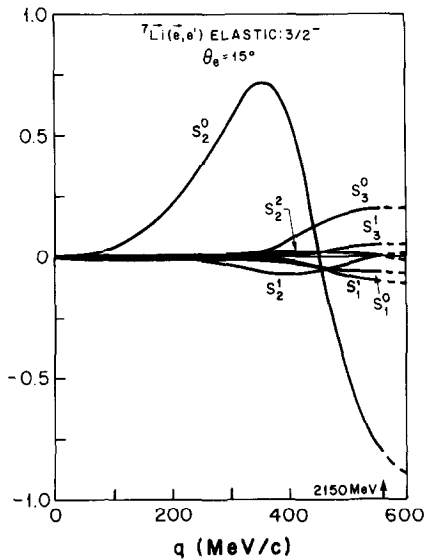


FIG. 18. Elastic electron scattering from polarized ${}^7\text{Li}(\frac{3}{2}^-)$. The polarization tensors S_j^k are displayed as functions of the momentum transfer for a fixed scattering angle of 15° .

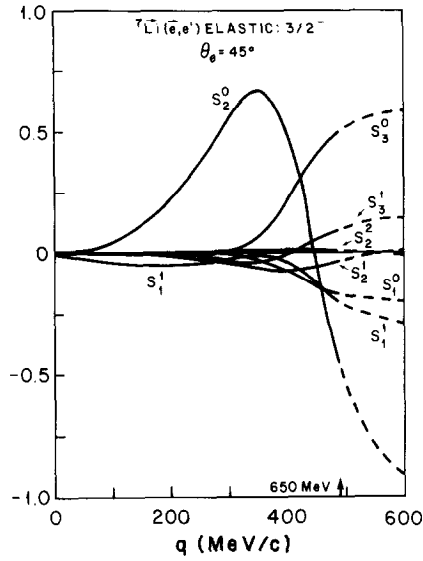


FIG. 19. Elastic electron scattering from polarized ${}^7\text{Li}(\frac{3}{2}^-)$. The polarization tensors S_j^k are displayed as functions of the momentum transfer for a fixed scattering angle of 45° .

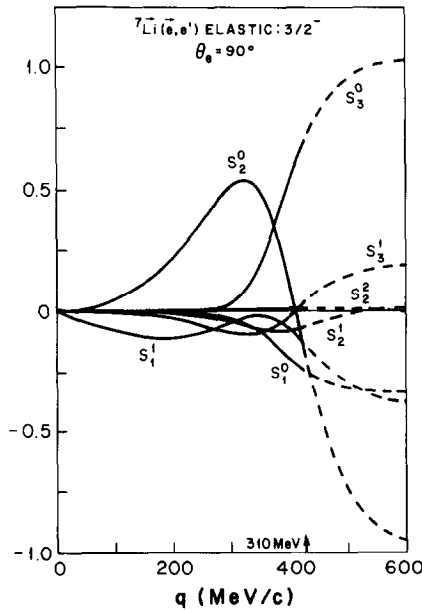


FIG. 20. Elastic electron scattering from polarized ${}^7\text{Li}(\frac{3}{2}^-)$. The polarization tensors S_j^k are displayed as functions of the momentum transfer for a fixed scattering angle of 90° .

kinematic factors contained in Δ compensates for the $1/Z$ suppression in the ratio Δ/Σ . Finally, we display the dependence of Σ and Δ/Σ on the polarization angles θ^* and ϕ^* in Fig. 17; as can be seen, significant differences result when the polarization direction is changed, and so this dependence may provide a very useful way to isolate the various $S_{\mathcal{J}}^{\mu}$. For instance, S_2^0 is not associated with any ϕ^* dependence, while the terms S_2^1 and S_2^2 involve $\cos \phi^*$ and $\cos 2\phi^*$, respectively; thus, it follows that S_2^1 can be separated by taking the combination $\Sigma(\phi^*=0^\circ) - \Sigma(\phi^*=180^\circ)$, while S_2^2 can be determined by considering $\Sigma(\phi^*=0^\circ) - 2\Sigma(\phi^*=90^\circ) + \Sigma(\phi^*=180^\circ)$.

At this point, we would like to emphasize that, while we have only discussed the behaviours of the various asymmetries and polarization ratios, the quantities of actual interest are the $S_{\mathcal{J}}^{\mu}(q, \theta_e)$ defined by Eq. (2.74), which involve the form factors and the kinematic factors v_K , but not the Fano tensors $f_{\mathcal{J}}^{(i)}$; the polarization tensors are displayed in Figs. 18 through 21 for a variety of scattering angles. The dashed curves indicate that Σ_L has fallen below the practical limit of $10^{-33} \text{ cm}^2/\text{sr}$ for these momentum transfers, and the electron energy corresponding to the critical value of Σ_L is displayed at the bottom of the graphs. Note that the $S_{\mathcal{J}}^{\mu}$ exhibit a strong dependence on the scattering angle due to the kinematic factors v_K ; at large angles, the effect of the Coulomb form factors has been suppressed relative to the transverse ones.

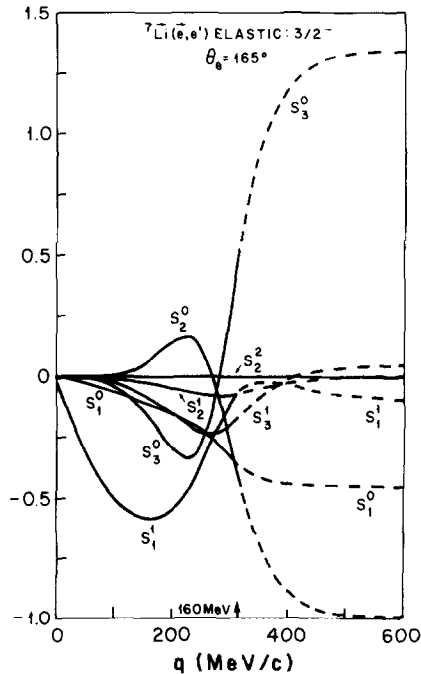


FIG. 21. Elastic electron scattering from polarized ${}^7\text{Li}(\frac{3}{2}^-)$. The polarization tensors $S_{\mathcal{J}}^{\mu}$ are displayed as functions of the momentum transfer for a fixed scattering angle of 165° .

To investigate the sensitivity of the various quantities of experimental interest to changes in the nuclear structure, we will now consider the cases for which the magnetic form factors have been suppressed and enhanced by 50% from the values obtained using our shell-model wavefunctions (which, in fact, yield form factors F_L^2 and F_T^2 in substantial agreement with experiment for $q < 400$ MeV/c). First, let us examine the effects of suppressing the M1 and M3 form factors; for the most part, the basic shapes of the various curves remain unaffected by the suppression, although the actual values can vary significantly. First, let us consider the asymmetries A_{ij} . Then, the only significant change in A_{NS} occurs for momentum transfers between 300 and 550 MeV/c; the asymmetry is lower in value beyond 300 MeV/c, and reaches its local minimum of about -105% at 370 MeV/c before passing through zero at 475 MeV/c (the fact that $|A_{ij}|$ can exceed 100% is due to our definition of the asymmetries; see the beginning of this section). Similar behaviour is observed for A_{LN} , except that in this case the asymmetry is greater in value beyond 350 MeV/c, reaching its local maximum of 35% at about 400 MeV/c and becoming zero at about 460 MeV/c; the effects of the suppression of the

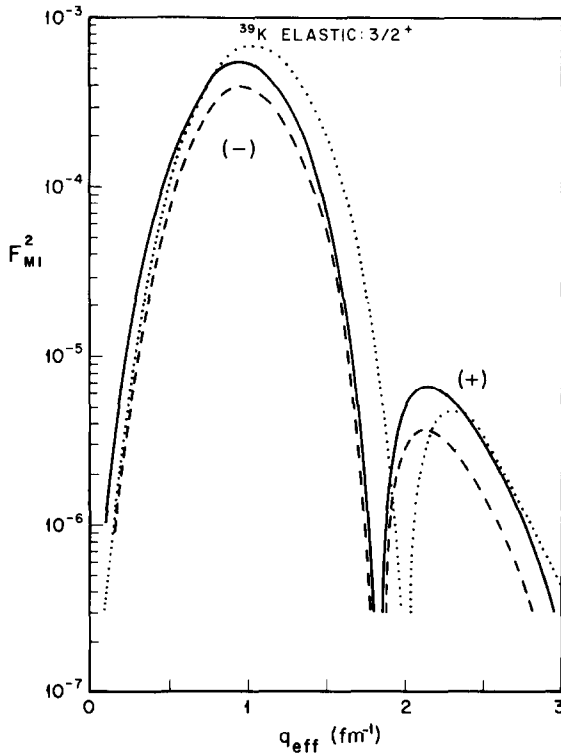


FIG. 22. M1 form factor for elastic scattering from ^{39}K as calculated by Suzuki *et al.* [66]; result for the extreme-single-particle model (\cdots); results when the effects of core-polarization ($---$), and core-polarization plus meson-exchange currents ($-$) are included.

magnetic form factors is small beyond 570 MeV/c. Finally, A_{LS} displays significant differences between 325 and 525 MeV/c in that it is lower in value when the M1 and M3 multipoles are suppressed; the asymmetry attains its local minimum of -80% at 350 MeV/c and its maximum value of -2% at 500 MeV/c. As far as the polarization ratios are concerned, $(\Delta/\Sigma)_L$ is increased in value by about 25 percentage points beyond 360 MeV/c. However, $(\Delta/\Sigma)_S$ displays larger differences, as the effect seen beyond 400 MeV/c is almost completely eliminated when the form factors are suppressed; $(\Delta/\Sigma)_S$ reaches its maximum value of about 5% at 475 MeV/c and then decreases steadily until it attains the value of -12% at 600 MeV/c.

Similarly, if the magnetic form factors are enhanced by 50% relative to their usual values, then A_{NS} is increased in value by about 10 percentage points between 300 and 500 MeV/c; A_{LN} is decreased by 5 percentage points between 350 and 475 MeV/c, while A_{LS} is increased by about 10 percentage points for $320 < q < 520$ MeV/c. Also, we have that $(\Delta/\Sigma)_L$ is decreased in value by about 5 percentage points between 350 and 475 MeV/c, while $(\Delta/\Sigma)_S$ is increased by about 50% from its usual value at momentum transfers above 400 MeV/c.

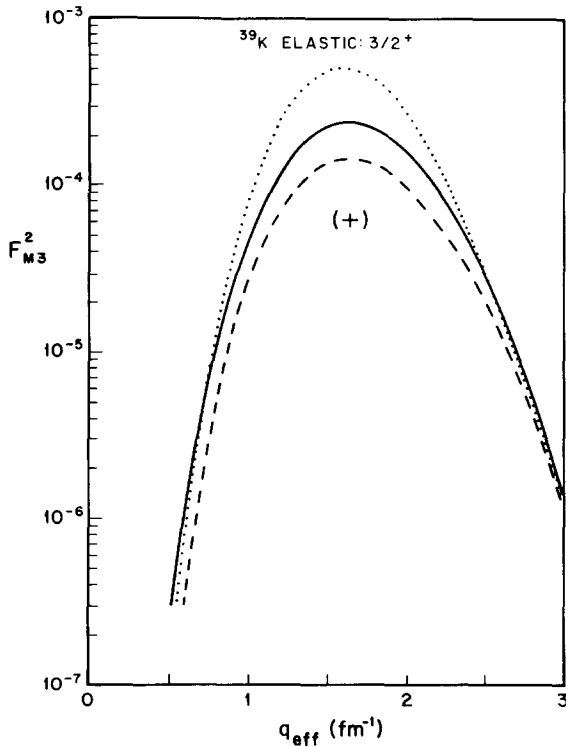


FIG. 23. M3 form factor for elastic scattering from ^{39}K as calculated by Suzuki *et al.* [66]; result for the extreme-single-particle model (\cdots); results when the effects of core-polarization ($---$), and core-polarization plus meson-exchange currents ($-$) are included.

Now, consider elastic electron scattering from another spin- $\frac{3}{2}$ nucleus, ^{39}K (as noted above, this case, along with ^7Li , is an alkali, and so is also known to be advantageous when it comes to producing practical polarized targets [23]). We describe the ground state of ^{39}K in terms of the extreme-single-particle model as a $1d_{3/2}$ proton hole relative to ^{40}Ca , where again we use harmonic oscillator wavefunctions (with $b=2.0$ fm). In this case, we include the effects of core polarization and meson-exchange currents on the transverse M1 and M3 form factors as calculated by Suzuki *et al.* [66]; the transverse form factors are displayed in Figs. 22 and 23. In particular, the M1 multipole is suppressed for momentum transfers between 200 and 375 MeV/c and enhanced between 400 and 500 MeV/c; similarly, the M3 form factor is suppressed between 150 and 500 MeV/c, with a reduction to 70% of the single-particle value at its maximum at 320 MeV/c. In this case, Σ_L exceeds 10^{-33} cm²/sr at an energy $\varepsilon = 300$ MeV for $q < 500$ MeV/c; as the energy is increased, the limiting value of q also increases. The coherent Coulomb monopole has zeros at about 235 and 370 MeV/c; the existence of two such zeros will greatly increase the range of momentum transfer for which the asymmetries and polarization ratios will be significant, because the large magnitudes for the A_{ij} and

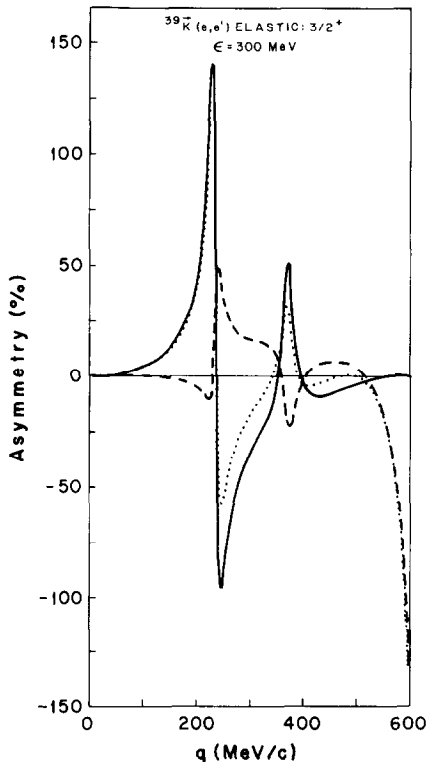


FIG. 24. Elastic electron scattering from polarized $^{39}\text{K}(\frac{3}{2}^+)$. The three asymmetries defined in Eq. (3.1) are shown using the convention of (3.3): A_{NS} (—), A_{LN} (---), and A_{LS} (···).

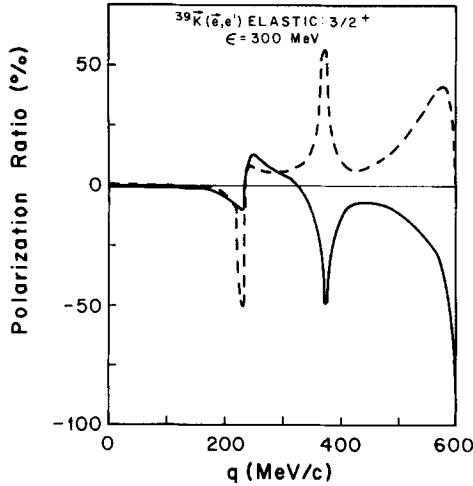


FIG. 25. Elastic electron scattering from polarized $^{39}\text{K}(\frac{3}{2}^+)$. The two polarization ratios defined at the beginning of the section are shown using the convention of (3.4): $(\Delta/\Sigma)_L$ (—), and $(\Delta/\Sigma)_S$ (---); $(\Delta/\Sigma)_N$ is identically zero.

Δ/Σ will persist over the region between these zeros. The asymmetries A_{ij} differ significantly from zero for momentum transfers between 150 and 500 MeV/c. Again, rapid variations can be seen near the zeros of the charge form factor, as shown in Fig. 24. For the polarization ratios $(\Delta/\Sigma)_i$, the effects of the zeros are not as large, as can be seen from Fig. 25. Again, there is a rapid variation near these two points, but the ratios tend to be smaller in magnitude, except for the sharp peak at 235 MeV/c for $(\Delta/\Sigma)_S$. For completeness, we display the dependence of the cross section and polarization ratio on the choice of the polarization direction (θ^*, ϕ^*) in Fig. 26; as can be seen, these quantities have a significant effect on the Σ and Δ .

When we compare these results to those obtained from the extreme-single-particle model, we find observable differences in the asymmetries beyond 300 MeV/c, where the Coulomb monopole form factor no longer overwhelms the others (note that the extremely large differences reported in a preliminary discussion of ^{39}K [21, 22] stemmed from the use of different wavefunctions for the calculations with and without the inclusion of meson-exchange and core-polarization effects, and are superseded by the present results). The fact that the effects of core polarization and meson-exchange currents on the asymmetries are not as significant as the corresponding effects on the individual form factors is a result of the complicated dependence of the A_{ij} on the form factors; because the asymmetries involve combinations of interferences between all of the possible form factors, the large effects seen in the form factors (Figs. 22 and 23) tend to be suppressed. However, these large differences would become evident after an analysis of the experimentally measured reduced response functions along the lines of Eqs. (3.21) through (3.25), since one is in principle able to extract all of the individual form factors from measurements of the cross section Σ alone.

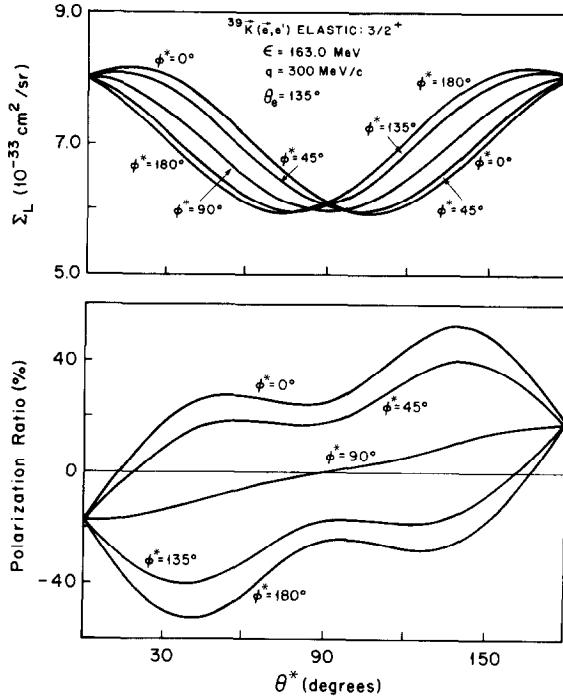


FIG. 26. Elastic electron scattering from polarized $^{39}\text{K}(\frac{3}{2}^+)$. The cross section Σ and the polarization ratio A/Σ are displayed as functions of the polarization direction (θ^* , ϕ^*) for given electron scattering kinematics.

(vi) *Inelastic Scattering*: $J_i = \frac{3}{2}$, $J_f = \frac{1}{2}$, $\Delta\pi = no$

For this nuclear transition, we have the M1, C2, and E2 electromagnetic multipoles

$$F_{M1}(q) = \frac{1}{2} \langle \frac{1}{2} \| i\hat{T}_1^{\text{mag}}(q) \| \frac{3}{2} \rangle, \quad \text{M1} \quad (3.26a)$$

$$F_{C2}(q) = \frac{1}{2} \langle \frac{1}{2} \| \hat{M}_2(q) \| \frac{3}{2} \rangle, \quad \text{C2} \quad (3.26b)$$

and

$$F_{E2}(q) = \frac{1}{2} \langle \frac{1}{2} \| \hat{T}_2^{\text{el}}(q) \| \frac{3}{2} \rangle, \quad \text{E2} \quad (3.26c)$$

and so $F_L^2(q)^{\text{fi}} = F_{C2}^2(q)$ and $F_T^2(q)^{\text{fi}} = F_{M1}^2(q) + F_{E2}^2(q)$. The cross section then takes the same form as was the case for elastic scattering from a $J_i = \frac{3}{2}$ nucleus (see Eqs. (3.13a) and (3.19)), except that from Table C16 we have

$$R_0^2(q, \theta_e)_R = -f_2^{(i)} \{ 2v_L F_{C2}^2 + v_T (F_{E2}^2 - F_{M1}^2 - 2\sqrt{3} F_{E2} F_{M1}) \} / F^2(q, \theta_e)^{\text{fi}}, \quad (3.27a)$$

$$R_2^2(q, \theta_e)_R = v_{TL} f_2^{(i)} \{ 2F_{C2}(F_{M1} + (1/\sqrt{3}) F_{E2}) \} / F^2(q, \theta_e)^{\text{fi}}, \quad (3.27b)$$

$$R_2^2(q, \theta_e)_{\bar{n}} = v_{TT} f_2^{(i)} \left\{ \frac{1}{2} (F_{E2}^2 - F_{M1}^2) + (2/\sqrt{3}) F_{E2} F_{M1} \right\} / F^2(q, \theta_e)_{\bar{n}}, \quad (3.27c)$$

$$R_1^0(q, \theta_e)_{\bar{n}} = -v_{T'} f_1^{(i)} \left\{ \sqrt{5} (F_{M1}^2 + \frac{3}{5} F_{E2}^2 + \frac{2}{5} \sqrt{3} F_{E2} F_{M1}) \right\} / F^2(q, \theta_e)_{\bar{n}}, \quad (3.27d)$$

$$R_1^1(q, \theta_e)_{\bar{n}} = -v_{TL} f_1^{(i)} \left\{ (2/\sqrt{5}) F_{C2} (F_{M1} + 3 \sqrt{3} F_{E2}) \right\} / F^2(q, \theta_e)_{\bar{n}}, \quad (3.27e)$$

$$R_3^0(q, \theta_e)_{\bar{n}} = v_{T'} f_3^{(i)} \left\{ (4/\sqrt{5}) F_{E2} (F_{E2} - \sqrt{3} F_{M1}) \right\} / F^2(q, \theta_e)_{\bar{n}}, \quad (3.27f)$$

and

$$R_3^1(q, \theta_e)_{\bar{n}} = v_{TL} f_3^{(i)} \left\{ (4/\sqrt{15}) F_{C2} (F_{E2} - \sqrt{3} F_{M1}) \right\} / F^2(q, \theta_e)_{\bar{n}}. \quad (3.27g)$$

As an example of such a transition, we consider the case of inelastic scattering from ${}^7\text{Li}$ for the transition $\frac{3}{2}^- \mapsto \frac{1}{2}^-$ (0.478 MeV), where we are again using Cohen and Kurath wavefunctions [56] with an harmonic oscillator basis with $b = 1.65$ fm; then, we find that $\Sigma_L > 10^{-33}$ cm²/sr for $q < 450$ MeV/c at an energy of 400 MeV. As can be seen from Fig. 27, the asymmetries vary from -150 to $+150\%$ over the range of useful momentum transfers, and in fact A_{LN} and A_{NS} tend to be very large even for low momentum transfers. Thus, measurements of these quantities could be

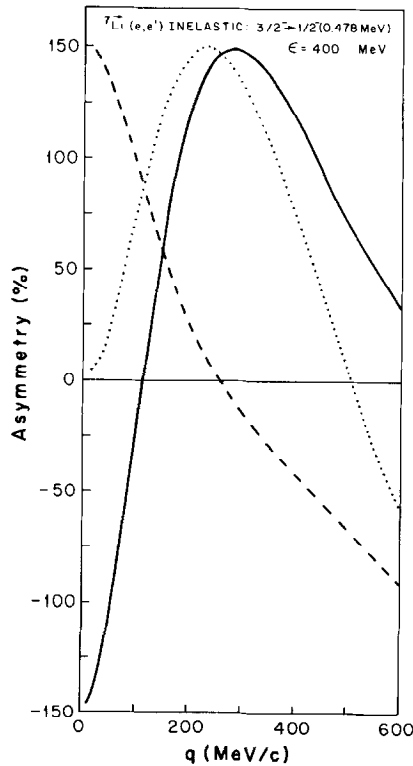


FIG. 27. Inelastic electron scattering from polarized ${}^7\text{Li}$ ($\frac{3}{2}^- \mapsto \frac{1}{2}^-$). The three asymmetries defined in Eq. (3.1) are shown using the convention of (3.3): A_{NS} (—), A_{LN} (---), and A_{LS} (···).

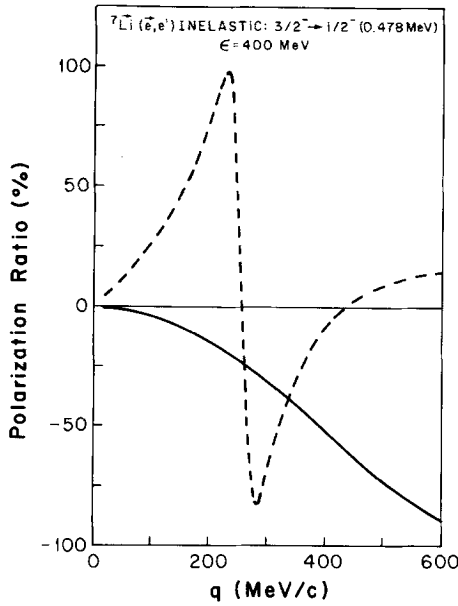


FIG. 28. Inelastic electron scattering from polarized ${}^7\text{Li}(\frac{3}{2}^- \rightarrow \frac{1}{2}^-)$. The two polarization ratios defined at the beginning of the section are shown using the convention of (3.4): $(\Delta/\Sigma)_L$ (—), and $(\Delta/\Sigma)_S$ (---); $(\Delta/\Sigma)_N$ is identically zero.

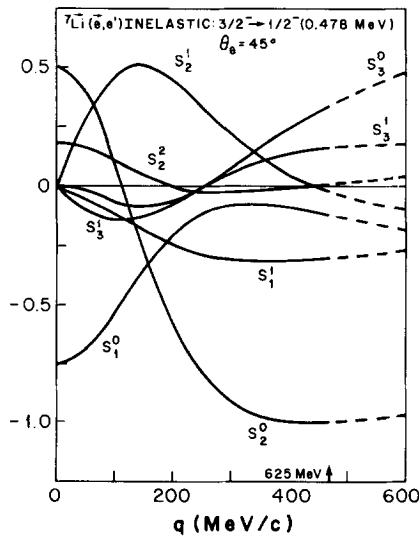


FIG. 29. Inelastic electron scattering from polarized ${}^7\text{Li}(\frac{3}{2}^- \rightarrow \frac{1}{2}^-)$. The polarization tensors S_i^j are displayed as functions of the momentum transfer for a fixed scattering angle of 45° .

performed over the entire range of q out to 450 MeV/c. Note that this is a general property for inelastic scattering, since, in contrast to elastic scattering, the absence of the typically overwhelmingly large coherent Coulomb monopole form factor implies that there can be considerable interference between the other form factors even at low momentum transfers.

Also, consider the polarization ratios $(A/\Sigma)_i$ as displayed in Fig. 28; as can be seen, the ratios are quite large up to 450 MeV/c. This is true even at small scattering angles for $(A/\Sigma)_S$, and is due to the peak of the C2 form factor near 200 MeV/c. When θ_e is held fixed rather than ϵ , relatively little variation can be seen for $(A/\Sigma)_L$ as the energy (and thus the momentum transfer) is increased, and the ratio differs significantly from zero as long as the scattering angle is not near zero. However, this is not true for $(A/\Sigma)_S$, which exhibits a very large variation and quite large magnitudes unless we are dealing with rather forward or backward scattering. For completeness, the polarization tensors $S_{ij}^{\mu\nu}$ for this transition are shown in Fig. 29 for $\theta_e = 45^\circ$; note that the inelastic nature of the transition results in a large variation in the behaviour of these quantities over the entire range of useful momentum transfers.

If we now consider the dependence of Σ and A/Σ on the polarization direction as defined by θ^* and ϕ^* , then, as shown in Figs. 30 and 31, there is again quite a lot of structure evident in these functions. In both cases, there is a very strong dependence on ϕ^* , and A/Σ varies over the entire range of possible values (from -100 to $+100\%$); thus, it can be seen that varying the polarization direction can provide a useful way to separate the various polarization tensors.

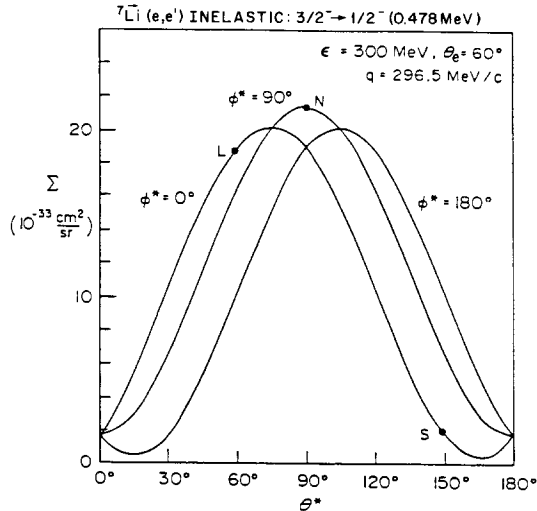


FIG. 30. Inelastic electron scattering from polarized ${}^7\text{Li}$ ($\frac{3}{2}^- \rightarrow \frac{1}{2}^-$). The cross section Σ is displayed as a function of the polarization direction of the nucleus (θ^* , ϕ^*) for given electron scattering kinematics.

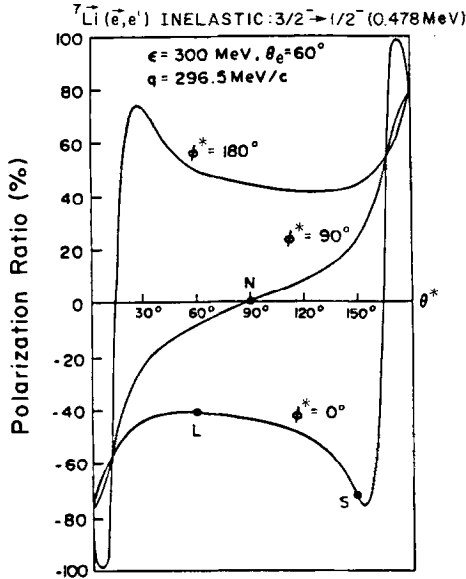


FIG. 31. Inelastic electron scattering from polarized ${}^7\text{Li}(\frac{3}{2}^- \rightarrow \frac{1}{2}^-)$. The polarization ratio Δ/Σ is displayed as a function of the polarization direction of the nucleus (θ^* , ϕ^*) for given electron scattering kinematics.

Let us now discuss the sensitivity of our results to changes in the nuclear structure input being used. Again, we will examine the effect of suppressing and enhancing the magnetic M1 form factor by 50%. For the most part, the basic shapes of the various curves are unaffected by these changes, because the magnetic dipole has zeros at 0 and 315 MeV/c; thus, the curves are constrained to intersect their "normal" values at these momentum transfers, and this limits the variations which are possible with this ansatz. For example, the maximum value of about 150% reached by all of the asymmetries is completely unaffected by the change in the dipole form factor, since the maxima are attained in the vicinity of 0 and 275 MeV/c where the M1 multipole is close to zero. However, the A_{NS} and A_{LS} curves become broadened when the form factor is suppressed, and these asymmetries are significantly increased in value away from the peaks; A_{NS} is zero at 75 MeV/c (rather than 115 MeV/c) and attains the value of 75% at 600 MeV/c, while A_{LS} increases twice as fast as usual near $q = 0$, is zero at about 560 MeV/c, and has the value of about -25% at 600 MeV/c. Finally, A_{LN} decreases much faster from its maximum at zero momentum transfer, passing through zero at 225 MeV/c; however, no significant differences are evident beyond about 300 MeV/c. Similarly, $(\Delta/\Sigma)_L$ is essentially unchanged over the entire range of the momentum transfer, while the locations of the peaks in $(\Delta/\Sigma)_S$ near 250 MeV/c are decreased by about 30 MeV/c, although the magnitude of the peaks is increased by less than 5 percentage points; however, this polarization ratio increases beyond 300 MeV/c until it reaches the value of

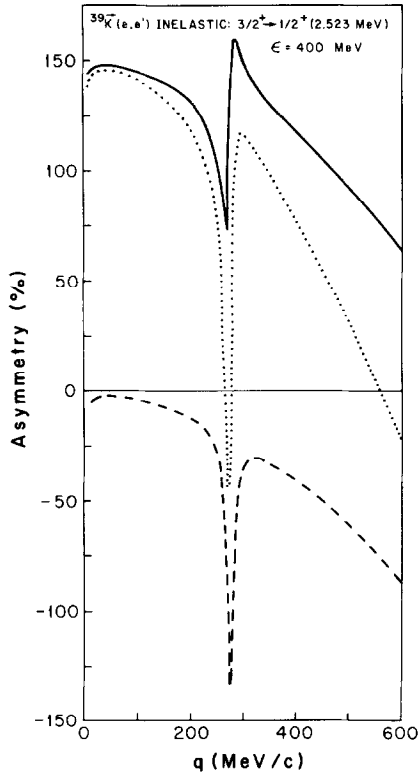


FIG. 32. Inelastic electron scattering from polarized $^{39}\text{K}(\frac{3}{2}^+ \rightarrow \frac{1}{2}^+)$. The three asymmetries defined in Eq. (3.1) are shown using the convention of (3.3): A_{NS} (—), A_{LN} (---), and A_{LS} (···).

–10% at 600 MeV/c, and the positive results which are observed in the absence of the suppression never appear.

If we now enhance the M1 factor, then the peaks in A_{NS} and A_{LS} become noticeably narrower, although the sizes of the peaks are again unchanged. A_{NS} is now reduced in value away from the peaks, reaching zero at the higher momentum transfer of 150 MeV/c and attaining the value of 5% at 600 MeV/c; similar results apply to A_{LS} , except that a zero occurs at 480 MeV/c (rather than 510 MeV/c as was the case in the absence of the enhancement) and A_{LS} has the value of –75% at 600 MeV/c. However, the only changes in A_{LN} are the increase in value of the asymmetry by about 15 percentage points between 100 and 250 MeV/c and beyond 500 MeV/c. Again, $(\Delta/\Sigma)_{\text{L}}$ is unaffected by the change in the dipole form factor, while $(\Delta/\Sigma)_{\text{S}}$ is increased by about 25 percentage points beyond 400 MeV/c.

Next, we consider the transition $\frac{3}{2}^+ \rightarrow \frac{1}{2}^+$ (2.523 MeV) for the nucleus ^{39}K , where we are describing the excited state as a $2s_{1/2}$ proton hole below ^{40}Ca in the extreme-single-particle model with an harmonic oscillator basis with $b = 2.0$ fm. In this case, the C2, E2, and M1 form factors exhibit much more structure than was the case for

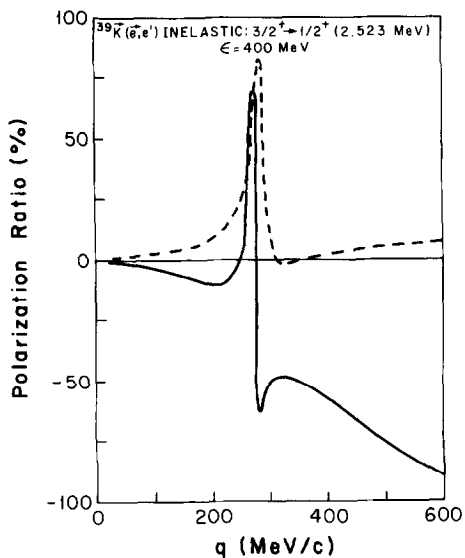


FIG. 33. Inelastic electron scattering from polarized $^{39}\text{K} (\frac{3}{2}^+ \rightarrow \frac{1}{2}^+)$. The two polarization ratios defined at the beginning of the section are shown using the convention of (3.4): $(d/\Sigma)_L$ (—), and $(d/\Sigma)_S$ (---); $(d/\Sigma)_N$ is identically zero.

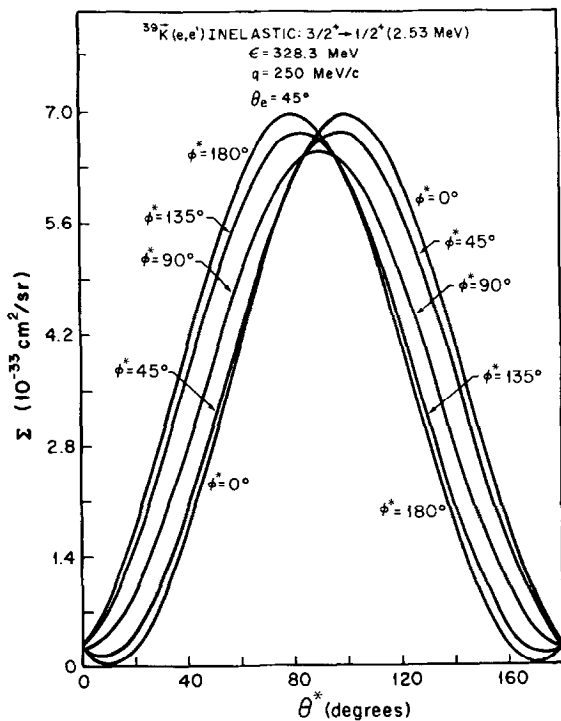


FIG. 34. Inelastic electron scattering from polarized $^{39}\text{K} (\frac{3}{2}^+ \rightarrow \frac{1}{2}^+)$. The cross section Σ is displayed as a function of the polarization direction of the nucleus (θ^*, ϕ^*) for given electron scattering kinematics.

${}^7\text{Li}$; the Coulomb quadrupole dominates only for $q < 200$ MeV/c. Then, we find that $\Sigma_L > 10^{-33}$ cm²/sr for $q < 450$ MeV/c at $\varepsilon = 300$ MeV/c; as the energy increases, so does this limiting value of q . The asymmetries A_{ij} are shown in Fig. 32 for an electron energy of 400 MeV; note that they are very large over essentially the entire momentum range. The extremely large and rapid variations observed at about 280 MeV/c are due to the fact that both the C2 and M1 form factors have zeros near that value of the momentum transfer; in addition, the electric quadrupole form factor has a zero at about 255 MeV/c, and so also contributes to this effect.

A similar rapid variation at the same momentum transfer can be seen for the $(\Delta/\Sigma)_i$ (see Fig. 33). Note that $(\Delta/\Sigma)_L$ is significant over an extended range of q , while $(\Delta/\Sigma)_S$ tends to be quite small beyond the peak at 280 MeV/c. Finally, we consider the variation of Σ and Δ/Σ as the polarization direction varies. As a result of the absence of the coherent Coulomb monopole for inelastic scattering, Σ is very sensitive to the value of θ^* , since the unpolarized part of the cross section, which is independent of the choice of the polarization direction, is no longer dominant; also, Σ can be seen to have a significant dependence on ϕ^* . In addition, Δ/Σ tends to be small under the same kinematic conditions except for values of θ^* within 30° of 0 and 180° (see Figs. 34 and 35).

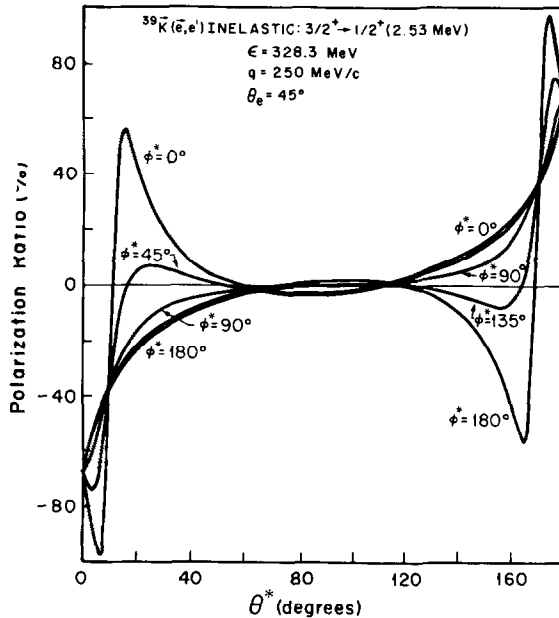


FIG. 35. Inelastic electron scattering from polarized ${}^{39}\text{K}(\frac{3}{2}^+ \rightarrow \frac{1}{2}^+)$. The polarization ratio Δ/Σ is displayed as a function of the polarization direction of the nucleus (θ^* , ϕ^*) for given electron scattering kinematics.

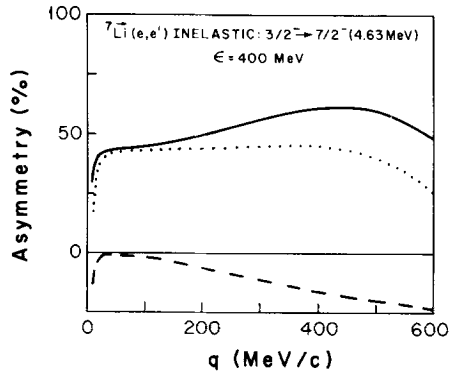


FIG. 36. Inelastic electron scattering from polarized ${}^7\text{Li}(\frac{3}{2}^- \rightarrow \frac{7}{2}^-)$. The three asymmetries defined in Eq. (3.1) are shown using the convention of (3.3): A_{NS} (—), A_{LN} (---), and A_{LS} (···).

(vii) *Inelastic Scattering*: $J_i = \frac{3}{2}$, $J_f = \frac{7}{2}$, $\Delta\pi = no$

In general, the electromagnetic form factors which are possible for this transition include the C2, C4, E2, E4, M3, and M5 multipoles. If we restrict ourselves to a $1s-1p$ model space and one-body electromagnetic current operators, then only the C2, E2, and M3 form factors are nonvanishing for the resulting shell-model calculations. However, if we include the effects of the two-body meson-exchange currents, then the transverse E4 and M5 multipoles can be nonzero [67]; similarly, extending our model space to include single-particle admixtures beyond the $1p$ shell would result in nonzero contributions to the C4, E4, M3, and M5 form factors. Then, we can see that the use of electron and nuclear polarizations as a “multipole

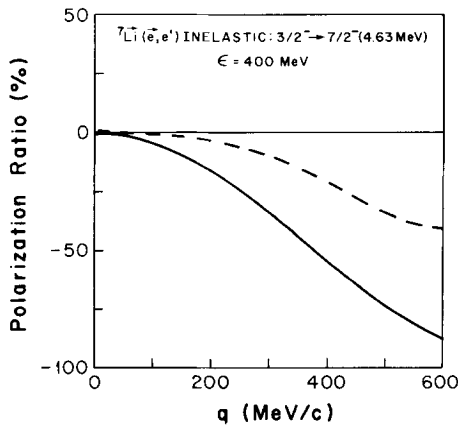


FIG. 37. Inelastic electron scattering from polarized ${}^7\text{Li}(\frac{3}{2}^- \rightarrow \frac{7}{2}^-)$. The two polarization ratios defined at the beginning of the section are shown using the convention of (3.4): $(A/S)_L$ (—), and $(A/S)_S$ (---); $(A/S)_N$ is identically zero.

meter" to separate the various form factors from each other may be a very nice way to demonstrate the effects of meson-exchange currents and/or configuration admixtures on the electromagnetic structure of the ${}^7\text{Li}$ nucleus.

In particular, certain combinations of the reduced response functions \mathcal{W}_J^K which eliminate the F_{C2}^2 , F_{E2}^2 , and F_{M3}^2 terms can be considered in order to see the presence of any additional effects. For instance, it follows from Eq. (2.64) that, for this transition,

$$\mathcal{W}_0^L + \frac{7}{2}\mathcal{W}_2^L = 4F_{C4}(F_{C4} - (3\sqrt{5}/2)F_{C2}) \quad (3.28a)$$

and

$$\begin{aligned} \mathcal{W}' &\equiv \mathcal{W}_0^T + \frac{22}{89}\mathcal{W}_2^T - \frac{600}{89}\mathcal{W}_2^{TT} - \frac{43}{89}\mathcal{W}_1^{T'}, \\ &= \frac{1}{89} \left(\frac{2016}{5}(F_{M5})^2 + \frac{1544}{5}(F_{E4})^2 - 144\sqrt{2}F_{M3}F_{M5} + 40\sqrt{6}F_{E2}F_{E4} \right. \\ &\quad \left. + 72\sqrt{7}F_{E4}F_{M3} - (888\sqrt{14}/5)F_{E4}F_{M5} \right), \end{aligned} \quad (3.28b)$$

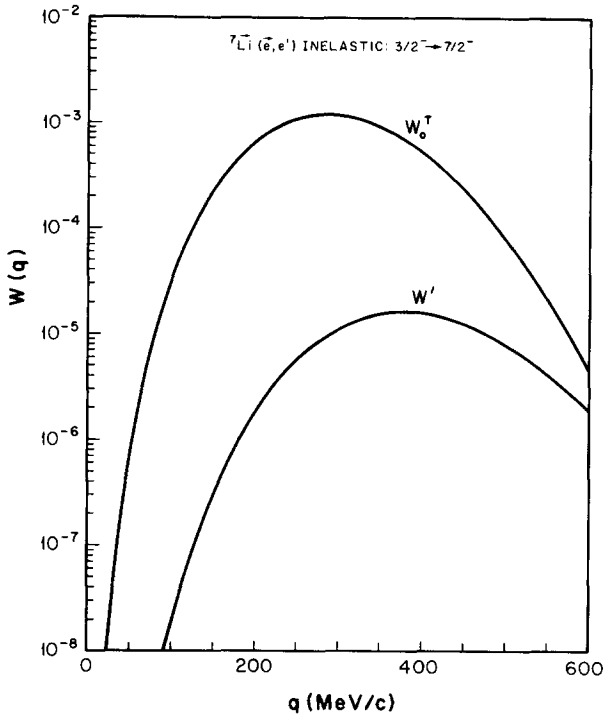


FIG. 38. Inelastic electron scattering from polarized ${}^7\text{Li}(\frac{3}{2}^- \rightarrow \frac{7}{2}^-)$. The response function \mathcal{W}_0^T is displayed for the shell model, while the function \mathcal{W}' defined in Eq. (3.28b) is displayed when the meson-exchange-current effects are taken into account.

and so both of these combinations would vanish identically in the absence of meson-exchange currents and configuration admixtures beyond the $1s-1p$ shell.

An example of this nuclear transition consists of the electro-excitation of the $\frac{3}{2}^-$ ground state of ${}^7\text{Li}$ to the $\frac{7}{2}^-$ (4.63 MeV) excited state. In this case, we will be comparing the results of a Cohen and Kurath $1s-1p$ shell-model description when the effects of meson-exchange currents are or are not included [56]. In both cases, Σ_L exceeds the practical limit of $10^{-33} \text{ cm}^2/\text{sr}$ for momentum transfers below 450 MeV/c at an energy of 400 MeV. As can be seen in Fig. 36, the asymmetries A_{ij} for the shell-model case are significant even if they do not display very much variation over the entire range of q , and similar results are valid for the polarization ratios $(A/\Sigma)_i$, as can be seen from Fig. 37. To examine the effects of meson-exchange currents (MEC), we consider the usual transverse form factor $\mathcal{W}_0^T = 2(F_{E2}^2 + F_{E4}^2 + F_{M3}^2 + F_{M5}^2)$, in the absence of any MEC effects, and the quantity \mathcal{W}' , including these effects. As can be seen from Fig. 38, \mathcal{W}' is about two orders of magnitude below \mathcal{W}_0^T , indicating the roughly 10% effect of the meson-exchange currents on the various transverse form factors. Since \mathcal{W}' would be identically zero in the absence of the MEC or extended-model-space effects, one could hope that a measurement of the various reduced response functions contained in \mathcal{W}' would provide an indication of the existence of the E4, M3, and M5 multipoles for the transition, thereby revealing important nuclear structure information about ${}^7\text{Li}$.

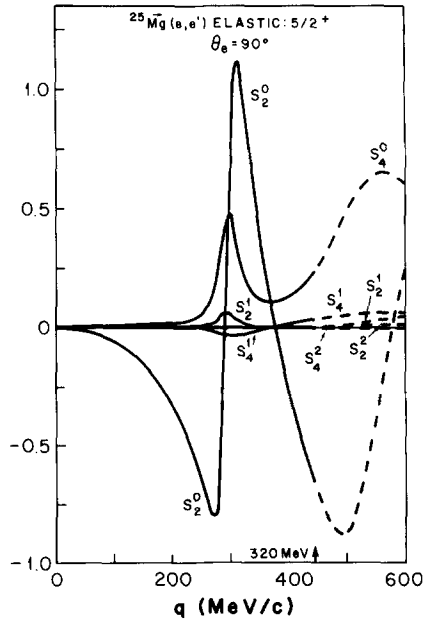


FIG. 39. Elastic electron scattering from polarized ${}^{25}\text{Mg}$ ($\frac{5}{2}^+$). The polarization tensors $S_{ij}^{\mathcal{G}}$ with even \mathcal{G} are displayed as functions of the momentum transfer for a fixed scattering angle of 90° .

(viii) *Elastic Scattering*: $J_i = J_f = \frac{5}{2}$

For this case, we will consider elastic scattering from the ground states of ^{25}Mg and ^{27}Al . Again, it will not be very useful to write out the explicit forms for the $S_{\mathcal{J}}^{\mathcal{H}}(q, \theta_e)$ in terms of the multipole form factors; anyone interested in the expansions should consult Eq. (2.64). The multipoles which are possible include the C0, C2, C4, M1, M3, and M5 form factors. We consider the case of ^{25}Mg , where we will compare the results of a shell-model calculation [56] to those of the deformed Nilsson model. The harmonic oscillator parameter was taken to be 1.70 fm for both models (that is, the magnetic form factors for the Nilsson model were calculated using this value). First, we examine the behaviour of the $S_{\mathcal{J}}^{\mathcal{H}}$ for \mathcal{J} even, as dis-

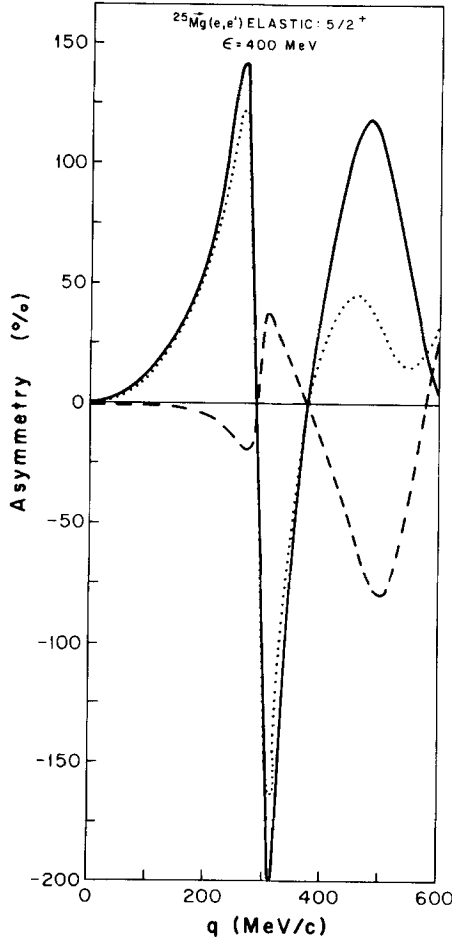


FIG. 40. Elastic electron scattering from polarized $^{25}\text{Mg}(\frac{5}{2}^+)$. The three asymmetries defined in Eq. (3.1) are shown using the convention of (3.3): A_{NS} (—), A_{LN} (---), and A_{LS} (···).

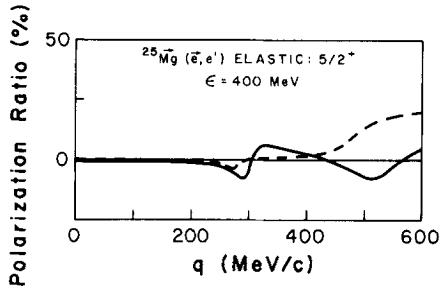


FIG. 41. Elastic electron scattering from polarized ^{25}Mg ($\frac{5}{2}^+$). The two polarization ratios defined at the beginning of the section are shown using the convention of (3.4): $(\Delta/\Sigma)_L$ (—), and $(\Delta/\Sigma)_S$ (---); $(\Delta/\Sigma)_N$ is identically zero.

played in Fig. 39 for $\theta_e = 90^\circ$ for the shell model; as can be seen, there is considerable variation in these functions. Now, we examine the asymmetries which are displayed in Fig. 40 as obtained for the shell model; as can be seen, large variations can occur over the entire range of useful momentum transfer, due to the fact that the Coulomb monopole does not overwhelm the other form factors beyond 300 MeV/c. However, such effects are not observed for the polarization ratios (see Fig. 41), and the $(\Delta/\Sigma)_i$ have magnitudes of more than 10% only beyond 500 MeV/c, since the scattering angle θ_e is then close to 180° .

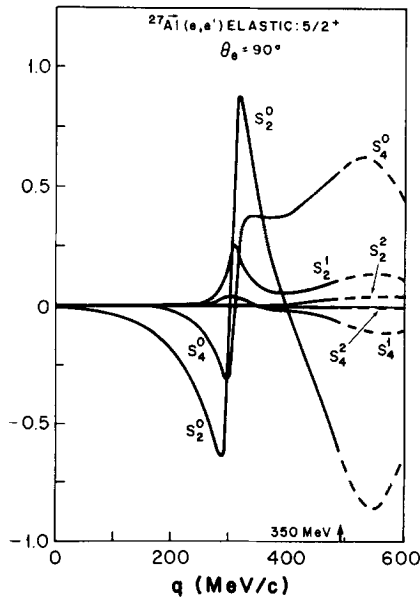


FIG. 42. Elastic electron scattering from polarized ^{27}Al ($\frac{5}{2}^+$). The polarization tensors S_j^k with even j are displayed as functions of the momentum transfer for a fixed scattering angle of 90° .

Next, we consider the Nilsson model, for which the Coulomb form factors were determined using a deformed three-parameter Fermi parameterization for the charge density; the transverse form factors were calculated using the Nilsson model for the applicable $\frac{5}{2}^+ [202]$ configuration [37, 68]. The asymmetries and polarization ratios resulting from this model are qualitatively similar to the shell-model results, although significant quantitative differences can be seen for the A_{ij} . For instance, A_{NS} and A_{LS} rise somewhat more rapidly at low q , and the values at the peaks are increased by about 10 percentage points. At higher momentum transfers, larger differences can be observed; the peaks seen near 450 MeV/c for these two asymmetries are increased in value by about 20 percentage points and shifted to a lower momentum transfer by about 50 MeV/c, and both A_{NS} and A_{LS} then decrease in value to about -35% at 500 MeV/c. Finally, A_{LN} shows somewhat smaller differences, as the peaks near 300 MeV/c are lowered in value by under 5 percentage points and their locations are decreased by about 10 MeV/c.

As another spin- $\frac{5}{2}$ ground state, we consider the case for which the target nucleus is ^{27}Al , which we will describe in terms of both the extreme-single-particle model

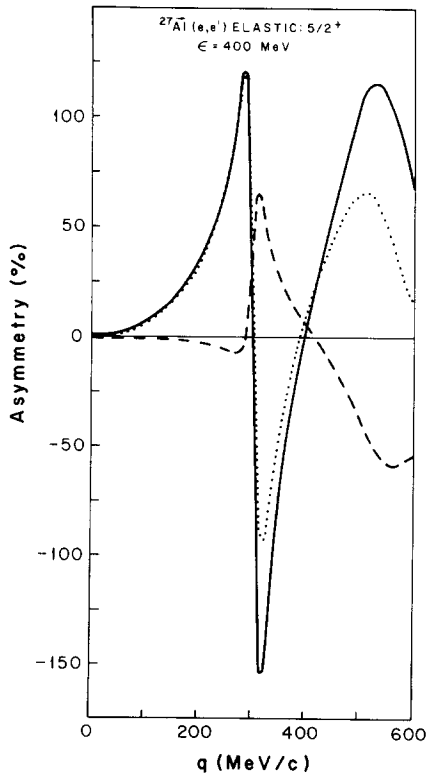


FIG. 43. Elastic electron scattering from polarized $^{27}\text{Al}(\frac{5}{2}^+)$. The three asymmetries defined in Eq. (3.1) are shown using the convention of (3.3): A_{NS} (—), A_{LN} (---), and A_{LS} (···).

(i.e., as a $1d_{5/2}$ proton below ^{28}Si), and the shell model [56]; in either model, we take harmonic oscillator wavefunctions with $b = 1.59$ fm. In this case, the practical limit on the cross section is reached for a momentum transfer of 550 MeV/c for an energy of 300 MeV; at higher energies, this limit is reached for larger values of q . The polarization tensors S_{ij}^{μ} which are accessible in the absence of any electron polarization are shown in Fig. 42 for a scattering angle of 90° for the shell model. As can be seen, a great deal of variation is observable beyond 250 MeV/c. If we examine the behaviour of the asymmetries A_{ij} as shown in Fig. 43 for the shell model, we can see that the existence of two zeros for the charge form factor (at $q \approx 310$ and 635 MeV/c) results in an extremely large variation in the asymmetries extending over essentially the entire accessible range of the momentum transfer. If we now consider the polarization ratios $(\Delta/\Sigma)_i$, as shown in Fig. 44 for the shell model, we can see the usual peaks corresponding to the first zero of the Coulomb monopole near 300 MeV/c; however, in this case, the peaks have a magnitude of less than 15%, and very little additional structure can be seen at higher momentum transfers.

If we now compare the results for the shell model with those obtained using the extreme-single-particle model, we find that the qualitative behaviours of the asymmetries and polarization ratios are very similar for the two models, although reasonably large differences in magnitude can be observed. For instance, the large peaks seen near 310 MeV/c for the asymmetries are reduced by about 25 percentage points for the single-particle model, while the peaks in A_{NS} and A_{LS} beyond 500 MeV/c are reduced in value by approximately 10 percentage points and displaced by about 20 MeV/c toward higher values of the momentum transfer. Also, A_{LN} is increased in value by about 10 percentage points between 400 and 500 MeV/c, and reaches the value of -100% at 600 MeV/c. Finally, $(\Delta/\Sigma)_L$ exhibits significant differences only beyond 400 MeV/c, where it decreases to 5% at 440 MeV/c and then rapidly increases in value at higher momentum transfers until

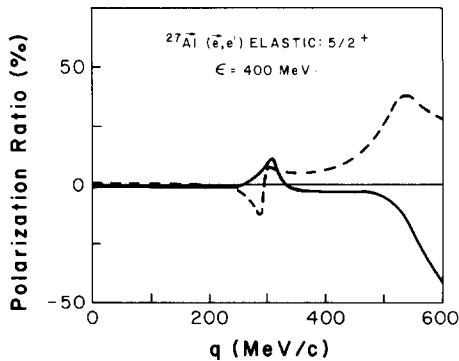


FIG. 44. Elastic electron scattering from polarized ^{27}Al ($\frac{5}{2}^+$). The two polarization ratios defined at the beginning of the section are shown using the convention of (3.4): $(\Delta/\Sigma)_L$ (—), and $(\Delta/\Sigma)_S$ (---); $(\Delta/\Sigma)_N$ is identically zero.

it peaks at the value of 80% at 600 MeV/c; however, $(\Delta/\Sigma)_S$ does not exhibit the same drastic effects, although it is twice as large as the shell-model results between 350 and 500 MeV/c, and 25% smaller beyond 550 MeV/c.

(ix) *Inelastic Scattering*: $J_i = \frac{5}{2}$, $J_f = \frac{1}{2}, \frac{3}{2}, \frac{5}{2}, \frac{7}{2}$, and $\frac{9}{2}$, $\Delta\pi = no$

As examples of these transitions, we consider the electro-excitation of ^{25}Mg to its first nine positive-parity excited states; the level scheme for this nucleus is given in Fig. 45 [69]. The multipoles which are possible for these values of J_f are C2, E2, and M3 for $J_f = \frac{1}{2}$; C2, C4, E2, E4, M1, and M3 for $J_f = \frac{3}{2}$; C0, C2, C4, E2, E4, M1, M3, and M5 for $J_f = \frac{5}{2}$; C2, C4, C6, E2, E4, E6, M1, M3, and M5 for $J_f = \frac{7}{2}$; and C2, C4, C6, E2, E4, E6, M3, M5, and M7 for $J_f = \frac{9}{2}$. All of the values of J_f , with the exception of $J_f = \frac{9}{2}$, occur for two different levels, and so we will be able to demonstrate the effect of nuclear structure on the quantities of interest. For all of the transitions under consideration, we will be using the shell model [56]; in addition, we will also discuss the transitions to the $\frac{7}{2}^+$ (1.614 MeV) and the $\frac{9}{2}^+$ (3.405 MeV) states in the context of the deformed Nilsson model, since these levels are in the same $\frac{5}{2}^+$ [202] rotational band as the ground state.

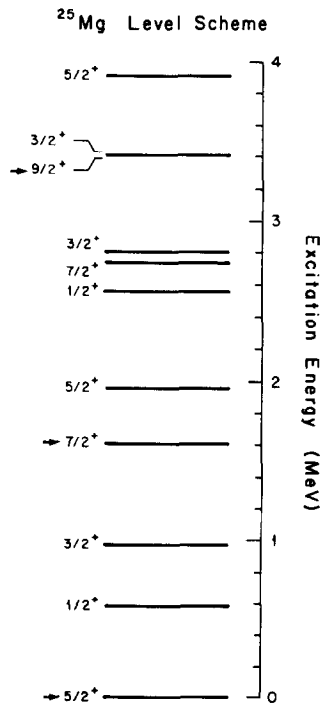


FIG. 45. Nuclear level scheme for ^{25}Mg (from [69]). The levels in the ground state rotational band are indicated by arrows.

As can be seen in Figs. 46–49 for $J_f = \frac{1}{2}$, Figs. 50–53 for $J_f = \frac{3}{2}$, and Figs. 54–57 for $J_f = \frac{5}{2}$, extremely large differences for the asymmetries and polarization ratios can be observed over large ranges of the momentum transfer for different excited states with the same spin. For $J_f = \frac{7}{2}$, we again observe radically different behaviours in these quantities for the two excited states (see Figs. 58–62); in addition, large variations are evident when we compare the shell and deformed models for the $\frac{7}{2}^+$ (1.614 MeV) state (see Figs. 58 and 59, respectively). Similar results are valid for the $J_f = \frac{9}{2}$ excited state, as can be seen by examining the behaviour of the asymmetries for the shell and deformed models as shown in Figs. 63 and 64, respectively. Note especially the fact that the signs of the A_{ij} are reversed for the two models

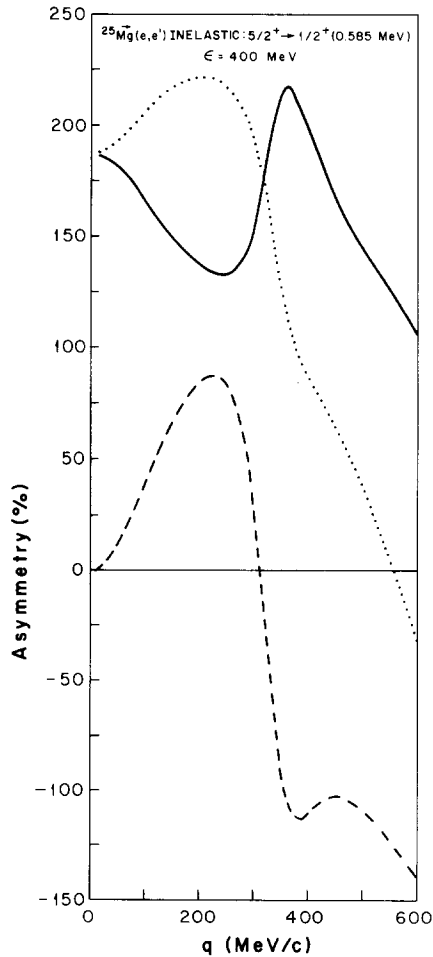


FIG. 46. Inelastic electron scattering from polarized $^{25}\text{Mg}(\frac{5}{2}^+ \mapsto \frac{1}{2}^+ \neq 1)$. The three asymmetries defined in Eq. (3.1) are shown using the convention of (3.3): A_{NS} (—), A_{LN} (---), and A_{LS} (···).

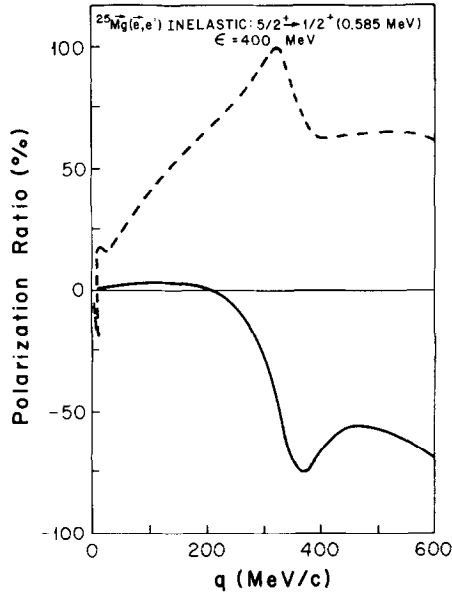


FIG. 47. Inelastic electron scattering from polarized $^{25}\text{Mg}(\frac{5}{2}^+ \rightarrow \frac{1}{2}^+ \#1)$. The two polarization ratios defined at the beginning of the section are shown using the convention of (3.4): $(\Delta/\Sigma)_L$ (—), and $(\Delta/\Sigma)_S$ (---); $(\Delta/\Sigma)_N$ is identically zero.

beyond 375 MeV/c. Finally, we show the polarization ratios $(\Delta/\Sigma)_i$ for the transition to this state in Fig. 65 for the shell model.

(x) *Elastic Scattering*: $J_i = J_f = \frac{7}{2}$

An example of such a nucleus is provided by ^{59}Co , which we treat in the deformed Nilsson model as a $\frac{7}{2}^- [303]$ configuration which becomes a $1f_{7/2}$ proton in the spherical limit [37]. Again, we calculate the Coulomb form factors from a deformed two-parameter Fermi fit while using the Nilsson model with harmonic oscillator wavefunctions having $b = 1.9$ fm for the magnetic form factors. At an energy of 300 MeV/c, Σ_L exceeds the practical limit of 10^{-33} cm²/sr for momentum transfers below 500 MeV/c. As can be seen from Fig. 66, extremely large variations occur for the asymmetries A_{ij} over the entire range of q , especially in the vicinity of the zeros of the coherent Coulomb monopole form factor at 250, 350, and 440 MeV/c.

At this point, we would like to emphasize that we are *not* taking into account the effects of the distortion of the electron wavefunctions in the Coulomb field of the nucleus under consideration. Because our formalism was developed using the PWBA, there is no easy way to determine the effects of such distortion on our results (with the exception of the first-order effect whereby the momentum transfer q is replaced by the usual effective momentum transfer). However, a simple analysis

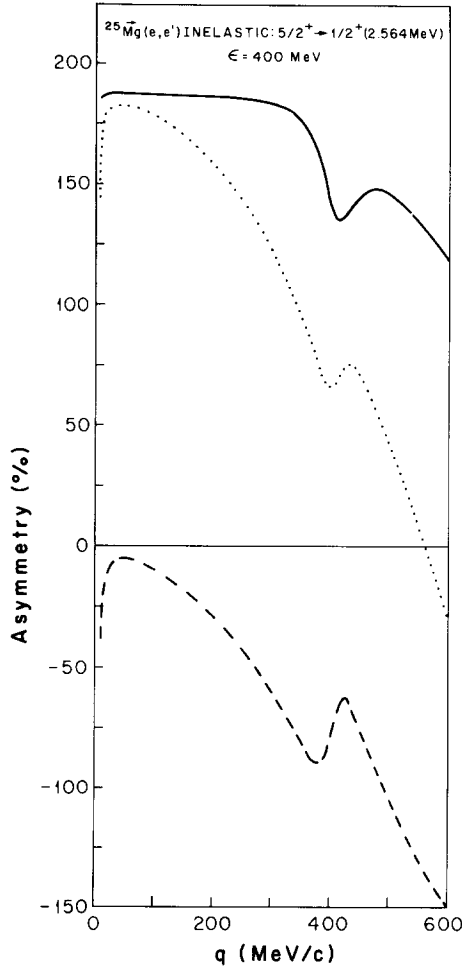


FIG. 48. Inelastic electron scattering from polarized $^{25}\text{Mg}(\frac{5}{2}^+ \mapsto \frac{1}{2}^+ \#2)$. The three asymmetries defined in Eq. (3.1) are shown using the convention of (3.3): A_{NS} (—), A_{LN} (---), and A_{LS} (···).

which we have performed for this problem (in effect, allowing regions about the diffraction minima to be filled in and to have arbitrary signs) indicates the large magnitudes of the asymmetries and polarization ratios which were obtained are not spurious; thus, although the filling-in of the zeros in the form factors, most importantly of the coherent CO contribution, due to the distortion will have an effect on our results, we expect our calculations to reflect at least the qualitative behaviour of the polarization cross sections. In spite of this, we feel that it is not very useful to pursue the PWBA in discussing elastic scattering from nuclei with high Z (such as ^{165}Ho and ^{181}Ta , which are potentially interesting cases), although we will consider the borderline cases of elastic scattering from ^{87}Sr and ^{93}Nb . We expect this

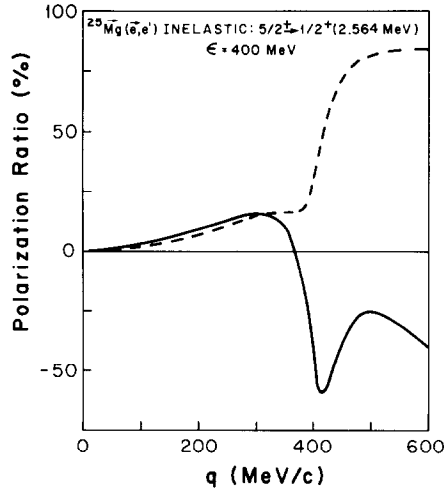


FIG. 49. Inelastic electron scattering from polarized $^{25}\text{Mg}(\frac{5}{2}^+ \mapsto \frac{1}{2}^+ \neq 2)$. The two polarization ratios defined at the beginning of the section are shown using the convention of (3.4): $(\Delta/\Sigma)_L$ (—), and $(\Delta/\Sigma)_S$ (---); $(\Delta/\Sigma)_N$ is identically zero.

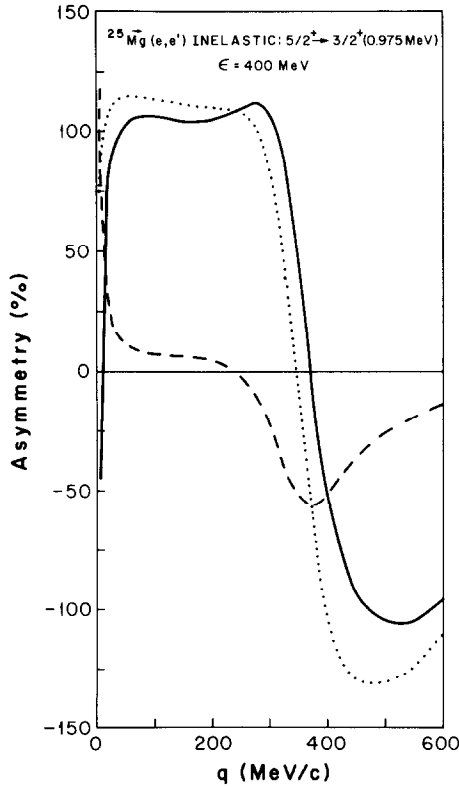


FIG. 50. Inelastic electron scattering from polarized $^{25}\text{Mg}(\frac{5}{2}^+ \mapsto \frac{3}{2}^+ \neq 1)$. The three asymmetries defined in Eq. (3.1) are shown using the convention of (3.3): A_{NS} (—), A_{LN} (---), and A_{LS} (···).

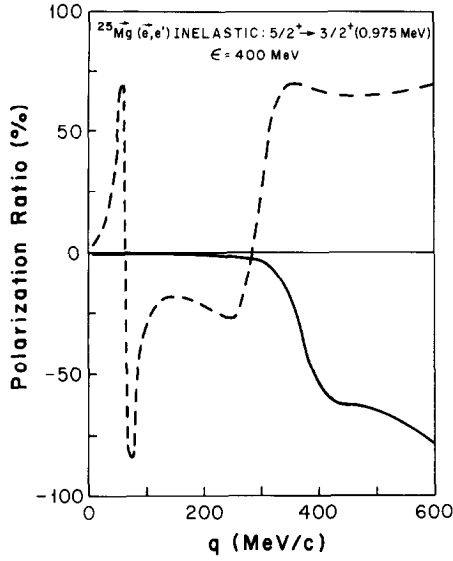


FIG. 51. Inelastic electron scattering from polarized $^{25}\text{Mg}(\frac{5}{2}^+ \mapsto \frac{3}{2}^+ \#1)$. The two polarization ratios defined at the beginning of the section are shown using the convention of (3.4): $(A/\Sigma)_L$ (—), and $(A/\Sigma)_S$ (---); $(A/\Sigma)_N$ is identically zero.

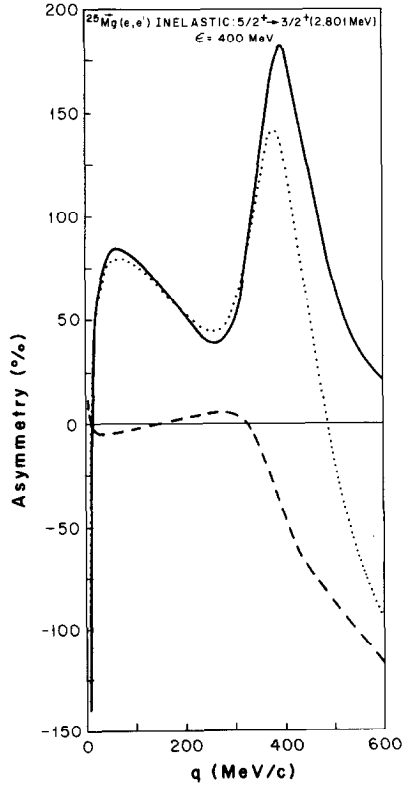


FIG. 52. Inelastic electron scattering from polarized $^{25}\text{Mg}(\frac{5}{2}^+ \mapsto \frac{3}{2}^+ \#2)$. The three asymmetries defined in Eq. (3.1) are shown using the convention of (3.3): A_{NS} (—), A_{LN} (---), and A_{LS} (···).

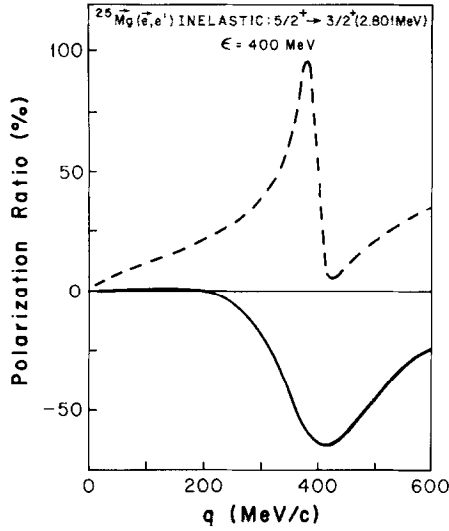


FIG. 53. Inelastic electron scattering from polarized $^{25}\text{Mg}(\frac{5}{2}^+ \mapsto \frac{3}{2}^+ \neq 2)$. The two polarization ratios defined at the beginning of the section are shown using the convention of (3.4): $(\Delta/\Sigma)_L$ (—), and $(\Delta/\Sigma)_S$ (---); $(\Delta/\Sigma)_N$ is identically zero.

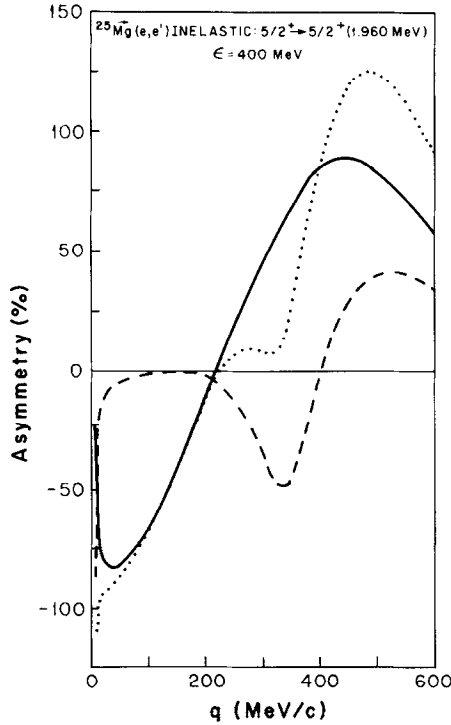


FIG. 54. Inelastic electron scattering from polarized $^{25}\text{Mg}(\frac{5}{2}^+ \mapsto \frac{5}{2}^+ \neq 1)$. The three asymmetries defined in Eq. (3.1) are shown using the convention of (3.3): A_{NS} (—), A_{LN} (---), and A_{LS} (···).

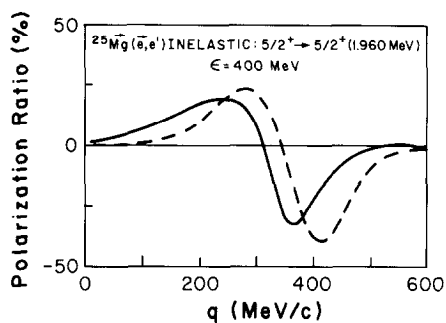


FIG. 55. Inelastic electron scattering from polarized $^{25}\text{Mg}(\frac{5}{2}^+ \mapsto \frac{5}{2}^+ \#1)$. The two polarization ratios defined at the beginning of the section are shown using the convention of (3.4): $(A/\Sigma)_L$ (—), and $(A/\Sigma)_S$ (---); $(A/\Sigma)_N$ is identically zero.

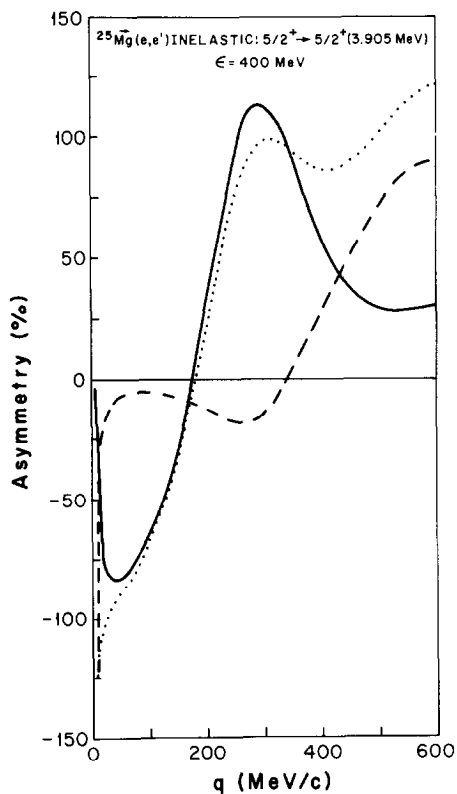


FIG. 56. Inelastic electron scattering from polarized $^{25}\text{Mg}(\frac{5}{2}^+ \mapsto \frac{5}{2}^+ \#2)$. The three asymmetries defined in Eq. (3.1) are shown using the convention of (3.3): A_{NS} (—), A_{LN} (---), and A_{LS} (···).

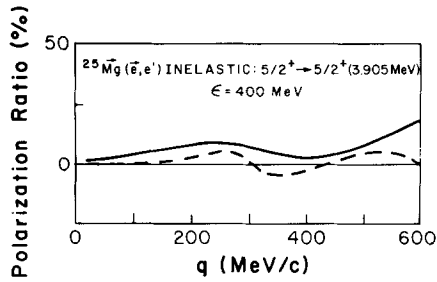


FIG. 57. Inelastic electron scattering from polarized ^{25}Mg ($\frac{5}{2}^+ \mapsto \frac{5}{2}^+ \#2$). The two polarization ratios defined at the beginning of the section are shown using the convention of (3.4): $(A/S)_L$ (—), and $(A/S)_S$ (---); $(A/S)_N$ is identically zero.

problem to be much less severe for inelastic scattering where the coherent C0 form factors do not occur and in fact we will consider the case of ^{181}Ta in the following subsection.

Returning to conclude our discussion of elastic scattering from ^{59}Co , we expect to find that this distortion would significantly reduce the magnitudes of the peaks in the A_{ij} at 180, 225, 275, and 375 MeV/c, although these peaks would not be drastically suppressed. As far as the polarization ratios are concerned, we find that they tend to be less than 5% except near the zeros of the Coulomb monopole and

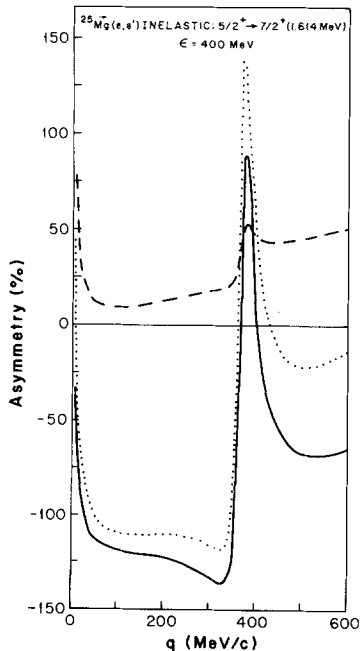


FIG. 58. Inelastic electron scattering from polarized ^{25}Mg ($\frac{3}{2}^+ \mapsto \frac{7}{2}^+ \#1$). The three asymmetries defined in Eq. (3.1) are shown using the convention of (3.3): A_{NS} (—), A_{LN} (---), and A_{LS} (···).

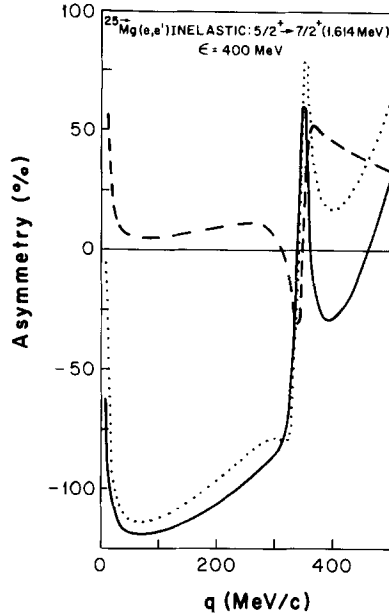


FIG. 59. Inelastic electron scattering from polarized $^{25}\text{Mg} (\frac{5}{2}^+ \mapsto \frac{7}{2}^+ \neq 1)$. The three asymmetries defined in Eq. (3.1) are shown using the convention of (3.3): A_{NS} (—), A_{LN} (---), and A_{LS} (···). Note that the results shown correspond to the deformed model.

at momentum transfers beyond 400 MeV/c, due to the dominance of the Coulomb form factor over an extended range of q .

(xi) *Inelastic Scattering*: $J_i = \frac{7}{2}$, $J_f = \frac{9}{2}$ and $\frac{11}{2}$, $\Delta\pi = no$

As examples of these transitions, we consider the excitation of the $\frac{7}{2}^+$ ground state of ^{181}Ta to the $\frac{9}{2}^+$ (0.136 MeV) and $\frac{11}{2}^+$ (0.302 MeV) states. These three states all belong to the same rotational band of the ground state, which in the deformed

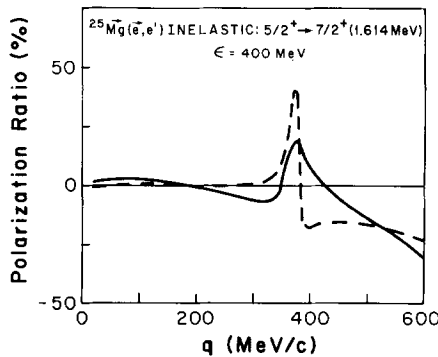


FIG. 60. Inelastic electron scattering from polarized $^{25}\text{Mg} (\frac{5}{2}^+ \mapsto \frac{7}{2}^+ \neq 1)$. The two polarization ratios defined at the beginning of the section are shown using the convention of (3.4): $(A/\Sigma)_L$ (—), and $(A/\Sigma)_S$ (---); $(A/\Sigma)_N$ is identically zero.

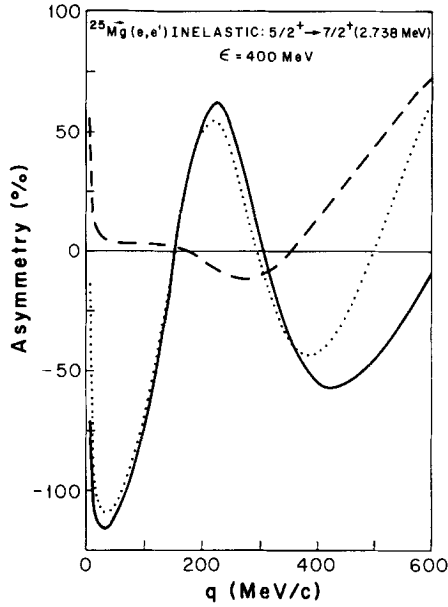


FIG. 61. Inelastic electron scattering from polarized $^{25}\text{Mg}(\frac{5}{2}^+ \rightarrow \frac{7}{2}^+ \# 2)$. The three asymmetries defined in Eq. (3.1) are shown using the convention of (3.3): A_{NS} (—), A_{LN} (---), and A_{LS} (···).

Nilsson model is the $\frac{7}{2}^+$ [404] proton intrinsic state with $\delta = 0.3$ [37, 68]. Again, we use a deformed two-parameter Fermi fit in order to calculate the Coulomb form factors, while the transverse electric and magnetic form factors are determined in the Nilsson model with harmonic oscillator wavefunctions with parameter $b = 2.0$ fm.

The form factors which are possible for the first transition include the C2, C4, C6, C8, E2, E4, E6, E8, M1, M3, M5, and M7 multipoles, although the E8 form

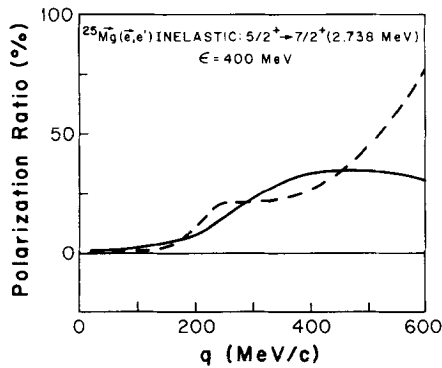


FIG. 62. Inelastic electron scattering from polarized $^{25}\text{Mg}(\frac{5}{2}^+ \rightarrow \frac{7}{2}^+ \# 2)$. The two polarization ratios defined at the beginning of the section are shown using the convention of (3.4): $(A/\Sigma)_L$ (—), and $(A/\Sigma)_S$ (---); $(A/\Sigma)_N$ is identically zero.

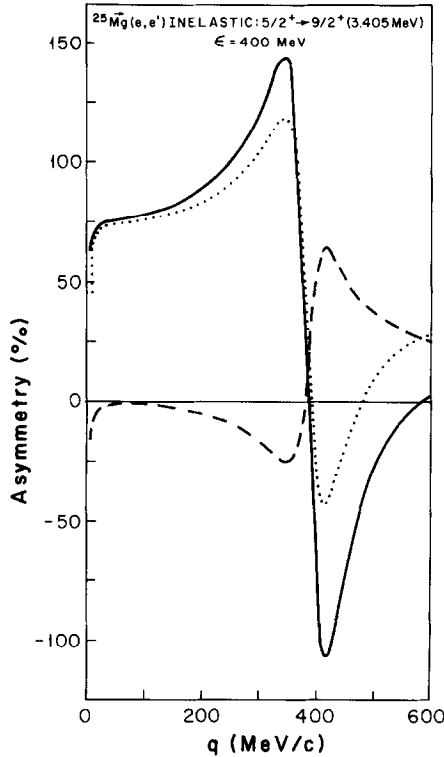


FIG. 63. Inelastic electron scattering from polarized $^{25}\text{Mg}(\frac{5}{2}^+ \rightarrow \frac{9}{2}^+)$. The three asymmetries defined in Eq. (3.1) are shown using the convention of (3.3): A_{NS} (—), A_{LN} (---), and A_{LS} (···).

factor is the only electric one which does not vanish in the Nilsson model [37]. Then, we find that Σ_L is above the practical limit for values of q of 450 MeV/c and below, for an energy of 300 MeV (again, as ε increases, so does the limiting value of q), and significant variations can be observed in the asymmetries as displayed in Fig. 67. Note that the effects from the collective core (which are not included here) are significant at low values of the momentum transfer, and so we do not show the asymmetries below 200 MeV/c. The effects seen near 200, 320, and 430 MeV/c are due to the zeros of the Coulomb quadrupole form factor, and so we expect that the distortion of the electron wavefunctions will soften the observed extreme behaviour (see subsect. (x) for a discussion of this point). In spite of this, the A_{ij} can be seen to be significantly large over the entire range of accessible momentum transfers. On the other hand, the polarization ratios $(\Delta/\Sigma)_i$ tend to be less than 5% except near the C2 zeros and so we do not display them here.

Similar results are obtained for inelastic scattering to the $\frac{11}{2}^+$ state, for which an M9 form factor is now permitted, while the M1 multipole is not. As shown in Fig. 68, the asymmetries are extremely large over the entire range of q and again

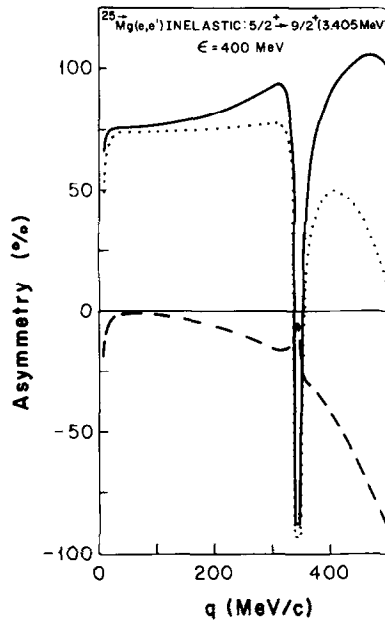


FIG. 64. Inelastic electron scattering from polarized $^{25}\text{Mg}(\frac{5}{2}^+ \rightarrow \frac{9}{2}^+)$. The three asymmetries defined in Eq. (3.1) are shown using the convention of (3.3): A_{NS} (—), A_{LN} (---), and A_{LS} (···). Note that the results shown correspond to the deformed model.

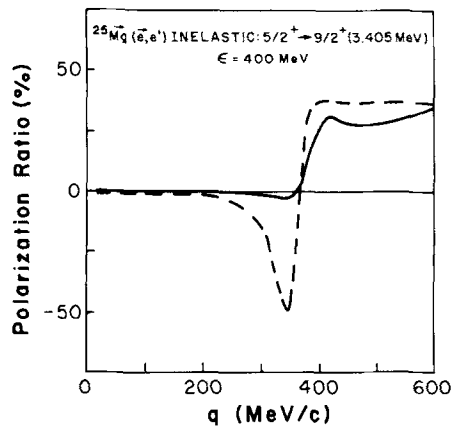


FIG. 65. Inelastic electron scattering from polarized $^{25}\text{Mg}(\frac{5}{2}^+ \rightarrow \frac{9}{2}^+)$. The two polarization ratios defined at the beginning of the section are shown using the convention of (3.4): $(A/\Sigma)_L$ (—), and $(A/\Sigma)_S$ (---); $(A/\Sigma)_N$ is identically zero.

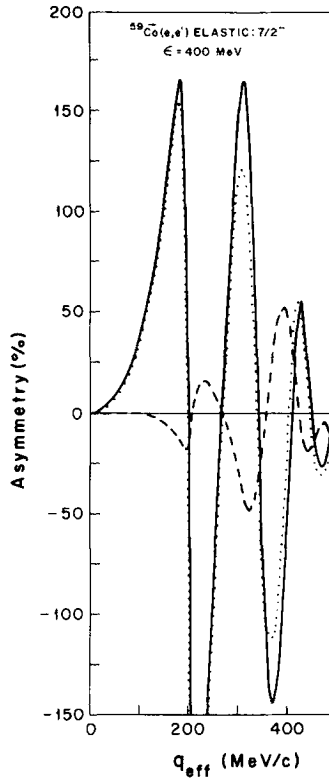


FIG. 66. Elastic electron scattering from polarized ^{59}Co ($\frac{7}{2}^-$). The three asymmetries defined in Eq. (3.1) are shown using the convention of (3.3): A_{NS} (—), A_{LN} (---), and A_{LS} (···).

exhibit extreme variations in the vicinity of the zero of the Coulomb quadrupole form factor, and the polarization ratios again are only significant near these zeros.

(xii) *Elastic Scattering*: $J_i = J_f = \frac{9}{2}$

Examples of such high-spin nuclei are ^{87}Sr , which may be treated as a single $1g_{9/2}$ neutron hole below a ^{88}Sr core, and ^{93}Nb , which we consider to be a $1g_{9/2}$ proton above ^{92}Zr [37]. For both nuclei, the electromagnetic multipoles which are possible are the C0, C2, C4, C6, C8, M1, M3, M5, M7, and M9 ones. Because these nuclei have relatively large charges, we expect that the distortion of the electron wavefunctions will have an important effect on our results and so the predictions made here should only be taken at the qualitative level (see subject. (x) for a discussion of this point). For the first case, we take $b = 2.0$ fm, and we have that $\Sigma_L > 10^{-33}$ cm²/sr for momentum transfers of 450 MeV/c and below, for an energy of 400 MeV. If we consider the asymmetries A_{ij} as shown in Fig. 69, we see that they are nearly zero below 400 MeV/c except in the vicinity of the zeros of the

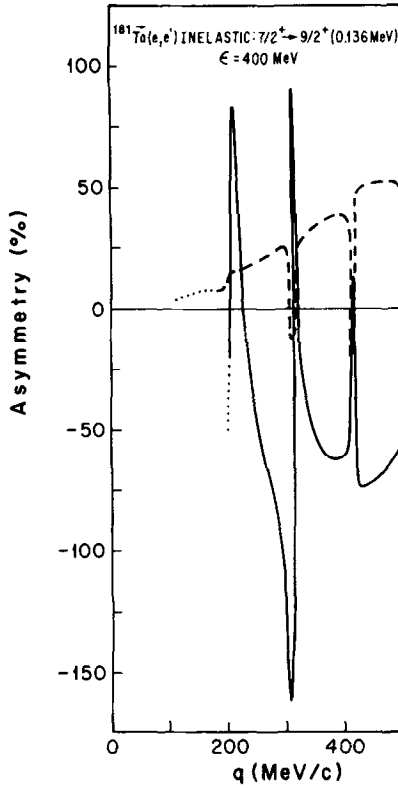


FIG. 67. Inelastic electron scattering from polarized $^{181}\text{Ta}(\frac{7}{2}^+ \rightarrow \frac{9}{2}^+)$. The asymmetries defined in Eq. (3.1) are shown using the convention of (3.3): A_{NS} (—) and A_{LN} (---).

charge form factor at 210, 335, and 485 MeV/c; because the nucleus has $Z \gg 1$, the asymmetries are severely suppressed between the first two zeros, in contrast to the low- Z cases discussed above. Again, the large asymmetries for $q > 520$ MeV/c are due to the $\tan \theta_e/2$ dependence of the kinematic factors (as $\theta_e \rightarrow 180^\circ$). As far as the polarization ratios A/Σ are concerned, the behaviour is similar to that for the asymmetries (see Fig. 70).

However, for the case of ^{93}Nb , for which we take $b = 2.03$ fm, a great deal of structure can be observed in the asymmetries over the entire range of the momentum transfer (see Fig. 71). For electron energies beyond 400 MeV, the cross section exceeds the practical limit below 450 MeV/c; in fact, at higher energies, this limit is pushed out to higher q (e.g., 600 MeV/c at 1 GeV). In addition, the polarization ratios as displayed in Fig. 72 indicate the effect that the choice of the polarization direction can have on the measured quantities; $(\Sigma/A)_L$ can be seen to be much greater in magnitude than $(\Sigma/A)_S$. Comparison of the results for these two spin- $\frac{9}{2}$ nuclei indicate the dependence of the form factors on whether the single particle is a neutron or a proton. As can be seen, the fact that the valence nucleon for ^{93}Nb is a

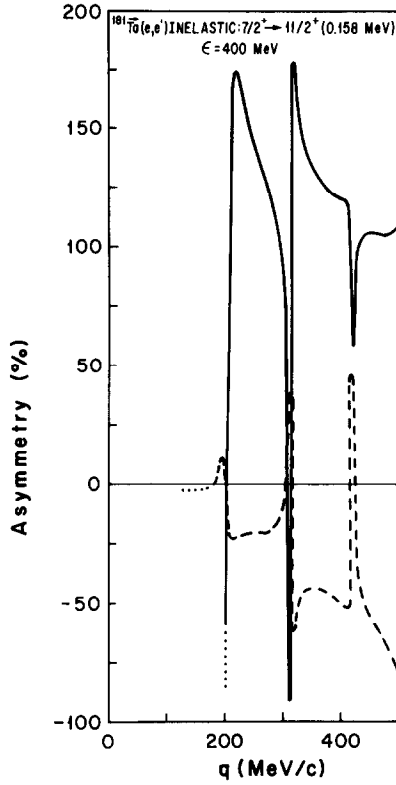


FIG. 68. Inelastic electron scattering from polarized $^{181}\text{Ta}(\frac{7}{2}^+ \rightarrow \frac{11}{2}^+)$. The asymmetries defined in Eq. (3.1) are shown using the convention of (3.3): A_{NS} (—) and A_{LN} (---).

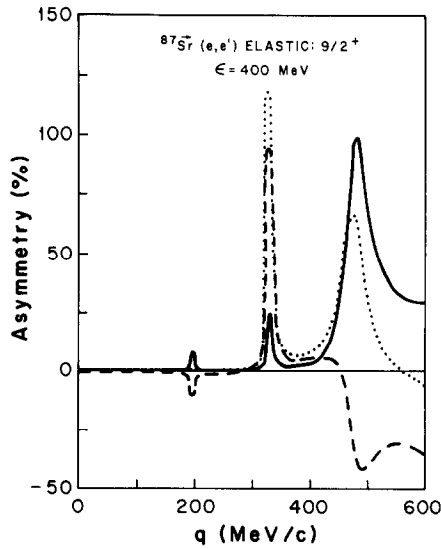


FIG. 69. Elastic electron scattering from polarized $^{87}\text{Sr}(\frac{9}{2}^+)$. The three asymmetries defined in Eq. (3.1) are shown using the convention of (3.3): A_{NS} (—), A_{LN} (---), and A_{LS} (···).

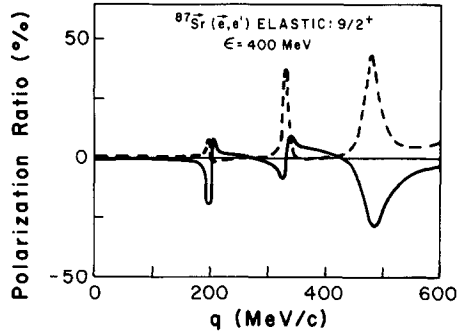


FIG. 70. Elastic electron scattering from polarized $^{87}\text{Sr}(\frac{9}{2}^+)$. The two polarization ratios defined at the beginning of the section are shown using the convention of (3.4): $(A/\Sigma)_L$ (—), and $(A/\Sigma)_S$ (---); $(A/\Sigma)_N$ is identically zero.

proton causes the asymmetries and polarization ratios to exhibit considerable structure over the entire range of momentum transfer, in contrast with the results for ^{87}Sr where a neutron is involved. This statement holds true because the closed proton shells have no contribution to the C2, C4, C6, and C8 multipole form factors, and so these multipoles are identically zero for ^{87}Sr within the context of this simple model. On the other hand, the valence proton in ^{93}Nb results in significantly

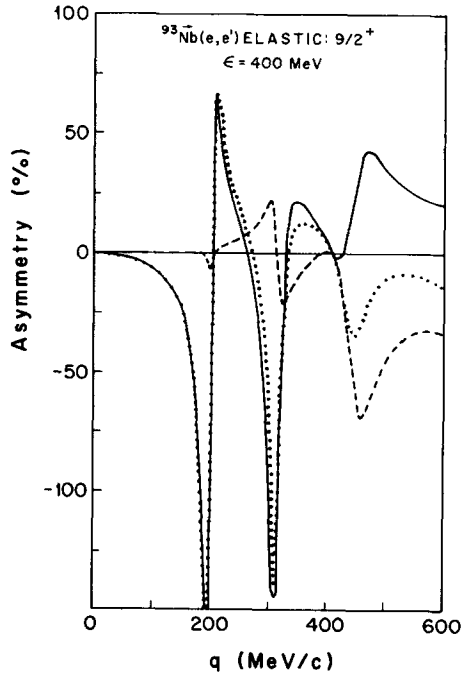


FIG. 71. Elastic electron scattering from polarized $^{93}\text{Nb}(\frac{9}{2}^+)$. The three asymmetries defined in Eq. (3.1) are shown using the convention of (3.3): A_{NS} (—), A_{LN} (---), and A_{LS} (···).

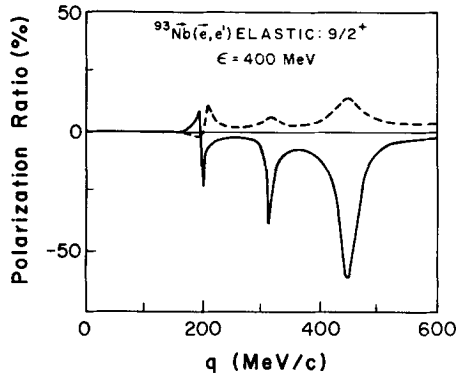


FIG. 72. Elastic electron scattering from polarized $^{93}\text{Nb}(\frac{9}{2}^+)$. The two polarization ratios defined at the beginning of the section are shown using the convention of (3.4): $(A/S)_L$ (—), and $(A/S)_S$ (---); $(A/S)_N$ is identically zero.

large Coulomb multipoles other than the C_0 ; all of the additional Coulomb form factors reach the level of the monopole at about 300 MeV/c, and the various interferences between the Coulomb and magnetic form factors results in the observed behaviour of the quantities of interest for this nucleus.

This concludes our discussion of polarization experiments for the selected illustrative nuclei. We will now summarize the results of Sections 2 and 3, and will give our conclusions concerning the usefulness of polarization studies for nuclear physics.

4. CONCLUSIONS

As discussed in this paper, the polarization degrees of freedom inherent in the inclusive electron-nucleus scattering process may be used as a powerful tool in extracting nuclear structure information. The required formalism was developed in Section 2, and was then applied to a variety of different nuclei and nuclear transitions in Section 3. The nuclei considered in the latter section ranged from low- A ones, such as the nucleon and the deuteron, to high- A nuclei, such as ^{181}Ta , and had spins ranging from $\frac{1}{2}-\frac{9}{2}$. In all cases, the use of the polarization degrees of freedom was seen to lead to significant effects in the scattering cross section, thereby indicating the usefulness of polarization in inclusive electron-nucleus scattering experiments.

There are four distinct classes of such scattering experiments which are possible, depending on whether or not the electrons and/or the nucleus are polarized:

- (1) Unpolarized electrons and an unpolarized nucleus.

In this case, only two quantities are accessible, F_L^2 and F_T^2 , the usual longitudinal and transverse form factors of Eq. (2.73). These contributions, which contain the

incoherent sums of the squares of the Coulomb and the transverse (electric and magnetic) multipole matrix elements respectively, may be separated from one another using the familiar Rosenbluth analysis. However, for nuclei with spins beyond $\frac{1}{2}$, the number of distinct electromagnetic multipole matrix elements which are possible from angular momentum, parity, and time-reversal-invariance considerations is greater than two, and so in general it is not possible in such experiments to determine these matrix elements individually.

(2) Unpolarized electrons, but a polarized nucleus.

In this case, new information is available, since we can now make a "super-Rosenbluth" separation of the electron-spin-averaged cross section Σ by varying the kinematic conditions while leaving the energy and momentum transfers fixed. This allows the determination of the L, T, TT, and TL response functions defined in Eq. (2.66). Furthermore, by varying the direction of nuclear polarization, as specified by θ^* and ϕ^* , it is possible to decompose each of these response functions into a larger number of terms involving specific interferences between the multipole matrix elements. Thus, in a mixed-multipole situation, in general much more information is now accessible than was possible for case (1) in the absence of any polarization.

(3) Polarized electrons, but an unpolarized nucleus.

In this case, the electron-polarization cross section Δ vanishes if parity is conserved, leading to a situation which is equivalent to case (1). Of course, the effects of parity violation, which in fact must occur due to the presence of the weak interaction, may be explored from a measurement of Δ as obtained by measuring the cross section for two different electron beam polarizations. In the present work we have assumed the conservation of parity and so have not considered such effects.

(4) Polarized electrons and a polarized nucleus.

This case is very similar to case (2), except that now the polarization of the electron beam may be used together with the "super-Rosenbluth" decomposition in order to determine the T' and TL' response functions of Eq. (2.66) along with the previous four response functions mentioned for case (2). The remainder of the analysis (i.e., the angular decomposition) is equivalent to that of case (2), and so it is apparent that the two additional response functions will provide us with more information than was possible in the absence of electron polarization.

In summary, it can be seen that at least nuclear polarization is necessary to extract from electron scattering additional nuclear structure information beyond that available from the usual Rosenbluth separation in the absence of any polarization; significantly more information can in principle be obtained if nuclear polarization is available. In addition, the use of a polarized electron beam allows the determination of still more information due to the presence of the two extra response functions. While it may not be possible in general to determine unambiguously all of the multipole matrix elements for inelastic scattering (as discussed in Appendix B), it should be noted that this problem was encountered in a more

severe form for the simpler Rosenbluth analysis in the absence of any electron or nuclear polarization. Thus, it can be seen that it is worthwhile to develop the necessary experimental facilities (electron stretcher rings, polarized targets, polarized electron beams, high-energy high-efficiency polarimeters for use with cw electron beams, etc.). In practice, the electron and nuclear polarizations which are required for such experiments appear to be attainable based on the level of technology which is presently available or being developed, and the resulting polarization studies which will be possible will provide an important means of extending the usefulness of electron scattering experiments in the not-too-distant future for the measurement of the electromagnetic properties of nuclei.

APPENDIX A: NOTATION AND CONVENTIONS

In this paper, we use the conventions of Bjorken and Drell [30], and we take physical units such that $\hbar = c = 1$. We denote Lorentz four-vectors by capital letters and three-vectors by boldface lowercase letters: $A \mapsto A^\mu = (A^0, \mathbf{a})$. The magnitude of a three-vector is written as a lowercase letter, $a = |\mathbf{a}|$. The scalar product of two four-vectors is denoted by $A \cdot B \equiv g_{\mu\nu} A^\mu B^\nu = A_\mu B^\mu = A^0 B^0 - \mathbf{a} \cdot \mathbf{b}$, where we have adopted the usual convention of summing repeated upper and lower Greek indices from zero to three and where we have taken the metric tensor to be

$$g_{\mu\nu} = g^{\mu\nu} = \begin{pmatrix} 1 & 0 & 0 & 0 \\ 0 & -1 & 0 & 0 \\ 0 & 0 & -1 & 0 \\ 0 & 0 & 0 & -1 \end{pmatrix}.$$

We use a caret above a quantity (as in \hat{T}) to denote that we are dealing with a second-quantization operator acting in the nuclear Hilbert space.

The Coulomb, electric, and magnetic operators are those considered in [25, 33]; their single-particle matrix elements are discussed and tabulated in [38, 39]. In these last references, several useful multipole identities are summarized. Throughout this paper, we use the angular momentum conventions of Edmonds [34].

APPENDIX B: INVERSE PROBLEM—REDUCED RESPONSE FUNCTIONS \mapsto FORM FACTORS

In this Appendix, we summarize a few identities which provide relationships among the various reduced response functions and then discuss the problem of determining the electromagnetic form factors given measurements of the set of $\mathcal{W}_g^{K'}$'s for a specific nuclear transition. To begin with, it is useful to define new

quantities involving sums of the reduced response functions weighted with 3-j coefficients,

$$U_m^L \equiv \sum_{\mathcal{J}} P_{\mathcal{J}}^+ [\mathcal{J}] (-1)^{J_i - m} \begin{pmatrix} J_i & J_i & \mathcal{J} \\ m & -m & 0 \end{pmatrix} \mathcal{W}_{\mathcal{J}}^L, \quad (\text{B.1a})$$

$$U_m^T \equiv \sum_{\mathcal{J}} P_{\mathcal{J}}^+ [\mathcal{J}] (-1)^{J_i - m} \begin{pmatrix} J_i & J_i & \mathcal{J} \\ m & -m & 0 \end{pmatrix} \mathcal{W}_{\mathcal{J}}^T, \quad (\text{B.1b})$$

$$U_m^{T'} \equiv \sum_{\mathcal{J}} P_{\mathcal{J}}^- [\mathcal{J}] (-1)^{J_i - m} \begin{pmatrix} J_i & J_i & \mathcal{J} \\ m & -m & 0 \end{pmatrix} \mathcal{W}_{\mathcal{J}}^{T'}, \quad (\text{B.1c})$$

$$U_m^{\text{TL}} \equiv (\sqrt{2}/4) \sum_{\mathcal{J}} P_{\mathcal{J}}^+ [\mathcal{J}] \sqrt{\mathcal{J}(\mathcal{J}+1)} (-1)^{J_i - (m+1)} \begin{pmatrix} J_i & J_i & \mathcal{J} \\ 1+m & -m & -1 \end{pmatrix} \mathcal{W}_{\mathcal{J}}^{\text{TL}}, \quad (\text{B.1d})$$

$$U_m^{\text{TL}'} \equiv (\sqrt{2}/4) \sum_{\mathcal{J}} P_{\mathcal{J}}^- [\mathcal{J}] \sqrt{\mathcal{J}(\mathcal{J}+1)} (-1)^{J_i - (m+1)} \begin{pmatrix} J_i & J_i & \mathcal{J} \\ 1+m & -m & -1 \end{pmatrix} \mathcal{W}_{\mathcal{J}}^{\text{TL}'}, \quad (\text{B.1e})$$

and

$$U_m^{\text{TT}} \equiv \sum_{\mathcal{J}} P_{\mathcal{J}}^+ [\mathcal{J}] \sqrt{(\mathcal{J}-1)\mathcal{J}(\mathcal{J}+1)(\mathcal{J}+2)} (-1)^{J_i - (m+2)} \begin{pmatrix} J_i & J_i & \mathcal{J} \\ 2+m & -m & -2 \end{pmatrix} \mathcal{W}_{\mathcal{J}}^{\text{TT}}. \quad (\text{B.1f})$$

By construction, the m 's are restricted to the following range:

$$\begin{aligned} -J_i \leq m \leq J_i & \quad \text{for L, T, T'}, \\ -J_i \leq m \leq J_i - 1 & \quad \text{for TL, TL}', \\ -J_i \leq m \leq J_i - 2 & \quad \text{for TT,} \end{aligned}$$

and from the symmetry properties of the 3-j coefficients [34] we have the following relationships:

$$U_{-m}^L = U_m^L, \quad (\text{B.2a})$$

$$U_{-m}^T = U_m^T, \quad (\text{B.2b})$$

$$U_{-m}^{T'} = -U_m^{T'}, \quad (\text{B.2c})$$

$$U_{-(1+m)}^{\text{TL}} = -U_m^{\text{TL}}, \quad (\text{B.2d})$$

$$U_{-(1+m)}^{\text{TL}'} = U_m^{\text{TL}'}, \quad (\text{B.2e})$$

and

$$U_{-(2+m)}^{\text{TT}} = U_m^{\text{TT}}. \quad (\text{B.2f})$$

It may be shown that various inequalities must be satisfied; in particular, we have that

$$U_m^L \geq 0, \quad (\text{B.3a})$$

$$U_m^T \geq |U_m^{T'}| \geq 0, \quad (\text{B.3b})$$

and thus it is natural to define the following nonnegative quantities:

$$V_m^L \equiv \sqrt{U_m^L} = V_{-m}^L \geq 0 \quad (\text{B.4a})$$

and

$$V_m^T \equiv \sqrt{U_m^T + U_m^{T'}} \geq 0. \quad (\text{B.4b})$$

Then, using Eqs. (B.2b) and (B.2c), we also have that

$$V_{-m}^T = \sqrt{U_m^T - U_m^{T'}} \geq 0. \quad (\text{B.4c})$$

Upon examining the specific expressions for the reduced response functions (Eq. (2.64)), it is possible to show that the magnitudes of the U_m^K for $K = \text{TL}, \text{TL}',$ and TT are determined by the quantities defined in Eq. (B.4),

$$|U_m^{\text{TL}} + U_m^{\text{TL}'}| = V_m^T V_{-(1+m)}^L, \quad (\text{B.5a})$$

$$|U_m^{\text{TT}}| = V_m^T V_{-(2+m)}^T, \quad (\text{B.5b})$$

and, using the symmetry properties of the U_m^K 's (see Eq. (B.2)),

$$|U_m^{\text{TL}} - U_m^{\text{TL}'}| = V_m^L V_{-(1+m)}^T. \quad (\text{B.5c})$$

These equations immediately yield a set of relationships (i.e., for the allowed ranges of m -values) that must be satisfied by the reduced response functions themselves. As just one example, let us consider odd-A nuclei and take $m = -\frac{1}{2}$ in Eq. (B.5a); this yields

$$|U_{-1/2}^{\text{TL}} + U_{-1/2}^{\text{TL}'}| = V_{-1/2}^T V_{-1/2}^L.$$

Upon substituting the above expressions for the U 's and V 's, we obtain

$$\begin{aligned} & \left[\sum_{\mathcal{J}} [\mathcal{J}] \begin{pmatrix} J_i & J_i & \mathcal{J} \\ -\frac{1}{2} & \frac{1}{2} & 0 \end{pmatrix} P_{\mathcal{J}}^+ \mathcal{W}_{\mathcal{J}}^L \right] \left[\sum_{\mathcal{J}} [\mathcal{J}] \begin{pmatrix} J_i & J_i & \mathcal{J} \\ -\frac{1}{2} & \frac{1}{2} & 0 \end{pmatrix} (P_{\mathcal{J}}^+ \mathcal{W}_{\mathcal{J}}^T + P_{\mathcal{J}}^- \mathcal{W}_{\mathcal{J}}^{T'}) \right] \\ & = \frac{1}{8} \left[\sum_{\mathcal{J}} [\mathcal{J}] \sqrt{\mathcal{J}(\mathcal{J}+1)} \begin{pmatrix} J_i & J_i & \mathcal{J} \\ -\frac{1}{2} & -\frac{1}{2} & 1 \end{pmatrix} P_{\mathcal{J}}^- \mathcal{W}_{\mathcal{J}}^{\text{TL}'} \right]^2 \end{aligned}$$

To be even more explicit, let us take $J_i = \frac{1}{2}$; then, for the L and T cases only $\mathcal{J} = 0$

occurs, while for the T' and TL' cases only $J = 1$ occurs. Evaluating the 3-j coefficients we obtain

$$(\mathcal{W}_1^{\text{TL}'})^2 = 2\mathcal{W}_0^{\text{L}}(\mathcal{W}_0^{\text{T}} - \mathcal{W}_1^{\text{T}'}) \quad \text{for } J_i = \frac{1}{2};$$

similarly, if we repeat this analysis for $J_i = \frac{3}{2}$, we find that

$$(\mathcal{W}_1^{\text{TL}'} - 3\mathcal{W}_3^{\text{TL}'})^2 = \frac{5}{2}(\mathcal{W}_0^{\text{L}} - \mathcal{W}_2^{\text{L}})[(\mathcal{W}_0^{\text{T}} - \mathcal{W}_2^{\text{T}}) - (1/\sqrt{5})(\mathcal{W}_1^{\text{T}'} - 3\mathcal{W}_3^{\text{T}'})].$$

Note that the above expressions are independent of the final spin J_f (although the \mathcal{W} 's themselves do depend on it).

Returning to the general case, let us proceed to invert the problem completely and to determine the form factors from the (experimentally accessible) quantities defined above. What we wish to determine are the following linear combinations of longitudinal and transverse matrix elements:

$$L_m \equiv \sum_J [J] \begin{pmatrix} J_f & J & J_i \\ -m & 0 & m \end{pmatrix} Q_J^\pi t_{CJ}, \quad (\text{B.6a})$$

$$T_m \equiv \sum_J [J] \begin{pmatrix} J_f & J & J_i \\ -(1+m) & 1 & m \end{pmatrix} (Q_J^\pi t_{EJ} + \pi Q_J^{-\pi} t_{MJ}), \quad (\text{B.6b})$$

where we have defined the quantities

$$Q_J^+ \equiv P_J^+ (-1)^{J/2} \quad (\text{B.7a})$$

and

$$Q_J \equiv P_J^- (-1)^{(J-1)/2}. \quad (\text{B.7b})$$

Note that π in Eq. (B.6) is the parity change which occurs in the transition $J_i^{\pi_i} \mapsto J_f^{\pi_f}$: $\pi = \pi_i \pi_f$. If the L's and T's in Eq. (B.6) are known, then the multipole matrix elements (and hence the form factors) are known as well:

$$t_{CJ} = Q_J^\pi [J] \sum_m \begin{pmatrix} J_f & J & J_i \\ -m & 0 & m \end{pmatrix} L_m, \quad (\text{B.8a})$$

$$t_{EJ} = Q_J^\pi [J] \sum_m \begin{pmatrix} J_f & J & J_i \\ -(1+m) & 1 & m \end{pmatrix} T_m, \quad (\text{B.8b})$$

and

$$t_{MJ} = \pi Q_J^{-\pi} [J] \sum_m \begin{pmatrix} J_f & J & J_i \\ -(1+m) & 1 & m \end{pmatrix} T_m. \quad (\text{B.8c})$$

Thus, the inversion problem hinges on knowing the L's and T's.

From the defining equations above, we see that the following ranges of m -values are involved:

$$\text{for } L_m: \quad -m_0 \leq m \leq m_0, \quad \text{where } m_0 = \min(J_i, J_f);$$

$$\text{for } T_m: \quad -m_1 \leq m \leq m_2, \quad \text{where } m_1 = \min(J_i, J_f + 1) \text{ and } m_2 = \min(J_i, J_f - 1).$$

Let us begin by considering the transverse projections in the range $m \geq -1$. Using the explicit expressions for $\mathcal{W}_{\mathcal{J}}^T$ and $\mathcal{W}_{\mathcal{J}'}^T$, it may be shown that

$$T_m = \lambda_m V_m^T, \tag{B.9}$$

where the set of signs $\{\lambda_m = \pm\}$ remains to be determined. Furthermore, it may be shown that the V_m^T 's for the allowed range of m -values can only be zero accidentally. That is, for some specific values of q the various form factors in Eq. (B.6b) may interfere so as to make T_m (and hence V_m^T) vanish; however, at a slightly different value of q this will not be the case. Thus, we shall assume that the accidental zeros are avoided and so we may safely divide by T_m . We then have that

$$T_{-(2+m)} = \pi(-1)^{J_i+J_f} U_m^{TT} / T_m, \tag{B.10a}$$

where $\pi = \pm$ is the parity change as above, and so the rest of the transverse projections (those with $m < -1$) are determined. Of course, the magnitude of U_m^{TT} is given by Eq. (B.5b) and the only new (experimentally accessible) input now is its sign. Furthermore, we have that

$$L_{1+m} = -(U_m^{TL} + U_m^{TL'}) / T_m \tag{B.10b}$$

and

$$L_{-m} = \pi(-1)^{J_i+J_f} L_m, \tag{B.10c}$$

and so the complete set of longitudinal projections is also determined. Again, the magnitude of $U_m^{TL} + U_m^{TL'}$ is already known from Eq. (B.5a) and the only new input is from the sign of this combination. In summary to this point, the inversion process is complete except for the as yet unknown set of signs $\{\lambda_m\}$, where m lies in the range $(-m_1 \leq m \leq m_2) \cap (m \geq -1)$.

For *inelastic* scattering, we have exhausted the information that can be used and so we have a certain level of ambiguity. In particular, after removing one overall sign which may be chosen by convention, we are left with n arbitrary signs, where n is given in Table B1. Such results are not unexpected when one remembers that the cross sections involved bilinear combinations of the form factors and we have had to solve quadratic equations to determine the latter quantities. In any practical situation, it will usually be possible to select from the sets of solutions which occur when $n \geq 1$ the one that is physically the most reasonable (e.g., the one which most resembles some model calculation).

TABLE B1
Level of Ambiguity n for Inelastic Scattering

	$A = \text{even}$	$A = \text{odd}$
$J_f = J_i \equiv J_0$	J_0	$J_0 - \frac{1}{2}$
$J_f < J_i$	J_f	$J_f - \frac{1}{2}$
$J_f > J_i$	$J_i + 1^a$	$J_i + \frac{1}{2}$

^a Except for natural parity transitions where $J_i = 0$, in which case $n = 0$.

On the other hand, for *elastic* scattering we have a special situation: $J_i = J_f \equiv J_0$, and it follows from parity and time-reversal invariance that the electric multipoles $t_{EJ} = 0$ for all J . Then, Eq. (B.6b) reduces to

$$T_m = \sum_J [J] \begin{pmatrix} J_0 & J & J_0 \\ -(1+m) & 1 & m \end{pmatrix} Q_J^- t_{MJ}, \quad (\text{B.11})$$

and this yields a new symmetry:

$$T_{-(1+m)} = (-1)^{2J_0+1} T_m. \quad (\text{B.12})$$

Combining this with Eq. (B.10a) yields a recursion relation for the phases:

$$\lambda_{1+m} = -\lambda_m \text{sign } U_m^{\text{TT}} \quad (\text{B.13})$$

for the allowed range of m -values. Upon fixing the overall phase convention (e.g., by choosing the phase $\lambda_{m=\min\{m\}}$), all of the phases are now determined and the problem may be inverted to obtain the form factors from the measured reduced response functions without any ambiguity.

Finally, it is possible to use the additional symmetry (Eq. (B.12)) to derive relationships directly among the reduced response functions. For example, we have for *elastic scattering* that

$$\sum_{\mathcal{J}} \mathcal{J}(\mathcal{J}+1) \{ (\mathcal{W}_{\mathcal{J}}^{\text{TL}})^2 + (\mathcal{W}_{\mathcal{J}}^{\text{TL}'})^2 \} = 8 \sum_{\mathcal{J}} \mathcal{W}_{\mathcal{J}}^{\text{L}} \mathcal{W}_{\mathcal{J}}^{\text{T}} \quad (\text{B.14a})$$

and

$$\sum_{\mathcal{J}} (\mathcal{J}-1) \mathcal{J}(\mathcal{J}+1)(\mathcal{J}+2) (\mathcal{W}_{\mathcal{J}}^{\text{TT}})^2 = \sum_{\mathcal{J}} \{ (\mathcal{W}_{\mathcal{J}}^{\text{T}})^2 - (\mathcal{W}_{\mathcal{J}}^{\text{T}'})^2 \}. \quad (\text{B.14b})$$

Equation (B.14a) is obtained from a more general set of relationships which are valid for *elastic scattering* only,

$$\sum_{\mathcal{J}'\mathcal{J}} [\mathcal{J}'] [\mathcal{J}] \begin{Bmatrix} \mathcal{J}' & \mathcal{J} & K \\ J_0 & J_0 & J_0 \end{Bmatrix} \left\{ \sqrt{\mathcal{J}'(\mathcal{J}'+1)\mathcal{J}(\mathcal{J}+1)} \begin{pmatrix} \mathcal{J}' & \mathcal{J} & K \\ 1 & -1 & 0 \end{pmatrix} \right. \\ \times [P_{\mathcal{J}'}^+ \mathcal{W}_{\mathcal{J}'}^{\text{TL}} - P_{\mathcal{J}'}^- \mathcal{W}_{\mathcal{J}'}^{\text{TL}'}] [P_{\mathcal{J}}^+ \mathcal{W}_{\mathcal{J}}^{\text{TL}} - P_{\mathcal{J}}^- \mathcal{W}_{\mathcal{J}}^{\text{TL}'}] \\ \left. + 8 \begin{pmatrix} \mathcal{J}' & \mathcal{J} & K \\ 0 & 0 & 0 \end{pmatrix} P_{\mathcal{J}'}^+ \mathcal{W}_{\mathcal{J}'}^{\text{L}} [P_{\mathcal{J}}^+ \mathcal{W}_{\mathcal{J}}^{\text{T}} + P_{\mathcal{J}}^- \mathcal{W}_{\mathcal{J}}^{\text{T}'}] \right\} = 0, \quad (\text{B.15})$$

where taking $K=0$ yields the above result. Relationships of a similar kind, but involving the TT reduced response functions, can also be derived for *elastic scattering*,

$$\sum_{\mathcal{J}'\mathcal{J}} [\mathcal{J}'] [\mathcal{J}] \begin{Bmatrix} \mathcal{J}' & \mathcal{J} & K \\ J_0 & J_0 & J_0 \end{Bmatrix} \sqrt{\mathcal{J}(\mathcal{J}+1)} [P_{\mathcal{J}'}^+ \mathcal{W}_{\mathcal{J}'}^{\text{TL}} + P_{\mathcal{J}'}^- \mathcal{W}_{\mathcal{J}'}^{\text{TL}'}] \\ \times \left(\begin{pmatrix} \mathcal{J}' & \mathcal{J} & K \\ -2 & 1 & 1 \end{pmatrix} P_{\mathcal{J}'}^+ \mathcal{W}_{\mathcal{J}'}^{\text{TT}} - (-1)^K \begin{pmatrix} \mathcal{J}' & \mathcal{J} & K \\ 0 & -1 & 1 \end{pmatrix} [P_{\mathcal{J}'}^+ \mathcal{W}_{\mathcal{J}'}^{\text{T}} + P_{\mathcal{J}'}^- \mathcal{W}_{\mathcal{J}'}^{\text{T}'}] \right) = 0. \quad (\text{B.16})$$

In conclusion, we have found that, in general, a measurement of all of the reduced response functions for inelastic scattering will not allow the unambiguous determination of all of the form factors; there will usually be a degree of ambiguity which can be eliminated only through the use of additional physical input. However, the absence of the electric multipoles for elastic scattering implies that one is able to determine all of the form factors without any ambiguity (other than the overall sign) if all of the reduced response functions are known.

APPENDIX C: TABULATION OF REDUCED RESPONSE FUNCTIONS

Explanation of the Tables

In these tables, the coefficients required for the six reduced response functions $\mathcal{W}_{\mathcal{J}}^K(q)_{\bar{n}}$ are given. These can be written in the form

$$\mathcal{W}_{\mathcal{J}}^K(q)_{\bar{n}} = \sum_{\substack{J'J \\ \sigma\sigma'}} A_{\bar{n}}^{K:\sigma\sigma'}(\mathcal{J}, J', J) F_{\sigma'J'}(q)_{\bar{n}} F_{\sigma J}(q)_{\bar{n}},$$

where σ and σ' are labels corresponding to the type of electromagnetic form factor required in the expansion; σ and $\sigma' = \text{C, E, and M}$. The form factors are related to the matrix elements $t_{\sigma J}(q)_{\bar{n}}$ defined previously by

$$F_{\sigma J}(q)_{\bar{n}} \equiv \frac{1}{[J_i]} t_{\sigma J}(q)_{\bar{n}} = \frac{1}{[J_i]} \langle J_i \| \hat{T}_{\sigma J}(q) \| J_i \rangle.$$

All of the nonvanishing real coefficients $A_f^{K;\sigma'\sigma}(\mathcal{J}, J', J)$ are listed in the tables in columns corresponding to the appropriate response function for a selection of nuclear transitions $J_i^{n_i} \mapsto J_f^{n_f}$. Each table then refers to a specific angular momentum transition $J_i \mapsto J_f$ (in these tables, we include the transitions up to $2 \mapsto 2$), and includes the two possible nuclear parity cases (i.e., with and without a parity change). It should be noted that conservation of parity has been applied to the nuclear transition matrix elements. In the case of elastic scattering, all of the electric multipoles can be shown to vanish by time-reversal invariance; this fact is indicated in the tables for those cases with $J_i = J_f$ and no nuclear parity change by underlining those nuclear response function terms which are still required even if time-reversal invariance is applied. Finally, one should note that only the situation in which just the initial nuclear polarization is known is given in these tables; the case in which just the final nuclear polarization is determined can easily be found from these tables through the use of the "turn-around" relation

$$\mathcal{W}_{\mathcal{J}}^K(q)_a = \pm \left(\frac{2J_f + 1}{2J_i + 1} \right) \mathcal{W}_{\mathcal{J}}^K(q)_{a'}$$

where the plus sign occurs for $K = L, T, TT,$ and TL' and the minus sign occurs for $K = TL$ and T' .

Since the squares of all of the coefficients are rational numbers, it is the squares of these coefficients which are listed in the tables; negative coefficients are then indicated by the presence of an asterisk preceding the representation of the coefficient. Any integer can be expressed as a product of prime factors, and so, if we adopt the convention that the prime numbers are listed in ascending order from left to right, then each integer can be uniquely specified. A more compact notation consists of listing only the exponents of the prime factors; for example, $20 = 2^2 \times 3^0 \times 5^1 \mapsto 201$. Similarly, any rational fraction can be represented in the same way, if we use the convention that negative exponents are overbarred. Also, a number which is equal to 1 is indicated by a single zero. As an example, consider the coefficient

$$\begin{aligned} -\sqrt{1040/153} &= -\sqrt{(2^4 \times 5 \times 13)/(3^2 \times 17)} \\ &= -\sqrt{2^4 \times 3^{-2} \times 5^1 \times 7^0 \times 11^0 \times 13^1 \times 17^{-1}} \end{aligned}$$

which would be listed in the tables as $*4\bar{2}1001\bar{1}$. For the transitions which are listed in this appendix, only the first seven prime numbers 2, 3, 5, 7, 11, 13, and 17 will be required in order to specify the resulting coefficients.

EXAMPLE. $\frac{1}{2}^{\pm} \mapsto \frac{3}{2}^{\mp}$. This transition has $J_i = \frac{1}{2}$ and $J_f = \frac{3}{2}$, and the nucleus

Table C1 : $J_i = 0$ $J_f = 0$
 No Parity Change
 (1 term)

$$L: \begin{matrix} & C & C \\ J & J' & J \\ 0 & 0 & 0 & 0 \end{matrix}$$

Table C2 : $J_i = 0$ $J_f = 1$
 No Parity Change
 (1 term)

$$T: \begin{matrix} & M & M \\ J & J' & J \\ 0 & 1 & 1 & 0 \end{matrix}$$

Table C3 : $J_i = 0$ $J_f = 1$
 Parity Change
 (2 terms)

$$L: \begin{matrix} & C & C \\ J & J' & J \\ 0 & 1 & 1 & 0 \end{matrix}$$

$$T: \begin{matrix} & E & E \\ J & J' & J \\ 0 & 1 & 1 & 0 \end{matrix}$$

Table C4 : $J_i = 0$ $J_f = 2$
 No Parity Change
 (2 terms)

$$L: \begin{matrix} & C & C \\ J & J' & J \\ 0 & 2 & 2 & 0 \end{matrix}$$

$$T: \begin{matrix} & E & E \\ J & J' & J \\ 0 & 2 & 2 & 0 \end{matrix}$$

Table C5 : $J_i = 0$ $J_f = 2$
 Parity Change
 (1 term)

$$T: \begin{matrix} & M & M \\ J & J' & J \\ 0 & 2 & 2 & 0 \end{matrix}$$

Table C6 : $J_i = 1/2$ $J_f = 1/2$
 No Parity Change
 (4 terms)

$$L: \begin{matrix} & C & C \\ J & J' & J \\ 0 & 0 & 0 & 1 \end{matrix}$$

$$T: \begin{matrix} & M & M \\ J & J' & J \\ 0 & 1 & 1 & 1 \end{matrix}$$

$$T': \begin{matrix} & M & M \\ J & J' & J \\ 1 & 1 & 1 & \cdot 1 \end{matrix}$$

$$TL': \begin{matrix} & C & M \\ J & J' & J \\ 1 & 0 & 1 & \cdot 3 \end{matrix}$$

Table C7 : $J_i = 1/2$ $J_f = 1/2$
 Parity Change
 (4 terms)

$$L: \begin{matrix} & C & C \\ J & J' & J \\ 0 & 1 & 1 & 1 \end{matrix}$$

$$T: \begin{matrix} & E & E \\ J & J' & J \\ 0 & 1 & 1 & 1 \end{matrix}$$

$$T': \begin{matrix} & E & E \\ J & J' & J \\ 1 & 1 & 1 & \cdot 1 \end{matrix}$$

$$TL': \begin{matrix} & C & E \\ J & J' & J \\ 1 & 1 & 1 & \cdot 3 \end{matrix}$$

Table C8 : $J_i = 1/2$ $J_f = 3/2$
 No Parity Change
 (8 terms)

$$L: \begin{matrix} & C & C \\ J & J' & J \\ 0 & 2 & 2 & 1 \end{matrix}$$

$$T: \begin{matrix} & M & M \\ J & J' & J \\ 0 & 1 & 1 & 1 \end{matrix}$$

$$T': \begin{matrix} & M & M \\ J & J' & J \\ 1 & 1 & 1 & T \end{matrix}$$

$$T: \begin{matrix} & E & E \\ J & J' & J \\ 0 & 2 & 2 & 1 \end{matrix}$$

$$T': \begin{matrix} & E & E \\ J & J' & J \\ 1 & 2 & 2 & \cdot T \end{matrix}$$

$$T': \begin{matrix} & E & M \\ J & J' & J \\ 1 & 2 & 1 & \cdot 11 \end{matrix}$$

$$TL': \begin{matrix} & C & M \\ J & J' & J \\ 1 & 2 & 1 & \cdot 1 \end{matrix}$$

$$TL': \begin{matrix} & C & E \\ J & J' & J \\ 1 & 2 & 2 & \cdot 11 \end{matrix}$$

Table C9 : $J_i = 1/2$ $J_f = 3/2$
 Parity Change
 (8 terms)

$$L: \begin{matrix} & C & C \\ J & J' & J \\ 0 & 1 & 1 & 1 \end{matrix}$$

$$T: \begin{matrix} & M & M \\ J & J' & J \\ 0 & 2 & 2 & 1 \end{matrix}$$

$$T': \begin{matrix} & M & M \\ J & J' & J \\ 1 & 2 & 2 & \cdot T \end{matrix}$$

$$T: \begin{matrix} & E & E \\ J & J' & J \\ 0 & 1 & 1 & 1 \end{matrix}$$

$$T': \begin{matrix} & E & E \\ J & J' & J \\ 1 & 1 & 1 & T \end{matrix}$$

$$T': \begin{matrix} & E & M \\ J & J' & J \\ 1 & 1 & 2 & 11 \end{matrix}$$

$$TL': \begin{matrix} & C & M \\ J & J' & J \\ 1 & 1 & 2 & \cdot 11 \end{matrix}$$

$$TL': \begin{matrix} & C & E \\ J & J' & J \\ 1 & 1 & 1 & 1 \end{matrix}$$

Table C10 : $J_i = 1$ $J_f = 0$
 No Parity Change
 (4 terms)

$$T: \begin{matrix} & M & M \\ J & J' & J \\ 0 & 1 & 1 & 01 \\ 2 & 1 & 1 & T1 \end{matrix}$$

$$T': \begin{matrix} & M & M \\ J & J' & J \\ 1 & 1 & 1 & \cdot T2 \end{matrix}$$

$$TT: \begin{matrix} & M & M \\ J & J' & J \\ 2 & 1 & 1 & \cdot 31 \end{matrix}$$

undergoes a parity change. Then, only the Coulomb dipole, the electric dipole, and the magnetic quadrupole form factors are nonvanishing,

$$F_{C1}(q)_{3/2,1/2} = (1/\sqrt{2}) \langle \frac{3}{2} \| \hat{M}_1(q) \| \frac{1}{2} \rangle,$$

$$F_{E1}(q)_{3/2,1/2} = (1/\sqrt{2}) \langle \frac{3}{2} \| \hat{T}_1^{el}(q) \| \frac{1}{2} \rangle,$$

and

$$F_{M2}(q)_{3/2,1/2} = (1/\sqrt{2}) \langle \frac{3}{2} \| i\hat{T}_2^{mag}(q) \| \frac{1}{2} \rangle,$$

where the subscript $\frac{3}{2} \frac{1}{2}$ refers to the transition $\frac{1}{2} \mapsto \frac{3}{2}$ and is consistent with the notation "fi." Then, the eight nonvanishing coefficients corresponding to this transition are given in Table C9. As an example, consider the reduced response function $\mathcal{W}_{\mathcal{J}}^T(q)_{3/2,1/2}$; then, as indicated in the table, only the $\mathcal{J} = 1$ term is nonvanishing:

T' :	M	M	
	\mathcal{J}	J'	J
	1	2	2 * $\bar{1}$
T'' :	E	E	
	\mathcal{J}	J'	J
	1	1	1 $\bar{1}$
T''' :	E	M	
	\mathcal{J}	J'	J
	1	1	2 11.

Then, we have that

$$\begin{aligned} \mathcal{W}_1^T(q)_{3/2,1/2} &= A_{3/2,1/2}^{T;MM}(1, 2, 2) F_{M2}(q)_{3/2,1/2} F_{M2}(q)_{3/2,1/2} \\ &+ A_{3/2,1/2}^{T;EE}(1, 1, 1) F_{E1}(q)_{3/2,1/2} F_{E1}(q)_{3/2,1/2} \\ &+ A_{3/2,1/2}^{T;EM}(1, 1, 2) F_{E1}(q)_{3/2,1/2} F_{M2}(q)_{3/2,1/2}, \end{aligned}$$

where $A_{3/2,1/2}^{T;MM}(1, 2, 2) = -\sqrt{2^{-1}}$, $A_{3/2,1/2}^{T;EE}(1, 1, 1) = +\sqrt{2^{-1}}$, and $A_{3/2,1/2}^{T;EM}(1, 1, 2) = +\sqrt{2^1 \times 3^1}$; thus,

$$\begin{aligned} \mathcal{W}_1^T(q)_{3/2,1/2} &= -(1/\sqrt{2})(F_{M2}(q)_{3/2,1/2})^2 + (1/\sqrt{2})(F_{E1}(q)_{3/2,1/2})^2 \\ &+ \sqrt{6}F_{E1}(q)_{3/2,1/2}F_{M2}(q)_{3/2,1/2}. \end{aligned}$$

Similarly, the other response functions can be determined from the table, and are given by

$$\begin{aligned} \mathcal{W}_0^L(q)_{3/2,1/2} &= \sqrt{2}(F_{C1}(q)_{3/2,1/2})^2, \\ \mathcal{W}_0^T(q)_{3/2,1/2} &= \sqrt{2}((F_{M2}(q)_{3/2,1/2})^2 + (F_{E1}(q)_{3/2,1/2})^2), \end{aligned}$$

Table C14: $J_i = 1$ $J_f = 2$
 No Parity Change
 (28 terms)

TT:	$J \begin{matrix} M \\ J' \\ J \end{matrix} \begin{matrix} M \\ J' \\ J \end{matrix}$			
	2 1 1	$\cdot 51\bar{E}$		
	2 3 1	$\bar{1}1\bar{E}$		
	2 3 3	$\cdot \bar{1}1\bar{E}$		
TT:	$J \begin{matrix} E \\ J' \\ J \end{matrix} \begin{matrix} E \\ J' \\ J \end{matrix}$			
	2 2 2	$\cdot 51$		
TT:	$J \begin{matrix} E \\ J' \\ J \end{matrix} \begin{matrix} M \\ J' \\ J \end{matrix}$			
	2 2 1	$\cdot 31T$		
	2 2 3	$\bar{1}1T$		
TL:	$J \begin{matrix} C \\ J' \\ J \end{matrix} \begin{matrix} M \\ J' \\ J \end{matrix}$	TL': $J \begin{matrix} C \\ J' \\ J \end{matrix} \begin{matrix} M \\ J' \\ J \end{matrix}$		
	2 2 1	$\cdot T2T$	1 2 1	$\cdot T3T$
	2 2 3	$\cdot 30T$	1 2 3	$\cdot 31T$
TL:	$J \begin{matrix} C \\ J' \\ J \end{matrix} \begin{matrix} E \\ J' \\ J \end{matrix}$	TL': $J \begin{matrix} C \\ J' \\ J \end{matrix} \begin{matrix} E \\ J' \\ J \end{matrix}$		
	2 2 2	$\cdot T$	1 2 2	$\cdot T1$

Table C15: $J_i = 1$ $J_f = 2$
 Parity Change
 (35 terms)

L:	$J \begin{matrix} C \\ J' \\ J \end{matrix} \begin{matrix} C \\ J' \\ J \end{matrix}$			
	0 1 1	01		
	0 3 3	01		
	2 1 1	$\cdot T1\bar{E}$		
	2 3 1	$\cdot 24\bar{E}$		
	2 3 3	$\cdot 31\bar{E}$		
T:	$J \begin{matrix} M \\ J' \\ J \end{matrix} \begin{matrix} M \\ J' \\ J \end{matrix}$	T': $J \begin{matrix} M \\ J' \\ J \end{matrix} \begin{matrix} M \\ J' \\ J \end{matrix}$		
	0 2 2	01	1 2 2	$\cdot 3$
	2 2 2	$\bar{3}1$		
T:	$J \begin{matrix} E \\ J' \\ J \end{matrix} \begin{matrix} E \\ J' \\ J \end{matrix}$	T': $J \begin{matrix} E \\ J' \\ J \end{matrix} \begin{matrix} E \\ J' \\ J \end{matrix}$		
	0 1 1	01	1 1 1	$\bar{3}2$
	0 3 3	01	1 3 3	$\cdot T$
	2 1 1	$\bar{3}1\bar{E}$		
	2 3 1	$\cdot 33\bar{E}$		
	2 3 3	$\cdot T3\bar{E}$		
T:	$J \begin{matrix} E \\ J' \\ J \end{matrix} \begin{matrix} M \\ J' \\ J \end{matrix}$	T': $J \begin{matrix} E \\ J' \\ J \end{matrix} \begin{matrix} M \\ J' \\ J \end{matrix}$		
	2 1 2	$\bar{1}3T$	1 1 2	$\bar{1}4T$
	2 3 2	$\bar{3}1T$	1 3 2	$\cdot 50T$
TT:	$J \begin{matrix} M \\ J' \\ J \end{matrix} \begin{matrix} M \\ J' \\ J \end{matrix}$			
	2 2 2	$\bar{5}1$		
TT:	$J \begin{matrix} E \\ J' \\ J \end{matrix} \begin{matrix} E \\ J' \\ J \end{matrix}$			
	2 1 1	$\bar{5}1\bar{E}$		
	2 3 1	$\cdot T1\bar{E}$		
	2 3 3	$\bar{1}1\bar{E}$		

Table C15: $J_i = 1$ $J_f = 2$
 Parity Change
 (35 terms)

TT:	$J \begin{matrix} E \\ J' \\ J \end{matrix} \begin{matrix} M \\ J' \\ J \end{matrix}$			
	2 1 2	$\cdot 31T$		
	2 3 2	$\bar{1}1T$		
TL:	$J \begin{matrix} C \\ J' \\ J \end{matrix} \begin{matrix} M \\ J' \\ J \end{matrix}$	TL': $J \begin{matrix} C \\ J' \\ J \end{matrix} \begin{matrix} M \\ J' \\ J \end{matrix}$		
	2 1 2	$\bar{1}1T$	1 1 2	$\cdot T4T$
	2 3 2	$\cdot 40T$	1 3 2	$\cdot 21T$
TL:	$J \begin{matrix} C \\ J' \\ J \end{matrix} \begin{matrix} E \\ J' \\ J \end{matrix}$	TL': $J \begin{matrix} C \\ J' \\ J \end{matrix} \begin{matrix} E \\ J' \\ J \end{matrix}$		
	2 1 1	$\bar{1}1\bar{E}$	1 1 1	$\bar{1}2$
	2 1 3	$\bar{5}1\bar{E}$	1 3 3	$\cdot 21$
	2 3 1	$\cdot 22\bar{E}$		
	2 3 3	$\bar{2}0\bar{E}$		

Table C16: $J_i = 3/2$ $J_f = 1/2$
 No Parity Change
 (21 terms)

L:	$J \begin{matrix} C \\ J' \\ J \end{matrix} \begin{matrix} C \\ J' \\ J \end{matrix}$			
	0 2 2	2		
	2 2 2	$\cdot 2$		
T:	$J \begin{matrix} M \\ J' \\ J \end{matrix} \begin{matrix} M \\ J' \\ J \end{matrix}$	T': $J \begin{matrix} M \\ J' \\ J \end{matrix} \begin{matrix} M \\ J' \\ J \end{matrix}$		
	0 1 1	2	1 1 1	$\cdot 001$
	2 1 1	0		
T:	$J \begin{matrix} E \\ J' \\ J \end{matrix} \begin{matrix} E \\ J' \\ J \end{matrix}$	T': $J \begin{matrix} E \\ J' \\ J \end{matrix} \begin{matrix} E \\ J' \\ J \end{matrix}$		
	0 2 2	2	1 2 2	$\cdot 02T$
	2 2 2	$\cdot 0$	3 2 2	$\cdot 40T$
T:	$J \begin{matrix} E \\ J' \\ J \end{matrix} \begin{matrix} M \\ J' \\ J \end{matrix}$	T': $J \begin{matrix} E \\ J' \\ J \end{matrix} \begin{matrix} M \\ J' \\ J \end{matrix}$		
	2 2 1	$\bar{2}1$	1 2 1	$\cdot 21T$
			3 2 1	$\cdot 41T$
TT:	$J \begin{matrix} M \\ J' \\ J \end{matrix} \begin{matrix} M \\ J' \\ J \end{matrix}$			
	2 1 1	$\cdot \bar{E}$		
TT:	$J \begin{matrix} E \\ J' \\ J \end{matrix} \begin{matrix} E \\ J' \\ J \end{matrix}$			
	2 2 2	\bar{E}		
TT:	$J \begin{matrix} E \\ J' \\ J \end{matrix} \begin{matrix} M \\ J' \\ J \end{matrix}$			
	2 2 1	$\bar{0}T$		
TL:	$J \begin{matrix} C \\ J' \\ J \end{matrix} \begin{matrix} M \\ J' \\ J \end{matrix}$	TL': $J \begin{matrix} C \\ J' \\ J \end{matrix} \begin{matrix} M \\ J' \\ J \end{matrix}$		
	2 2 1	2	1 2 1	$\cdot 20T$
			3 2 1	$\cdot 40T$
TL:	$J \begin{matrix} C \\ J' \\ J \end{matrix} \begin{matrix} E \\ J' \\ J \end{matrix}$	TL': $J \begin{matrix} C \\ J' \\ J \end{matrix} \begin{matrix} E \\ J' \\ J \end{matrix}$		
	2 2 2	$\bar{2}T$	1 2 2	$\cdot 23T$
			3 2 2	$\cdot 4T$

and

$$\mathcal{W}_1^{\text{TL}'}(q)_{3/2, 1/2} = \sqrt{2} F_{\text{C1}}(q)_{3/2, 1/2} (F_{\text{E1}}(q)_{3/2, 1/2} - \sqrt{3} F_{\text{M2}}(q)_{3/2, 1/2}).$$

As an example of the use of the "turnaround" relation (2.66), we now consider the nuclear transition $\frac{3}{2}^{\pm} \mapsto \frac{1}{2}^{\mp}$ for which the *final* nuclear polarization is measured. It then follows from the turnaround relation that

$$\mathcal{W}_J^{\text{K}}(q)_{1/2, 3/2} = \pm ((2 \cdot \frac{1}{2} + 1)/(2 \cdot \frac{3}{2} + 1)) \mathcal{W}_J^{\text{K}}(q)_{3/2, 1/2} = \pm \frac{1}{2} \mathcal{W}_J^{\text{K}}(q)_{3/2, 1/2},$$

where the $\mathcal{W}_J^{\text{K}}(q)_{3/2, 1/2}$ are given above, and so

$$\begin{aligned} \mathcal{W}_0^{\text{L}}(q)_{1/2, 3/2} &= (1/\sqrt{2})(F_{\text{C1}}(q)_{3/2, 1/2})^2, \\ \mathcal{W}_0^{\text{T}}(q)_{1/2, 3/2} &= (1/\sqrt{2})((F_{\text{M2}}(q)_{3/2, 1/2})^2 + (F_{\text{E1}}(q)_{3/2, 1/2})^2), \\ \mathcal{W}_1^{\text{T}}(q)_{1/2, 3/2} &= (\sqrt{2}/4)(F_{\text{M2}}(q)_{3/2, 1/2})^2 - (\sqrt{2}/4)(F_{\text{E1}}(q)_{3/2, 1/2})^2 \\ &\quad - \sqrt{3/2} F_{\text{E1}}(q)_{3/2, 1/2} F_{\text{M2}}(q)_{3/2, 1/2}, \end{aligned}$$

and

$$\mathcal{W}_1^{\text{TL}'}(q)_{1/2, 3/2} = (1/\sqrt{2}) F_{\text{C1}}(q)_{3/2, 1/2} (F_{\text{E1}}(q)_{3/2, 1/2} - \sqrt{3} F_{\text{M2}}(q)_{3/2, 1/2}),$$

where the form factors $F_{\sigma J}(q)_{3/2, 1/2}$ refer to the transition $\frac{1}{2} \mapsto \frac{3}{2}$.

However, we have that

$$F_{\sigma J}(q)_{\text{fi}} \equiv \frac{1}{[J_i]} \langle J_f \| \hat{T}_{\sigma J}(q) \| J_i \rangle$$

and

$$\langle J_i \| \hat{T}_{\sigma J}(q) \| J_f \rangle = (-1)^{J_f - J_i} (-1)^{J + \eta} \langle J_f \| \hat{T}_{\sigma J}(q) \| J_i \rangle,$$

where $\eta = 0$ for the Coulomb multipole operators and $\eta = 1$ for the transverse multipole operators [25, 33]. It then follows that

$$F_{\sigma J}(q)_{\text{fi}} = (-1)^{J_f - J_i} (-1)^{J + \eta} \frac{[J_f]}{[J_i]} F_{\sigma J}(q)_{\text{if}}.$$

Therefore,

$$\begin{aligned} F_{\text{C1}}(q)_{3/2, 1/2} &= +\sqrt{2} F_{\text{C1}}(q)_{1/2, 3/2}, \\ F_{\text{E1}}(q)_{3/2, 1/2} &= -\sqrt{2} F_{\text{E1}}(q)_{1/2, 3/2}, \end{aligned}$$

and

$$F_{\text{M2}}(q)_{3/2, 1/2} = +\sqrt{2} F_{\text{M2}}(q)_{1/2, 3/2},$$

Table C17: $J_i = 3/2$ $J_f = 1/2$
Parity Change (20 terms)

L:	$J \begin{smallmatrix} C \\ J' \\ J \end{smallmatrix} \begin{smallmatrix} C \\ J' \\ J \end{smallmatrix}$	
	0 1 1 2	
	2 1 1 +2	
T:	$J \begin{smallmatrix} M \\ J' \\ J \end{smallmatrix} \begin{smallmatrix} M \\ J' \\ J \end{smallmatrix}$	T': $J \begin{smallmatrix} M \\ J' \\ J \end{smallmatrix} \begin{smallmatrix} M \\ J' \\ J \end{smallmatrix}$
	0 2 2 2	1 2 2 +02T
	2 2 2 +0	3 2 2 40T
T:	$J \begin{smallmatrix} E \\ J' \\ J \end{smallmatrix} \begin{smallmatrix} E \\ J' \\ J \end{smallmatrix}$	T': $J \begin{smallmatrix} E \\ J' \\ J \end{smallmatrix} \begin{smallmatrix} E \\ J' \\ J \end{smallmatrix}$
	0 1 1 2	1 1 1 +001
	2 1 1 0	
T:	$J \begin{smallmatrix} E \\ J' \\ J \end{smallmatrix} \begin{smallmatrix} M \\ J' \\ J \end{smallmatrix}$	T': $J \begin{smallmatrix} E \\ J' \\ J \end{smallmatrix} \begin{smallmatrix} M \\ J' \\ J \end{smallmatrix}$
	2 1 2 +21	1 1 2 21T
		3 1 2 41T
TT:	$J \begin{smallmatrix} M \\ J' \\ J \end{smallmatrix} \begin{smallmatrix} M \\ J' \\ J \end{smallmatrix}$	
	2 2 2 +2	
TT:	$J \begin{smallmatrix} E \\ J' \\ J \end{smallmatrix} \begin{smallmatrix} E \\ J' \\ J \end{smallmatrix}$	
	2 1 1 2	
TT:	$J \begin{smallmatrix} E \\ J' \\ J \end{smallmatrix} \begin{smallmatrix} M \\ J' \\ J \end{smallmatrix}$	
	2 1 2 0T	
TL:	$J \begin{smallmatrix} C \\ J' \\ J \end{smallmatrix} \begin{smallmatrix} M \\ J' \\ J \end{smallmatrix}$	TL': $J \begin{smallmatrix} C \\ J' \\ J \end{smallmatrix} \begin{smallmatrix} M \\ J' \\ J \end{smallmatrix}$
	2 1 2 +2T	1 1 2 +21T
		3 1 2 61T
TL:	$J \begin{smallmatrix} C \\ J' \\ J \end{smallmatrix} \begin{smallmatrix} E \\ J' \\ J \end{smallmatrix}$	TL': $J \begin{smallmatrix} C \\ J' \\ J \end{smallmatrix} \begin{smallmatrix} E \\ J' \\ J \end{smallmatrix}$
	2 1 1 2	1 1 1 +201

Table C18: $J_i = 3/2$ $J_f = 3/2$
No Parity Change (37 terms)

L:	$J \begin{smallmatrix} C \\ J' \\ J \end{smallmatrix} \begin{smallmatrix} C \\ J' \\ J \end{smallmatrix}$	
	0 0 0 2	
	0 2 2 2	
	2 2 0 +4	
T:	$J \begin{smallmatrix} M \\ J' \\ J \end{smallmatrix} \begin{smallmatrix} M \\ J' \\ J \end{smallmatrix}$	T': $J \begin{smallmatrix} M \\ J' \\ J \end{smallmatrix} \begin{smallmatrix} M \\ J' \\ J \end{smallmatrix}$
	0 1 1 2	1 1 1 +20T
	0 3 3 2	1 3 3 +20T
	2 1 1 +402	3 3 1 51T
	2 3 1 +512	3 3 3 20T
	2 3 3 +222	
T:	$J \begin{smallmatrix} E \\ J' \\ J \end{smallmatrix} \begin{smallmatrix} E \\ J' \\ J \end{smallmatrix}$	T': $J \begin{smallmatrix} E \\ J' \\ J \end{smallmatrix} \begin{smallmatrix} E \\ J' \\ J \end{smallmatrix}$
	0 2 2 2	1 2 2 +20T
		3 2 2 +40T

Table C18: $J_i = 3/2$ $J_f = 3/2$
No Parity Change (37 terms)

T:	$J \begin{smallmatrix} E \\ J' \\ J \end{smallmatrix} \begin{smallmatrix} M \\ J' \\ J \end{smallmatrix}$	T': $J \begin{smallmatrix} E \\ J' \\ J \end{smallmatrix} \begin{smallmatrix} M \\ J' \\ J \end{smallmatrix}$
	2 2 1 41T	1 2 1 +612
	2 2 3 +50T	1 2 3 702
		3 2 1 412
		3 2 3 +502
TT:	$J \begin{smallmatrix} M \\ J' \\ J \end{smallmatrix} \begin{smallmatrix} M \\ J' \\ J \end{smallmatrix}$	
	2 1 1 202	
	2 3 1 112	
	2 3 3 +202	
TT:	$J \begin{smallmatrix} E \\ J' \\ J \end{smallmatrix} \begin{smallmatrix} M \\ J' \\ J \end{smallmatrix}$	
	2 2 1 21T	
	2 2 3 10T	
TL:	$J \begin{smallmatrix} C \\ J' \\ J \end{smallmatrix} \begin{smallmatrix} M \\ J' \\ J \end{smallmatrix}$	TL': $J \begin{smallmatrix} C \\ J' \\ J \end{smallmatrix} \begin{smallmatrix} M \\ J' \\ J \end{smallmatrix}$
	2 2 1 40T	1 0 1 -4
	2 2 3 +51T	1 2 1 -602
		1 2 3 -512
		3 0 3 3T
		3 2 1 402
		3 2 3 312
TL:	$J \begin{smallmatrix} C \\ J' \\ J \end{smallmatrix} \begin{smallmatrix} E \\ J' \\ J \end{smallmatrix}$	TL': $J \begin{smallmatrix} C \\ J' \\ J \end{smallmatrix} \begin{smallmatrix} E \\ J' \\ J \end{smallmatrix}$
	2 0 2 4T	1 2 2 -41T
		3 2 2 -41T

Table C19: $J_i = 3/2$ $J_f = 3/2$
Parity Change (43 terms)

L:	$J \begin{smallmatrix} C \\ J' \\ J \end{smallmatrix} \begin{smallmatrix} C \\ J' \\ J \end{smallmatrix}$	
	0 1 1 2	
	0 3 3 2	
	2 1 1 602	
	2 3 1 +422	
	2 3 3 +602	
T:	$J \begin{smallmatrix} M \\ J' \\ J \end{smallmatrix} \begin{smallmatrix} M \\ J' \\ J \end{smallmatrix}$	T': $J \begin{smallmatrix} M \\ J' \\ J \end{smallmatrix} \begin{smallmatrix} M \\ J' \\ J \end{smallmatrix}$
	0 2 2 2	1 2 2 +20T
		3 2 2 +40T
T:	$J \begin{smallmatrix} E \\ J' \\ J \end{smallmatrix} \begin{smallmatrix} E \\ J' \\ J \end{smallmatrix}$	T': $J \begin{smallmatrix} E \\ J' \\ J \end{smallmatrix} \begin{smallmatrix} E \\ J' \\ J \end{smallmatrix}$
	0 1 1 2	1 1 1 +20T
	0 3 3 2	1 3 3 +20T
	2 1 1 +402	3 3 1 51T
	2 3 1 +512	3 3 3 20T
	2 3 3 +222	

Table C19: $J_i = 3/2$ $J_f = 3/2$
 Parity Change (43 terms)

T:	$J \begin{smallmatrix} E \\ J' \\ J \end{smallmatrix} M$	T':	$J \begin{smallmatrix} E \\ J' \\ J \end{smallmatrix} M$
	2 1 2 +41 T		1 1 2 61 T
	2 3 2 50 T		1 3 2 +70 T
			3 1 2 +41 T
			3 3 2 50 T
TT:	$J \begin{smallmatrix} E \\ J' \\ J \end{smallmatrix} E$		
	2 1 1 +20 T		
	2 3 1 +17 T		
	2 3 3 20 T		
TT:	$J \begin{smallmatrix} E \\ J' \\ J \end{smallmatrix} M$		
	2 1 2 2TT		
	2 3 2 10 T		
TL:	$J \begin{smallmatrix} C \\ J' \\ J \end{smallmatrix} M$	TL':	$J \begin{smallmatrix} C \\ J' \\ J \end{smallmatrix} M$
	2 1 2 +4TT		1 1 2 +61 T
	2 3 2 6TT		1 3 2 +41 T
			3 1 2 +6TT
			3 3 2 +4TT
TL:	$J \begin{smallmatrix} C \\ J' \\ J \end{smallmatrix} E$	TL':	$J \begin{smallmatrix} C \\ J' \\ J \end{smallmatrix} E$
	2 1 1 +60 T		1 1 1 +40 T
	2 1 3 7TT		1 3 3 +51 T
	2 3 1 +40 T		3 1 3 3TT
	2 3 3 5TT		3 3 1 40 T
			3 3 3 3TT

Table C20: $J_i = 2$ $J_f = 0$
 No Parity Change (14 terms)

L:	$J \begin{smallmatrix} C \\ J' \\ J \end{smallmatrix} C$		
	0 2 2 0 01		
	2 2 2 +102 T		
	4 2 2 121 T		
T:	$J \begin{smallmatrix} E \\ J' \\ J \end{smallmatrix} E$	T':	$J \begin{smallmatrix} E \\ J' \\ J \end{smallmatrix} E$
	0 2 2 0 01		1 2 2 +T 01
	2 2 2 +T 02 T		3 2 2 101
	4 2 2 +3 01 T		
TT:	$J \begin{smallmatrix} E \\ J' \\ J \end{smallmatrix} E$		
	2 2 2 T 02 T		
	4 2 2 +T 21 T		
TL:	$J \begin{smallmatrix} C \\ J' \\ J \end{smallmatrix} E$	TL':	$J \begin{smallmatrix} C \\ J' \\ J \end{smallmatrix} E$
	2 2 2 1 T2 T		1 2 2 +111
	4 2 2 +111 T		3 2 2 1 T1

Table C21: $J_i = 2$ $J_f = 0$
 Parity Change (7 terms)

T:	$J \begin{smallmatrix} M \\ J' \\ J \end{smallmatrix} M$	T':	$J \begin{smallmatrix} M \\ J' \\ J \end{smallmatrix} M$
	0 2 2 0 01		1 2 2 +T 01
	2 2 2 +T 02 T		3 2 2 101
	4 2 2 +3 01 T		
TT:	$J \begin{smallmatrix} M \\ J' \\ J \end{smallmatrix} M$		
	2 2 2 +3 02 T		
	4 2 2 T 21 T		

Table C22: $J_i = 2$ $J_f = 1$
 No Parity Change (45 terms)

L:	$J \begin{smallmatrix} C \\ J' \\ J \end{smallmatrix} C$		
	0 2 2 0 01		
	2 2 2 +T 02 T		
	4 2 2 +3 01 T		
T:	$J \begin{smallmatrix} M \\ J' \\ J \end{smallmatrix} M$	T':	$J \begin{smallmatrix} M \\ J' \\ J \end{smallmatrix} M$
	0 1 1 0 01		1 1 1 +3 21
	0 3 3 0 01		1 3 3 +1 21
	2 1 1 T 001		3 3 1 101
	2 3 1 +3 00 T		3 3 3 T 01
	2 3 3 +1 20 T		
	4 3 1 +1 21 T		
	4 3 3 T 21 T		
T:	$J \begin{smallmatrix} E \\ J' \\ J \end{smallmatrix} E$	T':	$J \begin{smallmatrix} E \\ J' \\ J \end{smallmatrix} E$
	0 2 2 0 01		1 2 2 +3 23
	2 2 2 +3 02 T		
	4 2 2 5 21 T		

T:	$J \begin{smallmatrix} E \\ J' \\ J \end{smallmatrix} M$	T':	$J \begin{smallmatrix} E \\ J' \\ J \end{smallmatrix} M$
	2 2 1 T 011		1 2 1 +T 2
	2 2 3 +3 01 T		1 2 3 5 T
	4 2 3 1 T 4 T		3 2 1 +3
			3 2 3 +1
TT:	$J \begin{smallmatrix} M \\ J' \\ J \end{smallmatrix} M$		
	2 1 1 +5 001		
	2 3 1 T 20 T		
	2 3 3 +1 00 T		
	4 3 1 T 01 T		
	4 3 3 T 41 T		
TT:	$J \begin{smallmatrix} E \\ J' \\ J \end{smallmatrix} E$		
	2 2 2 T 02 T		
	4 2 2 1 T 1 T		

Table C22 : $J_i = 2$ $J_f = 1$
No Parity Change
(45 terms)

TT: $J \begin{matrix} E \\ J' \\ J \end{matrix} \begin{matrix} M \\ J \end{matrix}$

2	2	1	$\bar{3}\bar{2}11$
2	2	3	$\bar{1}01\bar{1}$
4	2	3	$\cdot\bar{3}\bar{4}2\bar{1}$

TL: $J \begin{matrix} C \\ J' \\ J \end{matrix} \begin{matrix} M \\ J \end{matrix}$

2	2	1	$\bar{1}\bar{1}11$
2	2	3	$\cdot\bar{3}\bar{1}1\bar{1}$
4	2	3	$\bar{1}\bar{1}2\bar{1}$

TL': $J \begin{matrix} C \\ J' \\ J \end{matrix} \begin{matrix} M \\ J \end{matrix}$

1	2	1	$\cdot\bar{1}\bar{1}$
1	2	3	$\cdot\bar{3}\bar{1}$
3	2	1	$\cdot\bar{3}\bar{1}$
3	2	3	$\bar{1}\bar{1}$

TL: $J \begin{matrix} C \\ J' \\ J \end{matrix} \begin{matrix} E \\ J \end{matrix}$

2	2	2	$\bar{1}\bar{1}2\bar{1}$
4	2	2	$3\bar{1}\bar{1}\bar{1}$

TL': $J \begin{matrix} C \\ J' \\ J \end{matrix} \begin{matrix} E \\ J \end{matrix}$

1	2	2	$\cdot\bar{1}\bar{1}3$
---	---	---	------------------------

Table C23 : $J_i = 2$ $J_f = 1$
Parity Change
(58 terms)

TT: $J \begin{matrix} E \\ J' \\ J \end{matrix} \begin{matrix} E \\ J \end{matrix}$

2	1	1	$\bar{5}001$
2	3	1	$\cdot\bar{1}\bar{2}0\bar{1}$
2	3	3	$100\bar{1}$
4	3	1	$\cdot\bar{3}01\bar{1}$
4	3	3	$\cdot\bar{1}\bar{4}1\bar{1}$

TT: $J \begin{matrix} E \\ J' \\ J \end{matrix} \begin{matrix} M \\ J \end{matrix}$

2	1	2	$\bar{3}\bar{2}11$
2	3	2	$\bar{1}01\bar{1}$
4	3	2	$\cdot\bar{3}\bar{4}2\bar{1}$

TL: $J \begin{matrix} C \\ J' \\ J \end{matrix} \begin{matrix} M \\ J \end{matrix}$

2	1	2	$\cdot\bar{1}\bar{2}11$
2	3	2	$4\bar{1}1\bar{1}$
4	3	2	$\cdot\bar{0}\bar{1}2\bar{1}$

TL': $J \begin{matrix} C \\ J' \\ J \end{matrix} \begin{matrix} M \\ J \end{matrix}$

1	1	2	$\cdot\bar{1}2$
1	3	2	$\cdot\bar{2}\bar{1}$
3	1	2	$6\bar{2}$
3	3	2	$\cdot\bar{0}\bar{1}$

Table C23 : $J_i = 2$ $J_f = 1$
Parity Change
(58 terms)

L: $J \begin{matrix} C \\ J' \\ J \end{matrix} \begin{matrix} C \\ J \end{matrix}$

0	1	1	001
0	3	3	001
2	1	1	$\cdot\bar{1}001$
2	3	1	$\cdot\bar{2}10\bar{1}$
2	3	3	$\cdot\bar{5}00\bar{1}$
4	3	1	$411\bar{1}$
4	3	3	$101\bar{1}$

T: $J \begin{matrix} M \\ J' \\ J \end{matrix} \begin{matrix} M \\ J \end{matrix}$

0	2	2	001
2	2	2	$\cdot\bar{3}02\bar{1}$
4	2	2	$5\bar{2}1\bar{1}$

T: $J \begin{matrix} E \\ J' \\ J \end{matrix} \begin{matrix} E \\ J \end{matrix}$

0	1	1	001
0	3	3	001
2	1	1	$\bar{3}001$
2	3	1	$\cdot\bar{3}00\bar{1}$
2	3	3	$\cdot\bar{1}20\bar{1}$
4	3	1	$\cdot\bar{1}21\bar{1}$
4	3	3	$\bar{1}\bar{2}1\bar{1}$

T: $J \begin{matrix} E \\ J' \\ J \end{matrix} \begin{matrix} M \\ J \end{matrix}$

2	1	2	$\cdot\bar{1}011$
2	3	2	$301\bar{1}$
4	3	2	$\cdot\bar{1}\bar{2}4\bar{1}$

TT: $J \begin{matrix} M \\ J' \\ J \end{matrix} \begin{matrix} M \\ J \end{matrix}$

2	2	2	$\cdot\bar{5}02\bar{1}$
4	2	2	$\cdot\bar{1}\bar{4}1\bar{1}$

Table C24 : $J_i = 2$ $J_f = 2$
No Parity Change
(96 terms)

L: $J \begin{matrix} C \\ J' \\ J \end{matrix} \begin{matrix} C \\ J \end{matrix}$

0	0	0	001
0	2	2	001
0	4	4	001
2	2	0	$\cdot\bar{2}01$
2	2	2	$\bar{1}22\bar{3}$
2	4	2	$\cdot\bar{6}21\bar{3}$
2	4	4	$\cdot\bar{1}04\bar{3}$
4	4	0	201
4	2	2	$321\bar{3}$
4	4	2	$304\bar{3}$
4	4	4	$\bar{1}41\bar{3}$

T: $J \begin{matrix} M \\ J' \\ J \end{matrix} \begin{matrix} M \\ J \end{matrix}$

0	1	1	001
0	3	3	001
2	1	1	$\cdot\bar{3}001$
2	3	1	$410\bar{1}$
2	3	3	$\cdot\bar{3}20\bar{1}$
4	3	1	$011\bar{1}$
4	3	3	$\cdot\bar{3}01\bar{1}$

T: $J \begin{matrix} E \\ J' \\ J \end{matrix} \begin{matrix} M \\ J \end{matrix}$

0	1	1	$\bar{1}2$
1	3	2	$\cdot\bar{5}\bar{2}$
3	1	2	3
3	3	2	1

T: $J \begin{matrix} M \\ J' \\ J \end{matrix} \begin{matrix} M \\ J \end{matrix}$

0	1	1	001
0	3	3	001
2	1	1	$\cdot\bar{3}001$
2	3	1	$\cdot\bar{4}10\bar{1}$
2	3	3	$\cdot\bar{3}20\bar{1}$
4	3	1	$011\bar{1}$
4	3	3	$\cdot\bar{3}01\bar{1}$

Table C25 : $J_i = 2$ $J_f = 2$				Table C25 : $J_i = 2$ $J_f = 2$																																																																																																																																																																
Parity Change (86 terms)				Parity Change (86 terms)																																																																																																																																																																
<p>T:</p> <table style="width: 100%; border-collapse: collapse;"> <tr><td style="text-align: center;">J</td><td style="text-align: center;">E</td><td style="text-align: center;">E</td><td></td></tr> <tr><td style="text-align: center;">J'</td><td style="text-align: center;">J'</td><td style="text-align: center;">J</td><td></td></tr> <tr><td style="text-align: center;">0</td><td style="text-align: center;">1</td><td style="text-align: center;">1</td><td style="text-align: center;">001</td></tr> <tr><td style="text-align: center;">0</td><td style="text-align: center;">3</td><td style="text-align: center;">3</td><td style="text-align: center;">001</td></tr> <tr><td style="text-align: center;">2</td><td style="text-align: center;">1</td><td style="text-align: center;">1</td><td style="text-align: center;">•3001</td></tr> <tr><td style="text-align: center;">2</td><td style="text-align: center;">3</td><td style="text-align: center;">1</td><td style="text-align: center;">•410T</td></tr> <tr><td style="text-align: center;">2</td><td style="text-align: center;">3</td><td style="text-align: center;">3</td><td style="text-align: center;">•320T</td></tr> <tr><td style="text-align: center;">4</td><td style="text-align: center;">3</td><td style="text-align: center;">1</td><td style="text-align: center;">011T</td></tr> <tr><td style="text-align: center;">4</td><td style="text-align: center;">3</td><td style="text-align: center;">3</td><td style="text-align: center;">•301T</td></tr> </table>	J	E	E		J'	J'	J		0	1	1	001	0	3	3	001	2	1	1	•3001	2	3	1	•410T	2	3	3	•320T	4	3	1	011T	4	3	3	•301T	<p>T':</p> <table style="width: 100%; border-collapse: collapse;"> <tr><td style="text-align: center;">J</td><td style="text-align: center;">E</td><td style="text-align: center;">E</td><td></td></tr> <tr><td style="text-align: center;">J'</td><td style="text-align: center;">J'</td><td style="text-align: center;">J</td><td></td></tr> <tr><td style="text-align: center;">1</td><td style="text-align: center;">1</td><td style="text-align: center;">1</td><td style="text-align: center;">•301</td></tr> <tr><td style="text-align: center;">1</td><td style="text-align: center;">3</td><td style="text-align: center;">3</td><td style="text-align: center;">•301</td></tr> <tr><td style="text-align: center;">3</td><td style="text-align: center;">3</td><td style="text-align: center;">1</td><td style="text-align: center;">011</td></tr> <tr><td style="text-align: center;">3</td><td style="text-align: center;">3</td><td style="text-align: center;">3</td><td style="text-align: center;">•301</td></tr> </table>	J	E	E		J'	J'	J		1	1	1	•301	1	3	3	•301	3	3	1	011	3	3	3	•301	<p>TT:</p> <table style="width: 100%; border-collapse: collapse;"> <tr><td style="text-align: center;">J</td><td style="text-align: center;">E</td><td style="text-align: center;">M</td><td></td></tr> <tr><td style="text-align: center;">J'</td><td style="text-align: center;">J'</td><td style="text-align: center;">J</td><td></td></tr> <tr><td style="text-align: center;">2</td><td style="text-align: center;">1</td><td style="text-align: center;">2</td><td style="text-align: center;">3T1</td></tr> <tr><td style="text-align: center;">2</td><td style="text-align: center;">3</td><td style="text-align: center;">2</td><td style="text-align: center;">201T</td></tr> <tr><td style="text-align: center;">2</td><td style="text-align: center;">3</td><td style="text-align: center;">4</td><td style="text-align: center;">T13T</td></tr> <tr><td style="text-align: center;">4</td><td style="text-align: center;">3</td><td style="text-align: center;">2</td><td style="text-align: center;">T22T</td></tr> <tr><td style="text-align: center;">4</td><td style="text-align: center;">1</td><td style="text-align: center;">4</td><td style="text-align: center;">•T</td></tr> <tr><td style="text-align: center;">4</td><td style="text-align: center;">3</td><td style="text-align: center;">4</td><td style="text-align: center;">•T0T</td></tr> </table>	J	E	M		J'	J'	J		2	1	2	3T1	2	3	2	201T	2	3	4	T13T	4	3	2	T22T	4	1	4	•T	4	3	4	•T0T	<p>TL:</p> <table style="width: 100%; border-collapse: collapse;"> <tr><td style="text-align: center;">J</td><td style="text-align: center;">C</td><td style="text-align: center;">M</td><td></td></tr> <tr><td style="text-align: center;">J'</td><td style="text-align: center;">J'</td><td style="text-align: center;">J</td><td></td></tr> <tr><td style="text-align: center;">2</td><td style="text-align: center;">1</td><td style="text-align: center;">2</td><td style="text-align: center;">•T11</td></tr> <tr><td style="text-align: center;">2</td><td style="text-align: center;">3</td><td style="text-align: center;">2</td><td style="text-align: center;">7T1T</td></tr> <tr><td style="text-align: center;">2</td><td style="text-align: center;">3</td><td style="text-align: center;">4</td><td style="text-align: center;">•003T</td></tr> <tr><td style="text-align: center;">4</td><td style="text-align: center;">1</td><td style="text-align: center;">4</td><td style="text-align: center;">T</td></tr> <tr><td style="text-align: center;">4</td><td style="text-align: center;">3</td><td style="text-align: center;">2</td><td style="text-align: center;">T12T</td></tr> <tr><td style="text-align: center;">4</td><td style="text-align: center;">3</td><td style="text-align: center;">4</td><td style="text-align: center;">T40T</td></tr> </table>	J	C	M		J'	J'	J		2	1	2	•T11	2	3	2	7T1T	2	3	4	•003T	4	1	4	T	4	3	2	T12T	4	3	4	T40T	<p>TL':</p> <table style="width: 100%; border-collapse: collapse;"> <tr><td style="text-align: center;">J</td><td style="text-align: center;">C</td><td style="text-align: center;">M</td><td></td></tr> <tr><td style="text-align: center;">J'</td><td style="text-align: center;">J'</td><td style="text-align: center;">J</td><td></td></tr> <tr><td style="text-align: center;">1</td><td style="text-align: center;">1</td><td style="text-align: center;">2</td><td style="text-align: center;">•T101</td></tr> <tr><td style="text-align: center;">1</td><td style="text-align: center;">3</td><td style="text-align: center;">2</td><td style="text-align: center;">•310T</td></tr> <tr><td style="text-align: center;">1</td><td style="text-align: center;">3</td><td style="text-align: center;">4</td><td style="text-align: center;">•002T</td></tr> <tr><td style="text-align: center;">3</td><td style="text-align: center;">1</td><td style="text-align: center;">2</td><td style="text-align: center;">•6T0T</td></tr> <tr><td style="text-align: center;">3</td><td style="text-align: center;">1</td><td style="text-align: center;">4</td><td style="text-align: center;">T02T</td></tr> <tr><td style="text-align: center;">3</td><td style="text-align: center;">3</td><td style="text-align: center;">2</td><td style="text-align: center;">•T10T</td></tr> <tr><td style="text-align: center;">3</td><td style="text-align: center;">3</td><td style="text-align: center;">4</td><td style="text-align: center;">T02T</td></tr> </table>	J	C	M		J'	J'	J		1	1	2	•T101	1	3	2	•310T	1	3	4	•002T	3	1	2	•6T0T	3	1	4	T02T	3	3	2	•T10T	3	3	4	T02T
J	E	E																																																																																																																																																																		
J'	J'	J																																																																																																																																																																		
0	1	1	001																																																																																																																																																																	
0	3	3	001																																																																																																																																																																	
2	1	1	•3001																																																																																																																																																																	
2	3	1	•410T																																																																																																																																																																	
2	3	3	•320T																																																																																																																																																																	
4	3	1	011T																																																																																																																																																																	
4	3	3	•301T																																																																																																																																																																	
J	E	E																																																																																																																																																																		
J'	J'	J																																																																																																																																																																		
1	1	1	•301																																																																																																																																																																	
1	3	3	•301																																																																																																																																																																	
3	3	1	011																																																																																																																																																																	
3	3	3	•301																																																																																																																																																																	
J	E	M																																																																																																																																																																		
J'	J'	J																																																																																																																																																																		
2	1	2	3T1																																																																																																																																																																	
2	3	2	201T																																																																																																																																																																	
2	3	4	T13T																																																																																																																																																																	
4	3	2	T22T																																																																																																																																																																	
4	1	4	•T																																																																																																																																																																	
4	3	4	•T0T																																																																																																																																																																	
J	C	M																																																																																																																																																																		
J'	J'	J																																																																																																																																																																		
2	1	2	•T11																																																																																																																																																																	
2	3	2	7T1T																																																																																																																																																																	
2	3	4	•003T																																																																																																																																																																	
4	1	4	T																																																																																																																																																																	
4	3	2	T12T																																																																																																																																																																	
4	3	4	T40T																																																																																																																																																																	
J	C	M																																																																																																																																																																		
J'	J'	J																																																																																																																																																																		
1	1	2	•T101																																																																																																																																																																	
1	3	2	•310T																																																																																																																																																																	
1	3	4	•002T																																																																																																																																																																	
3	1	2	•6T0T																																																																																																																																																																	
3	1	4	T02T																																																																																																																																																																	
3	3	2	•T10T																																																																																																																																																																	
3	3	4	T02T																																																																																																																																																																	
<p>T:</p> <table style="width: 100%; border-collapse: collapse;"> <tr><td style="text-align: center;">J</td><td style="text-align: center;">E</td><td style="text-align: center;">M</td><td></td></tr> <tr><td style="text-align: center;">J'</td><td style="text-align: center;">J'</td><td style="text-align: center;">J</td><td></td></tr> <tr><td style="text-align: center;">2</td><td style="text-align: center;">1</td><td style="text-align: center;">2</td><td style="text-align: center;">•T11</td></tr> <tr><td style="text-align: center;">2</td><td style="text-align: center;">3</td><td style="text-align: center;">2</td><td style="text-align: center;">601T</td></tr> <tr><td style="text-align: center;">2</td><td style="text-align: center;">3</td><td style="text-align: center;">4</td><td style="text-align: center;">•T13T</td></tr> <tr><td style="text-align: center;">4</td><td style="text-align: center;">3</td><td style="text-align: center;">2</td><td style="text-align: center;">004T</td></tr> <tr><td style="text-align: center;">4</td><td style="text-align: center;">1</td><td style="text-align: center;">4</td><td style="text-align: center;">002</td></tr> <tr><td style="text-align: center;">4</td><td style="text-align: center;">3</td><td style="text-align: center;">4</td><td style="text-align: center;">T32T</td></tr> </table>	J	E	M		J'	J'	J		2	1	2	•T11	2	3	2	601T	2	3	4	•T13T	4	3	2	004T	4	1	4	002	4	3	4	T32T	<p>T':</p> <table style="width: 100%; border-collapse: collapse;"> <tr><td style="text-align: center;">J</td><td style="text-align: center;">E</td><td style="text-align: center;">M</td><td></td></tr> <tr><td style="text-align: center;">J'</td><td style="text-align: center;">J'</td><td style="text-align: center;">J</td><td></td></tr> <tr><td style="text-align: center;">1</td><td style="text-align: center;">1</td><td style="text-align: center;">2</td><td style="text-align: center;">T101</td></tr> <tr><td style="text-align: center;">1</td><td style="text-align: center;">3</td><td style="text-align: center;">2</td><td style="text-align: center;">•600T</td></tr> <tr><td style="text-align: center;">1</td><td style="text-align: center;">3</td><td style="text-align: center;">4</td><td style="text-align: center;">T12T</td></tr> <tr><td style="text-align: center;">3</td><td style="text-align: center;">1</td><td style="text-align: center;">2</td><td style="text-align: center;">•310T</td></tr> <tr><td style="text-align: center;">3</td><td style="text-align: center;">3</td><td style="text-align: center;">2</td><td style="text-align: center;">000T</td></tr> <tr><td style="text-align: center;">3</td><td style="text-align: center;">1</td><td style="text-align: center;">4</td><td style="text-align: center;">•002T</td></tr> <tr><td style="text-align: center;">3</td><td style="text-align: center;">3</td><td style="text-align: center;">4</td><td style="text-align: center;">•T12T</td></tr> </table>	J	E	M		J'	J'	J		1	1	2	T101	1	3	2	•600T	1	3	4	T12T	3	1	2	•310T	3	3	2	000T	3	1	4	•002T	3	3	4	•T12T	<p>TL:</p> <table style="width: 100%; border-collapse: collapse;"> <tr><td style="text-align: center;">J</td><td style="text-align: center;">C</td><td style="text-align: center;">E</td><td></td></tr> <tr><td style="text-align: center;">J'</td><td style="text-align: center;">J'</td><td style="text-align: center;">J</td><td></td></tr> <tr><td style="text-align: center;">2</td><td style="text-align: center;">1</td><td style="text-align: center;">1</td><td style="text-align: center;">•T001</td></tr> <tr><td style="text-align: center;">2</td><td style="text-align: center;">1</td><td style="text-align: center;">3</td><td style="text-align: center;">0T0T</td></tr> <tr><td style="text-align: center;">2</td><td style="text-align: center;">3</td><td style="text-align: center;">1</td><td style="text-align: center;">•300T</td></tr> <tr><td style="text-align: center;">2</td><td style="text-align: center;">3</td><td style="text-align: center;">3</td><td style="text-align: center;">0T0T</td></tr> <tr><td style="text-align: center;">4</td><td style="text-align: center;">1</td><td style="text-align: center;">3</td><td style="text-align: center;">T11T</td></tr> <tr><td style="text-align: center;">4</td><td style="text-align: center;">3</td><td style="text-align: center;">1</td><td style="text-align: center;">T01T</td></tr> <tr><td style="text-align: center;">4</td><td style="text-align: center;">3</td><td style="text-align: center;">3</td><td style="text-align: center;">T11T</td></tr> </table>	J	C	E		J'	J'	J		2	1	1	•T001	2	1	3	0T0T	2	3	1	•300T	2	3	3	0T0T	4	1	3	T11T	4	3	1	T01T	4	3	3	T11T	<p>TL':</p> <table style="width: 100%; border-collapse: collapse;"> <tr><td style="text-align: center;">J</td><td style="text-align: center;">C</td><td style="text-align: center;">E</td><td></td></tr> <tr><td style="text-align: center;">J'</td><td style="text-align: center;">J'</td><td style="text-align: center;">J</td><td></td></tr> <tr><td style="text-align: center;">1</td><td style="text-align: center;">1</td><td style="text-align: center;">1</td><td style="text-align: center;">•T01</td></tr> <tr><td style="text-align: center;">1</td><td style="text-align: center;">3</td><td style="text-align: center;">3</td><td style="text-align: center;">•011</td></tr> <tr><td style="text-align: center;">3</td><td style="text-align: center;">1</td><td style="text-align: center;">3</td><td style="text-align: center;">T11</td></tr> <tr><td style="text-align: center;">3</td><td style="text-align: center;">3</td><td style="text-align: center;">1</td><td style="text-align: center;">T01</td></tr> <tr><td style="text-align: center;">3</td><td style="text-align: center;">3</td><td style="text-align: center;">3</td><td style="text-align: center;">•T11</td></tr> </table>	J	C	E		J'	J'	J		1	1	1	•T01	1	3	3	•011	3	1	3	T11	3	3	1	T01	3	3	3	•T11																													
J	E	M																																																																																																																																																																		
J'	J'	J																																																																																																																																																																		
2	1	2	•T11																																																																																																																																																																	
2	3	2	601T																																																																																																																																																																	
2	3	4	•T13T																																																																																																																																																																	
4	3	2	004T																																																																																																																																																																	
4	1	4	002																																																																																																																																																																	
4	3	4	T32T																																																																																																																																																																	
J	E	M																																																																																																																																																																		
J'	J'	J																																																																																																																																																																		
1	1	2	T101																																																																																																																																																																	
1	3	2	•600T																																																																																																																																																																	
1	3	4	T12T																																																																																																																																																																	
3	1	2	•310T																																																																																																																																																																	
3	3	2	000T																																																																																																																																																																	
3	1	4	•002T																																																																																																																																																																	
3	3	4	•T12T																																																																																																																																																																	
J	C	E																																																																																																																																																																		
J'	J'	J																																																																																																																																																																		
2	1	1	•T001																																																																																																																																																																	
2	1	3	0T0T																																																																																																																																																																	
2	3	1	•300T																																																																																																																																																																	
2	3	3	0T0T																																																																																																																																																																	
4	1	3	T11T																																																																																																																																																																	
4	3	1	T01T																																																																																																																																																																	
4	3	3	T11T																																																																																																																																																																	
J	C	E																																																																																																																																																																		
J'	J'	J																																																																																																																																																																		
1	1	1	•T01																																																																																																																																																																	
1	3	3	•011																																																																																																																																																																	
3	1	3	T11																																																																																																																																																																	
3	3	1	T01																																																																																																																																																																	
3	3	3	•T11																																																																																																																																																																	
<p>TT:</p> <table style="width: 100%; border-collapse: collapse;"> <tr><td style="text-align: center;">J</td><td style="text-align: center;">M</td><td style="text-align: center;">M</td><td></td></tr> <tr><td style="text-align: center;">J'</td><td style="text-align: center;">J'</td><td style="text-align: center;">J</td><td></td></tr> <tr><td style="text-align: center;">2</td><td style="text-align: center;">2</td><td style="text-align: center;">2</td><td style="text-align: center;">T22T</td></tr> <tr><td style="text-align: center;">2</td><td style="text-align: center;">4</td><td style="text-align: center;">2</td><td style="text-align: center;">0T2T</td></tr> <tr><td style="text-align: center;">2</td><td style="text-align: center;">4</td><td style="text-align: center;">4</td><td style="text-align: center;">•304T</td></tr> <tr><td style="text-align: center;">4</td><td style="text-align: center;">2</td><td style="text-align: center;">2</td><td style="text-align: center;">1T1T</td></tr> <tr><td style="text-align: center;">4</td><td style="text-align: center;">4</td><td style="text-align: center;">2</td><td style="text-align: center;">T31T</td></tr> <tr><td style="text-align: center;">4</td><td style="text-align: center;">4</td><td style="text-align: center;">4</td><td style="text-align: center;">T01T</td></tr> </table>	J	M	M		J'	J'	J		2	2	2	T22T	2	4	2	0T2T	2	4	4	•304T	4	2	2	1T1T	4	4	2	T31T	4	4	4	T01T	<p>TT:</p> <table style="width: 100%; border-collapse: collapse;"> <tr><td style="text-align: center;">J</td><td style="text-align: center;">E</td><td style="text-align: center;">E</td><td></td></tr> <tr><td style="text-align: center;">J'</td><td style="text-align: center;">J'</td><td style="text-align: center;">J</td><td></td></tr> <tr><td style="text-align: center;">2</td><td style="text-align: center;">1</td><td style="text-align: center;">1</td><td style="text-align: center;">•5001</td></tr> <tr><td style="text-align: center;">2</td><td style="text-align: center;">3</td><td style="text-align: center;">1</td><td style="text-align: center;">•0T0T</td></tr> <tr><td style="text-align: center;">2</td><td style="text-align: center;">3</td><td style="text-align: center;">3</td><td style="text-align: center;">T00T</td></tr> <tr><td style="text-align: center;">4</td><td style="text-align: center;">3</td><td style="text-align: center;">1</td><td style="text-align: center;">T11T</td></tr> <tr><td style="text-align: center;">4</td><td style="text-align: center;">3</td><td style="text-align: center;">3</td><td style="text-align: center;">T11T</td></tr> </table>	J	E	E		J'	J'	J		2	1	1	•5001	2	3	1	•0T0T	2	3	3	T00T	4	3	1	T11T	4	3	3	T11T																																																																																																							
J	M	M																																																																																																																																																																		
J'	J'	J																																																																																																																																																																		
2	2	2	T22T																																																																																																																																																																	
2	4	2	0T2T																																																																																																																																																																	
2	4	4	•304T																																																																																																																																																																	
4	2	2	1T1T																																																																																																																																																																	
4	4	2	T31T																																																																																																																																																																	
4	4	4	T01T																																																																																																																																																																	
J	E	E																																																																																																																																																																		
J'	J'	J																																																																																																																																																																		
2	1	1	•5001																																																																																																																																																																	
2	3	1	•0T0T																																																																																																																																																																	
2	3	3	T00T																																																																																																																																																																	
4	3	1	T11T																																																																																																																																																																	
4	3	3	T11T																																																																																																																																																																	

and so

$$\begin{aligned}
 \mathcal{W}_0^L(q)_{1/2,3/2} &= \sqrt{2}(F_{C1}(q)_{1/2,3/2})^2, \\
 \mathcal{W}_0^T(q)_{1/2,3/2} &= \sqrt{2}((F_{M2}(q)_{1/2,3/2})^2 + (F_{E1}(q)_{1/2,3/2})^2) \\
 \mathcal{W}_1^T(q)_{1/2,3/2} &= (1/\sqrt{2})(F_{M2}(q)_{1/2,3/2})^2 - (1/\sqrt{2})(F_{E1}(q)_{1/2,3/2})^2 \\
 &\quad + \sqrt{6}F_{E1}(q)_{1/2,3/2} F_{M2}(q)_{1/2,3/2},
 \end{aligned}$$

and

$$\mathcal{W}_1^{TL'}(q)_{1/2,3/2} = -\sqrt{2}F_{C1}(q)_{1/2,3/2}(F_{E1}(q)_{1/2,3/2} + \sqrt{3}F_{M2}(q)_{1/2,3/2}).$$

REFERENCES

1. T. W. DONNELLY AND J. D. WALECKA, *Ann. Rev. Nucl. Sci.* **25** (1975), 329.
2. J. D. WALECKA, in "Muon Physics," Vol. II (V. W. Hughes and C. S. Wu, Eds.) p. 113, Academic Press, New York, 1975.

3. T. W. DONNELLY AND R. D. PECCEI, *Phys. Lett. B* **65** (1976), 196.
4. M. N. ROSENBLUTH, *Phys. Rev.* **79** (1950), 615.
5. L. J. WEIGERT AND M. E. ROSE, *Nucl. Phys.* **51** (1964), 529.
6. T. W. DONNELLY, in "International School of Nuclear Physics, Nuclear and Subnuclear Degrees of Freedom and Lepton Scattering, Erice, Sicily" April 1984; *Prog. Part. Nucl. Phys.* **13** (1985), 183.
7. J. H. SCOFIELD, *Phys. Rev.* **113** (1959), 1599.
8. J. H. SCOFIELD, *Phys. Rev.* **141** (1966), 1352.
9. N. DOMBEY, *Rev. Mod. Phys.* **41** (1969), 236.
10. M. GOURDIN, *Phys. Rep.* **11C** (1974), 29.
11. A. I. AKHIEZER AND M. P. REKALO, *Fiz. Elem. Chastits Atom. Yadra* **4** (1973), 662; *Sov. J. Part. Nucl.* **4** (1974), 277.
12. M. J. ALGUARD *et al.*, *Phys. Rev. Lett.* **37** (1976), 1258.
13. F. L. RIDENER, JR., H. S. SONG, AND R. H. GOOD, JR., *Phys. Rev. D* **24** (1981), 631.
14. R. G. ARNOLD, C. E. CARLSON, AND F. GROSS, *Phys. Rev. C* **23** (1981), 363.
15. M. GOURDIN AND C. A. PIKETTY, *Nuovo Cimento* **32** (1964), 1137.
16. D. SCHILDKNECHT, *Z. Phys.* **185** (1965), 382.
17. H. S. SONG, F. L. RIDENER, JR., AND R. H. GOOD, JR., *Phys. Rev. D* **25** (1982), 61.
18. F. J. UHRHANE, J. S. MCCARTHY, AND M. R. YEARIAN, *Phys. Rev. Lett.* **26** (1971), 578.
19. D. G. RAVENHALL AND R. L. MERCER, *Phys. Rev. C* **13** (1976), 2324.
20. C. Y. PRESCOTT *et al.*, *Phys. Lett. B* **77** (1978), 347.
21. T. W. DONNELLY, "Physics with Polarized Electrons and Targets," Workshop on Polarized Targets in Storage Rings, p. 17, Argonne National Laboratory, ANL-84-50, May 1984.
22. Proposal for a CW Upgrade of the William H. Bates Linear Accelerator Center, June 1984.
23. R. J. HOLT, in "Proceedings of the Spectrometer Workshop, Williamsburg, Va.," 1983, d1; in "Workshop on Polarized Targets in Storage Rings," p. 103, Argonne National Laboratory, ANL-84-50, May 1984.
24. T. W. DONNELLY, "Coincidence and Polarization Measurements with High-Energy Electrons," CEBAF Workshop, June 1984.
25. T. DEFOREST, JR. AND J. D. WALECKA, *Advan. Phys.* **15** (1966), 1.
26. H. ÜBERALL, "Electron Scattering from Complex Nuclei. Parts A and B," Academic Press, New York 1971.
27. T. W. DONNELLY, in "Perspectives in Nuclear Physics at Intermediate Energies" (S. Boffi, C. Ciofi degli Atti, and M. M. Giannini, Eds.), p. 244, World Scientific, Trieste, Italy, 1984.
28. T. W. DONNELLY, "Super-Rosenbluth Physics," BUTG Workshop "Nucleon and Nuclear Structure and Exclusive Electromagnetic Reaction Studies," M. I. T., Cambridge, Mass., July 1984.
29. T. W. DONNELLY, "Polarized Electron Scattering from Polarized Nuclei," 6th Seminar "Electromagnetic Interactions of Nuclei at Low and Medium Energies," Moscow, December, 1984.
30. J. D. BJORKEN AND S. D. DRELL, "Relativistic Quantum Mechanics," McGraw-Hill, New York, 1964.
31. T. W. DONNELLY, A. S. RASKIN, AND G. RAWITSCHER, to be published.
32. T. W. DONNELLY, in "Symmetries in Nuclear Structure" (K. Abrahams, K. Allaart, and A. E. L. Dieperink, Eds.), p. 1, Plenum, New York, 1983.
33. T. W. DONNELLY AND J. D. WALECKA, *Nucl. Phys. A* **201** (1973), 81.
34. A. R. EDMONDS, "Angular Momentum in Quantum Mechanics," 3rd ed., Princeton Univ. Press, Princeton, 1974.
35. T. W. DONNELLY AND J. D. WALECKA, *Phys. Lett. B* **44** (1973), 330.
36. S. E. DARDEN, in "Polarization Phenomena in Nuclear Reactions" (H. H. Barschall and W. Haeberli, Eds.), p. 39, Univ. of Wisconsin Press, Madison, 1971; see the summary of the Madison Convention contained in this volume.
37. T. W. DONNELLY AND I. SICK, *Rev. Mod. Phys.* **56** (1984), 461.
38. T. W. DONNELLY AND W. C. HAXTON, *Atomic Data Nucl. Tables* **23** (1979), 103.
39. T. W. DONNELLY AND W. C. HAXTON, *Atomic Data Nucl. Tables* **25** (1980), 1.

40. R. G. ARNOLD AND F. GROSS, in "Future Directions in Electromagnetic Nuclear Physics," Workshop report, p. 141, 1981.
41. F. BORKOWSKI *et al.*, *Z. Phys. A* **275** (1975), 29.
42. F. BORKOWSKI *et al.*, *Nucl. Phys. B* **93** (1975), 461.
43. G. HÖHLER *et al.*, *Nucl. Phys. B* **114** (1976), 505.
44. G. G. SIMON *et al.*, *Z. Naturforsch. a* **35** (1980), 1.
45. M. GARI AND W. KRÜPELMANN, *Phys. Lett. B* **141** (1984), 295.
46. P. N. KIRK *et al.*, *Phys. Rev. D* **8** (1973), 63.
47. W. ALBRECHT *et al.*, *Phys. Lett. B* **26** (1968), 642.
48. S. ROCK *et al.*, *Phys. Rev. Lett.* **49** (1982), 1139.
49. C. Y. CHEUNG AND R. M. WOLOSHYN, *Phys. Lett. B* **127** (1983), 147.
50. B. BLANKLEIDER AND R. M. WOLOSHYN, *Phys. Rev. C* **29** (1984), 538.
51. H. COLLARD *et al.*, *Phys. Rev. B* **138** (1965), 57.
52. D. H. BECK, J. ASAI, AND D. M. SKOPIK, *Phys. Rev. C* **25** (1982), 1152.
53. D. H. BECK *et al.*, *Phys. Rev. C* **30** (1984), 1403.
54. R. G. ARNOLD *et al.*, *Phys. Rev. Lett.* **40** (1978), 1429; G. A. RETZLAFF AND D. M. SKOPIK, *Phys. Rev. C* **29** (1984), 1194.
55. J. S. MCCARTHY, I. SICK, AND R. R. WHITNEY, *Phys. Rev. C* **15** (1977), 1396; P. C. DUNN *et al.*, *Phys. Rev. C* **27** (1983), 71; for a discussion of the elastic magnetic form factor of ^3He including references to the original literature, see [37].
56. J. F. DUBACH, private communications.
57. W. W. ASH *et al.*, *Phys. Lett. B* **24** (1967), 165.
58. R. SIDDLER *et al.*, *Nucl. Phys. B* **35** (1971), 93.
59. C. MISTRETTA *et al.*, *Phys. Rev.* **184** (1969), 1487.
60. W. ALBRECHT *et al.*, *Nucl. Phys. B* **25** (1971), 1.
61. W. ALBRECHT *et al.*, *Nucl. Phys. B* **27** (1971), 615.
62. T. W. DONNELLY, A. S. RASKIN, AND J. F. DUBACH, to be published.
63. M. I. HAFTEL, L. MATHELITSCH, AND H. F. K. ZINGL, *Phys. Rev. C* **22** (1980), 1285.
64. M. E. SCHULTZE *et al.*, *Phys. Rev. Lett.* **52** (1984), 597.
65. R. J. HOLT, in "Future Directions in Electromagnetic Nuclear Physics," 1981, p. 169.
66. T. SUZUKI, *Phys. Lett. B* **120** (1983), 27; private communications.
67. J. DUBACH, J. H. KOCH, AND T. W. DONNELLY, *Nucl. Phys. A* **271** (1976), 279.
68. E. MOYA DE GUERRA AND A. E. L. DIEPERINK, *Phys. Rev. C* **18** (1978), 1596.
69. C. M. LEDERER AND V. S. SHIRLEY, Eds., "Table of Isotopes," 7th ed., Wiley, New York, 1978.